

The Role of *bHLHm1* in Phytohormone Signalling in Legume Nodules and Roots

A thesis submitted for the degree of Doctor of Philosophy at
The University of Sydney

School of Life and Environmental Sciences

Submitted by

Die Hu

June 2023

Table of Contents

List of Tables	IX
I. Abstract	X
II. Declaration	XIII
III. Acknowledgements	XIV
IV. Abbreviations	XVI
Chapter 1 Literature Review	1
1.1 Introduction.....	1
1.1.1 Nitrogen use efficiency is important for agriculture.....	1
1.1.2 Legumes are improving NUE.....	1
1.1.3 Soybean is an important legume crop for the economy.....	2
1.2 Nodulation	2
1.2.1 Symbiotic communication	3
1.2.2 The infection thread elongation	3
1.2.3 The bacteria invasion and nodule organogenesis.....	4
1.3 Structure of mature nodules	4
1.4 Autoregulation of nodulation.....	7
1.5 Phytohormone regulation of nodulation.....	10
1.5.1 Gibberellins.....	10
1.5.2 Auxin.....	13

1.6 Nitrogen fixation and N transport in the nodule.....	15
1.6.1 The AMT family	15
1.6.2 The AMF family	16
1.7 GmbHLHm1 and GmAMF3.....	17
Chapter 2 Functional analysis of <i>GmbHLHm1</i> in soybean roots through silencing and overexpression.	21
2.1 Introduction.....	21
2.2 Results	22
2.2.1 <i>GmbHLHm1</i> RNAi-silencing.....	22
2.2.2 <i>GmbHLHm1</i> Overexpression.....	23
2.3 Discussion.....	34
2.4 Materials and Methods.....	36
2.4.1 Plant material cultivation	36
2.4.2 RNAi silencing.....	36
2.4.3 Overexpression	37
2.4.4 RNA extraction and quantitative polymerase chain reaction (qPCR) analysis	37
2.4.5 Acetylene reduction assay (ARA)	38
Chapter 3 The interaction between <i>GmbHLHm1</i> and the plant hormones GA₃ and IAA... 39	39
3.1 Introduction.....	39
3.2 Results	42
3.2.1 GA affects the expression of nodulation genes and alters the activity of <i>GmbHLHm1</i> in nodules and roots.	42
3.2.2 Long-term GA treatment on <i>GmbHLHm1</i> expression in <i>bhlhm1</i>	43
3.2.3 Long-term GA treatment on <i>GmbHLHm1</i> -overexpressed (Overexpression) soybeans	44
3.2.4 <i>GmbHLHm1</i> expression in nodules and roots after a short-term IAA treatment.	45
3.2.5 Long-term IAA treatment on <i>GmbHLHm1</i> expression in <i>bhlhm1</i>	45

3.2.6 Long-term IAA treatment on <i>GmbHLHm1</i> -overexpressed (Overexpression) soybeans	46
3.3 Discussion	59
3.4 Material and Method	63
3.4.1 Plant material cultivation and treatment	63
Chapter 4 Genetic control of <i>GmbHLHm1</i> and <i>GmAMF3</i> promoters	64
4.1. Introduction	64
4.2. Result	65
4.3 Discussion	82
4.4. Material and method	84
4.4.2 Yeast One-Hybrid	86
Chapter 5 Functional analysis of the nodule transcription factor <i>LjbHLHm1.1</i> in <i>Lotus japonicus</i>	88
5.1 Introduction	88
5.2 Results	90
5.2.1 <i>L. japonicus</i> line selection and seedling genotyping	90
5.2.2 Promoter analysis and GA responsive element identification.	92
5.2.3 The effect of GA on the <i>L. japonicus</i> nodulation phenotype and <i>LjbHLHm1.1</i> expression	92
5.2.5 The effects of <i>LjbHLHm1.1</i> expression and long-term GA application on <i>L. japonicus</i> nodule phenotype and function	94
5.3 Discussion	111
5.4 Materials and method	112
5.4.1 Lotus line identification	112
5.4.2 Plant material preparation of <i>LORE1</i> line	113
5.4.3 RNA extraction and quantitative polymerase chain reaction (qPCR) analysis	114
5.4.4 Ammonium assay	115

Chapter 6 Conclusion and Future Directions	116
6.1 Function analysis of <i>GmbHLHm1</i> in soybean roots and nodules	116
6.2 Interaction between <i>bHLHm1</i> expression with N, GA₃, and IAA	118
6.3 Promoter analysis of <i>GmbHLHm1</i> and <i>GmAMF3</i>	121
Reference	124
Appendixes.....	140

List of Figures

- Figure 1. 1 The organogenesis of determinate and indeterminate nodules.** Steps 1 and 2 illustrate the first stage, steps 3-8 illustrate the second stage, and steps 9-10 demonstrate the third stage. The structures of the determinate and indeterminate nodules are shown in the bottom part of the picture. The picture was modified from Ferguson et al. (2010). 6
- Figure 1. 2 The CEP/CRA2, NIN/CLE/SUNN and NIN/miR172/NNC1 pathway models for Autoregulation of nodulation**..... 9
- Figure 1. 3 The molecular regulation of GA signalling via DELLA** 13
- Figure 1. 4 Hormone regulation of nodulation in different stages.** ET: ethylene; JA: jasmonic acid; GA: gibberellic acid; CK: cytokinin; AUX: auxin.(Roy et al., 2019) 14
- Figure 1. 5 N and GA treatment affect soybean shoot height** (A) The effects of *GmbHLHm1* silencing on shoot height of inoculated plants and non-inoculated plants (supplemented with 2.5mM NH_4NO_3) (B) GA treatments significantly induced shoot height. (Dehcheshmeh, 2013, unpublished result). 19
- Figure 2. 1 Map of pK7GWIWG2D(II) vector used for RNAi silencing of *GmbHLHm1*.** pK7GWIWG2D(II) was used in *Agrobacterium rhizogenes* K599 hairy root transformation of soybean hypocotyls (Mohammadi-Dehcheshmeh et al., 2014). The vector contains the selectable marker, *nptII*, which encodes neomycin phosphotransferase for kanamycin resistance, an enhanced green fluorescent protein (Egfp) driven by the 35S promoter (p35S) and streptomycin-spectinomycin resistance (Sm/SpR) for plasmid selection (Karimi et al., 2002). 25
- Figure 2. 2 *GmbHLHm1* expression in wild-type, empty vector (Vector), and *GmbHLHm1*RNAi-silenced mutant (*bhlhm1*) nodules and roots.** Comparison of *GmbHLHm1* expression in 28 d (A) Wild-type nodules and roots. The * indicates the significant differences between groups based on the Student T-test ($P < 0.05$). (B) wild-type and transgenic nodules. The

expression of *GmbHLHm1* was normalized with *Con6* as a reference gene and was calculated using the $2^{-\Delta\Delta Ct}$ method (Libault et al., 2008). Values were means \pm SE (n=4) biological replicates. The * indicate the significant differences compared to the Wild-type based on the Student T-test ($P < 0.05$). 26

Figure 2. 3 Egfp expression in pK7GWIWG2D(II) identified in transformed hairy roots and nodules. (A) The pK7GWIWG2D(II)-*GmbHLHm1* transformed hairy roots and nodules. (B) pK7GWIWG2D(II) empty vector transformed hairy roots and nodules. Transgenic hairy roots were made according to the protocol of (Mohammadi-Dehcheshmeh et al., 2014). Soybeans were grown in a mixed matrix of quartz sand and turf (1:1 ratio). B&D nutrient solution (Broughton and Dilworth, 1971) was applied twice a day using a semi-hydroponic growing system. 28 d nodules on wild-type roots and transgenic hairy roots were harvested for experiments and for **Egfp** detection. 27

Figure 2. 4 The effects of *GmbHLHm1* silencing on shoot height, nodulation, nodule growth and nodule N₂-fixation activity. (A) Shoot height, (B) nodule number, (C) nodule DW plant⁻¹, and (D) N₂-fixation rate (Acetylene Reduction Assay) (E) Average nodule dry weight (average nodule dry weight per plant /Average nodule number per plant) of *GmbHLHm1*RNAi-silenced and empty vector (Vector) plants. Plant tissues were analyzed 28 d after inoculation with rhizobia. Values are means \pm SE (n=5). Values with * indicate significant differences compared to Vector based on the Student T-test ($P < 0.05$). 28

Figure 2. 5 The effects of *GmbHLHm1* silencing on soybean growth. (A) Shoot and root phenotypes of 28-day-old empty vector, *GmbHLHm1* RNAi transformed hairy roots and untransformed wild-type plants. Representative nodules on roots (B) and nodule cross-sections (C) of wild-type, empty vector control, and *GmbHLHm1* RNAi (*bhlhm1*) soybean plants. 29

Figure 2. 6 Soybean shoot growth with/without rhizobium inoculation and exogenous nitrate. (A) Plant growth was reliant on nodule biological N₂-fixation (no supplied KNO₃) versus (B) non-inoculated plants grown solely on 5 mM KNO₃. Shoot height (C), shoot dry weight (D) of empty vector control, *GmbHLHm1*RNAi, and wild-type control plants supplied inoculum plus nitrate and no inoculum with nitrate. B&D nutrient solutions (Broughton and Dilworth, 1971) containing \pm 5 mM KNO₃ were supplied twice a day using a semi-hydroponic system. Twenty-eight-day-old plants were harvested for all experiments. Values are means \pm SE (n=5 plants). Values with different letters above each bar indicate significant differences between the treatments based on a one-way ANOVA ($P < 0.05$). 30

Figure 2. 7 Map of pFAST-G02 vector for gene overexpression. pFAST-G02 was used in *Agrobacterium rhizogenes* K599 hairy root transformation of soybean hypocotyls (Shimada et al., 2010). The vector contains a fusion gene encoding either GFP or RFP with an oil body membrane protein that is prominent in seeds and a marker gene for streptomycin-spectinomycin resistance (Sm/SpR) in *A. rhizogenes* (Shimada et al., 2010). Target genes of interest rely on the p35S promoter for gene transcription in planta. 31

Figure 2. 8 *GmbHLLHm1* expression in wild-type, empty vector (Vector), and *GmbHLLHm1*-overexpressed (*GmbHLLHm1* OEX) nodules. (A) Comparison of *GmbHLLHm1* expression in wild-type, empty vector, and *GmbHLLHm1*-overexpressed nodules. (B) Shoot height, (C) nodule number per plant, (D) nodule dry weight per plant, (E) nitrogenase activity per nodule dry weight, and (F) %N in leaves (G) Average nodule dry weight (average nodule dry weight per plant /Average nodule number per plant) of *GmbHLLHm1*-overexpressed plants and the empty vector control. Transgenic hairy roots were made according to Mohammadi-Dehcheshmeh et al. (2014). Soybeans were grown in a mixed matrix of quartz sand and turface (1:1 ratio). B&D nutrient solution (Broughton and Dilworth, 1971) was supplied twice a day using a semi-hydroponic system. Twenty-eight-day-old nodules on wild-type or transgenic hairy roots were harvested for experiments. The expression of *GmbHLLHm1* levels was normalized with *Con6* as a reference gene and was calculated using the $2^{-\Delta\Delta C_t}$ method (Libault et al., 2008). Values were means \pm SE (n = 4) of four biological plant replicates. The * above bars indicate the significant difference compared to wild-type (A) and /or Vector (B) to (F) based on the Student T-test (P < 0.05). 32

Figure 2. 9 The effect of *GmbHLLHm1* OEX on soybean growth. (A) Shoot and root phenotypes of 28-day-old empty vector, *GmbHLLHm1* OEX transformed hairy roots and untransformed wild-type plants. Nodules on roots (B) and nodule cross-sections (C) of wild-type, empty vector control, and *GmbHLLHm1* OEX..... 33

Figure 3. 1 *GmbHLLHm1*, *GASA6*, *MTO3* and *GAMMA-TIP* expression in nodules with/without long-term KNO_3 treatment. Nodulated plants were supplied \pm 5 mM KNO_3 in the nutrient solution for 10 days after an initial 18 days of growth in a minus N nutrient solution. The expression levels of (A) *GmbHLLHm1*, (B) *MTO3*, (C) *GASA6*, and (D) *GAMMA-TIP* in nodules were determined. The expression of gene levels was normalized with *Con6* as a reference gene and was calculated using the $2^{-\Delta\Delta C_t}$ method (Libault et al., 2008). Values were means \pm SE (n=5) of five biological replicates. The * above bars indicate the significant difference compared to Control based on the T-test (P < 0.05). 47

Figure 3. 2 *GmbHLLHm1*, *GASA6*, *MTO3*, and *GAMMA-TIP* expression in nodules with short-term GA treatment \pm KNO_3 in the nutrient solution. Nodulated plants were grown without N (-N) or with 5 mM KNO_3 for 18 days post-inoculation with rhizobia. (A) *GmbHLLHm1*, (B) *MTO3*, (C) *GASA6*, and (D) *GAMMA-TIP* expression levels in nodules after 1 h and 24 hrs of GA_3 treatment. The expressions of gene levels were normalized with *Con6* as a reference gene and were calculated using the $2^{-\Delta\Delta C_t}$ method (Libault et al., 2008). Values were means \pm SE (n=5) of five biological replicates. The letters above each bar indicate the significant differences between groups based on the one-way ANOVA (P < 0.05). 48

Figure 3. 3 The nitrogenase activity in the wild-type nodules after short-term GA treatments (0-48 h). (A) The ammonium levels per nodule dry weight and (B) nitrogen fixation rate (Acetylene Reduction Assay) after a short-term GA_3 treatment. 4ppm GA_3 was applied to the soil for a 48-h period. Values were means \pm SE (n=6) of six biological replicates. The letters above

each bar indicate the significant differences between groups based on the one-way ANOVA ($P < 0.05$). 49

Figure 3. 4 The effect of long-term GA treatment on *GmbHLHm1* expression in nodules. From the 5th day after inoculation, 4ppm of GA₃ solution was applied directly to the soil twice a week. 28-day-old plants were harvested and analyzed. (A) Expression levels of *GmbHLHm1* in wild-type, empty vector, and *bhlhm1* plants. (B) The nitrogen percentage of the leaves, (C) nitrogen fixation rate (ARA), (D) nodule dry weight, (E) nodule number, (F) root dry weight, (G) shoot dry weight, and (H) shoot height of empty vector (EV) and *bhlhm1* with GA treatment. The expression of *GmbHLHm1* levels was normalized with *Con6* as a reference gene and was calculated using the $2^{-\Delta\Delta Ct}$ method (Libault et al., 2008). Values were means \pm SE (n=4) of four biological replicates. The letters above each bar indicate the significant differences between groups based on the two-way ANOVA ($P < 0.05$). 50

Figure 3. 5 Visual images of (A)whole plant, (B) nodules on roots, and (C) nodule cross-section of empty vector and *bhlhm1* with GA treatment...... 51

Figure 3. 6 The effect of long-term GA treatment on *GmbHLHm1* expression in nodules. From the 5th day after inoculation, 4ppm of GA₃ solution was applied directly to the soil twice a week. 28-day-old plants on wild-type, empty vector, and *GmbHLHm1* overexpression hairy roots were harvested and analyzed. (A) Expression levels of *GmbHLHm1* in nodules. (B) The nitrogen percentage of the leaves, (C) nitrogen fixation rate (ARA), (D) nodule dry weight, (E) nodule number, (F) shoot dry weight, and (G) shoot height of empty vector and overexpression plants with GA treatment. The expression of *GmbHLHm1* levels was normalized with *Con6* as a reference gene and was calculated using the $2^{-\Delta\Delta Ct}$ method (Libault et al., 2008). Values were means \pm SE (n=6) of six biological replicates. The letters above each bar indicate the significant differences between groups based on the two-way ANOVA ($P < 0.05$). 52

Figure 3. 7 Visual images of (A)whole plant, (B) nodules on roots, and (C) nodule cross-section of plants on empty vector and *GmbHLHm1* overexpression hairy roots with GA treatment...... 53

Figure 3. 8 *GmbHLHm1* expression in nodules and roots after a short-term IAA (1 ppm) treatment. *GmbHLHm1* expression in roots (A) and nodules (B) showed no response with a short-term IAA treatment applied directly to the soil. The expression of *GmbHLHm1* levels was normalized with *Con6* as a reference gene and was calculated using the $2^{-\Delta\Delta Ct}$ method (Libault et al., 2008). Values were means \pm SE (n=5) of five biological replicates. The significant differences between groups based on the one-way ANOVA ($P < 0.05$). 54

Figure 3. 9 The effect of long-term IAA treatment on *GmbHLHm1* expression in nodules. From the 5th day after inoculation, 1ppm of IAA solution was applied directly to the soil twice a week. 28-day-old plants were harvested and analyzed. (A) Expression levels of *GmbHLHm1* in wild-type, empty vector, and *bhlhm1* plants. (B) The nitrogen percentage of the leaves, (C) nodule

dry weight, (D) nodule number, (E) root dry weight, (F) shoot dry weight and (G) shoot height of empty vector and *bhlhm1* with IAA treatment. The expression of *GmbHLHm1* levels was normalized with *Con6* as a reference gene and was calculated using the $2^{-\Delta\Delta C_t}$ method (Libault et al., 2008). Values were means \pm SE (n=4) of four biological replicates. The letters above each bar indicate the significant differences between groups based on the two-way ANOVA ($P < 0.05$). 55

Figure 3. 10 Visual images of (A)whole plant, (B) nodules on roots, and (C) nodule cross-section of empty vector and *bhlhm1* with IAA treatment. 56

Figure 3. 11 The effect of long-term IAA treatment on *GmbHLHm1* expression in nodules. From the 5th day after inoculation, 1ppm of IAA solution was applied directly to the soil twice a week. 28-day-old plants on wild-type, empty vector, and *GmbHLHm1* overexpression hairy roots were harvested and analyzed. (A) Expression levels of *GmbHLHm1* in nodules. (B) The nitrogen percentage of the leaves, (C) nitrogen fixation rate (ARA), (D) nodule dry weight, (E) nodule number, (F) shoot dry weight, and (G) shoot height of empty vector and overexpression plants with IAA treatment. The expression of *GmbHLHm1* levels was normalized with *Con6* as a reference gene and was calculated using the $2^{-\Delta\Delta C_t}$ method (Libault et al., 2008). Values were means \pm SE (n=6) of six biological replicates. The letters above each bar indicate the significant differences between groups based on the two-way ANOVA ($P < 0.05$). 57

Figure 3. 12 Visual images of (A)whole plant, (B) nodules on roots, and (C) nodule cross-section of plants on empty vector and *GmbHLHm1* overexpression hairy roots with GA treatment. 58

Figure 4. 1 Map of pKGWFS7 vector with inserted the *GmbHLHm1* promoter. pKGWFS7 was used in the *Agrobacterium rhizogenes* K599 hairy root transformation of soybean hypocotyls (Karimi et al., 2002; Mohammadi Dehcheshmeh, 2014). The vector contains the selectable marker, *nptII*, which encodes neomycin phosphotransferase for kanamycin resistance, an enhanced green fluorescent protein (eGFP) and a beta-glucuronidase (*gus*) driven by the *GmbHLHm1* promoter under study. Streptomycin-spectinomycin resistance (Sm/SpR) for plasmid selection (Karimi et al., 2002). 72

Figure 4. 2 *GmbHLHm1* promoter-driven GUS expression in nodules and roots. 28-day-old transgenic nodules were stained for GUS activity. (A) the whole root; (B) nodule cross sections after supply of either 1ppm IAA or 4ppm GA. *GmbHLHm1* gene expression levels in roots and nodules with either IAA or GA treatments; (C) and (D) GUS expression levels in roots and nodules with 1ppm IAA or 4ppm GA supply. The expression of GUS levels was normalized with *Con6* as a reference gene and was calculated using the $2^{-\Delta\Delta C_t}$ method (Libault et al., 2008). Values were means \pm SE (n=4) biological replicates. The letters indicate the significant differences between groups based on the one-way ANOVA ($P < 0.05$). 73

Figure 4. 3 Illustrations of edited *GmbHLHm1* promoters and their activation of GUS expression in soybean nodules. (A) Three Gibberellin-responsive elements of the *GmbHLHm1* promoter were edited respectively. Bases of each element were replaced with a similar number of adenine residues. (B) GUS expression of each edited construct in 28-day-old soybean nodules treated with water, 4ppm GA or 1ppm Auxin treatments for 5 days. GUS staining was developed over 5 hours. Images are representative samples of repeated nodule experiments..... 74

Figure 4. 4 *GmbHLHm1* promoter-GUS expression with/without GA treatment. 28-day-old soybean nodules were stained for GUS analysis (see methods 4.4.1). Plants were treated with water (A, C) or 4ppm GA₃ (B, D). Nodule cross sections identify the central infected region (IR), which contains infected cells (I). The IR is surrounded by the inner cortex (IC) with vascular bundles (VB) and the outer cortex (OC). In the IR (C and D), GUS staining is observed in both infected and uninfected cells including within the enlarged infected cell nucleus (N). GUS signal was less intense in those tissues receiving a GA treatment. Images are representative of multiple nodules treated with this experiment. 75

Figure 4. 5 Maps of vector pAbAi and vector pGADT7-Rec used for Yeast One-Hybrid promoter screening. (A) The pAbAi was used for constructing transgenic yeast strains with the promoter construct of interest and to provide AbA resistance. (B) The pGADT7-Rec was used for constructing the cDNA library from soybean nodules. Soybean nodule cDNA was ligated into pGADT7-Rec and the collective library of ligated cDNAs transformed in promoter:pAbAi transformed yeast. 76

Figure 4. 6 The growth of serial-diluted cultures of AbA resistance yeast lines, with *GmbHLHm1* promoter inserted in the genome. Serial diluted cells were plated onto solid yeast media (SD, leu, AbA²⁵⁰) and grown for 5 days at 28°C. 77

Figure 4. 7 The growth of serial-diluted cultures of AbA resistance yeast lines, with *GmAMF3* promoter inserted in the genome. Serial diluted cells were plated onto solid yeast media (SD, leu, AbA²⁵⁰) and grown for days at 28°C. 78

Figure 5. 1 Structure of *LjbHLHm1.1*, the LORE1 insertion site and genotyping result of line 30056892. (A) The LORE1 insert was in the second exon of the *LjbHLHm1* gene (Plant ID: 30056892). (B) Genotype analysis of 1st generation seedlings from Lotus Base seed. Primer combinations (LJPrimer F and LJPrimer R) were used to identify plant lines with or without the LORE1 insertion (565 bp products would identify genomic sequences without a LORE1 insertion). Primer combinations (LJPrimer F and LORE1-LC2-rev) were used to amplify the 5'-flanking DNA region at the insertion site. A positive PCR for LORE1 will amplify a 414 bp product. (C) PCR confirmation of homozygous plants with primers (LJPrimer F and LJPrimer R). Putative homozygous lines were examined using PCR with 5 min extension cycles. A positive PCR result is a band that is 5406 bp in size. 95

Figure 5. 2 The *LORE1* insertion in *LjbHLLHm1.1* disrupts gene expression (line 30056892). (A) *LORE1* insertion could be on one allele (heterozygous) or both alleles (homozygous, the *bhlhm1.1* mutant). (A) The *LORE1* insertion can be observed to disrupt *LjbHLLHm1* mRNA expression in both heterozygous and homozygous lines relative to the wild-type control. (B) The relative expression of *LjbHLLHm1* in nodules of wild-type and homozygous *bhlhm1.1* lines. The expression of *LjbHLLHm1* levels was normalized with *UBI* as a reference gene and was calculated using the $2^{-\Delta\Delta C_t}$ method (Libault et al., 2008). Values were means \pm SE (n=4) biological replicates. The * indicates the significant differences compared to wild-type based on the T-test ($P < 0.05$).
 96

Figure 5. 3 GA responsive elements in the promoter region of *LjbHLLHm1.1*...... 97

Figure 5. 4 Contrasting expression of *LjbHLLHm1.1* in nodules and roots of wild-type plants. *LjbHLLHm1.1* mRNA expression is measured in (A) separated nodules and roots or (B) Four-month-old wild-type plants were treated with/without 4ppm GA₃ (10⁻⁶ M) at 10 am followed by nodule harvests at 1, 3, 6, 24 and 48 h after treatment. The expression of *LjbHLLHm1.1* was normalized with *ubiquitin* as a reference gene and was calculated using the $2^{-\Delta\Delta C_t}$ method. Values were means \pm SE (n=4) of four biological replicates. 98

Figure 5. 5 The effects of long-term GA application on *Lotus japonicus* nodule and shoot growth. (A) Shoot height, (B) shoot dry weight, (C) nodule dry weight, and (D) nodule number per plant after 3 weeks of growth in the presence/absence of 10⁻⁶ M GA₃. At three months, plants were treated with/without GA₃ for three weeks. Values are means \pm SE (n=4). Values with different letters indicate significant differences between the treatments based on the two-way ANOVA ($P < 0.05$). 99

Figure 5. 6 *Lotus japonicas* phenotypes influenced by extended GA₃ treatment. Phenotypes of wild-type, heterozygous and homozygous *bhlhm1.1* mutant plants after 3 w (A) and 5 w GA₃ treatment. Seedlings were grown for 90 d in river sand and watered every day or supplied with B&D nutrient solution (Broughton and Dilworth 1971) containing 5 mM KNO₃ three times a week. The 10⁻⁶ M GA₃ solution was directly applied into pots every 48 h..... 100

Figure 5. 7 *Lotus japonicas* nodule size of wild-type, heterozygous and homozygous *bhlhm1.1* mutant plants with/without GA₃ treatment. 4ppm GA₃ was applied to 90 d old plants for 3 weeks. A random selection of nodules is presented from each treatment. 101

Figure 5. 8 Nodule cross-sections of wild-type, heterozygous and homozygous *bhlhm1.1* mutant plants with/without GA₃ treatment. The pink-to-orange area inside the nodule is the effective nitrogen fixation area. 90 d plants were treated with/without 4ppm GA₃ for 3 weeks and nodules were harvested and sectioned. 102

Figure 5. 9 NH₄⁺ concentration in *L. japonicus* GA₃ treated nodules. Nodulated 90 d plants were treated with/without 4ppm GA₃ for up to 3 weeks. Concentrations of NH₄⁺ were measured

in nodules by ammonium assay. (A) Reduced NH_4^+ in GA_3 treated nodules after 3 w. (B) Four-month-old nodules were treated with/without 4ppm GA_3 at 10 am, and four biological repeats for each treatment were harvested after 1, 3, 6, 24 and 48 h. Values are means \pm SE (n=4)..... 103

Figure 5. 10 The design of LORE1 genotyping primers. Forward and reverse primers are designed using Primer 3 and are located at least 100 and 200 bp away from the LORE1 insertion site, respectively. The LORE-LC2-rev primer binds to a region 264 bp downstream of the LORE1 5' LTR. Figure edited from Mun et al. (2017)..... 104

List of Tables

Table 4. 1 Identified soybean nodule cDNAs isolated through interactions with the promoter of <i>GmbHLHm1</i> in transgenic yeast (Aureobasidin A resistant). The BLAST result was generated using Phytozome (https://phytozome-next.jgi.doe.gov). The assembly version is <i>Glycine max Wm82.a4.v1</i>	79
Table 4. 2 Soybean nodule cDNAs were identified to bind to the <i>GmAMF3</i> promoter. The blast result was conducted using Phytozome (https://phytozome-next.jgi.doe.gov). The assembly version <i>Glycine max Wm82.a4.v1</i>	80
Table 4. 3 List of Primers for <i>GmbHLHm1</i> promoter-GUS construct editing.....	81
Table 5. 1 Information of <i>LORE1</i> lines and Primers for genotyping.....	105
Table 5. 2 PCR cycles for genotyping (A) and conformation (B).....	106
Table 5. 3 Genotype interpretation from gel electrophoresis results.....	107
Table 5. 4 Primers used for Real-time quantitative PCR.....	108
Table 5. 5 The reaction solution for ammonium assay.....	109
Table 5. 6 The survival seedling number and death rate of different genotypes (Line 30056892) with/without N supply	110

I. Abstract

The *GmbHLHm1* is characterized as a basic Helix-Loop-Helix membrane (bHLHm) DNA-binding transcription factor localized on the symbiosome cellular membrane. It plays a significant role in enhancing the function of NH_4^+ transporters (AMFs) and regulating the expression of nitrogen transporters (NRTs). To investigate the function of *GmbHLHm1* in nodulation via root hair infection and nitrogen fixation, in Chapter 2, the impact of RNAi silencing and overexpression of *GmbHLHm1* in soybean nodules was studied. RNAi-Silenced *GmbHLHm1* transgenic hairy roots led to reduced nodule size, nodule number, nitrogen fixation rate, and impaired plant growth. Overexpression of the *GmbHLHm1* significantly induced the nodule size, nodule dry weight, nitrogen fixation rate, and enhanced plant growth. These results indicate that *GmbHLHm1* plays an important role in nodulation and symbiotic nitrogen fixation. Interestingly, soybean grown with non-nodulated, RNAi-silenced *GmbHLHm1* transgenic hairy roots showed enhanced shoot growth with an exogenous N supply.

GA (gibberellic acid) responsive elements and Auxin-responsive elements were discovered in the promoter area of *GmbHLHm1*, indicating the potential role of these two phytohormones in regulating the expression of *GmbHLHm1* in soybean nodules and roots. The effect of GA and auxin on *GmbHLHm1* expression in nodules and how the expression affects plant growth and nodule development were studied in Chapter 3. With GA treatments, *GmbHLHm1* expression was reduced after 1h of supply but recovered after 3h. While the ammonium level and ARA (Acetylene reduction assay) of nodules did not significantly change within 48 h of the GA treatment. Long-term GA had a structural impact on the nodule, such as reduced nodule size and fixation area, leading to the reduced expression of *GmbHLHm1* and nitrogenase activity. Longer-term GA application promoted shoot height on both the wildtype and RNAi-Silenced *GmbHLHm1* transgenic hairy roots, indicating that induced shoot height is independent of *GmbHLHm1* expression in roots.

Auxin regulates nodulation by controlling cell cycle reactivation, vascular tissue differentiation, and rhizobial infection. In this study, short-term IAA (indole-3-acetic acid) treatments did not affect the *GmbHLHm1* expression in nodules. Extended IAA treatments induced *GmbHLHm1* expression and enlarged nodules, while not changing the nodule biomass at the whole plant level. IAA treatment on *GmbHLHm1*-silenced nodules showed induced nodule size but not an increase in the nitrogen fixation area, indicating that auxin only improves the size of nodules, not the nitrogen fixation capability.

Promoters play an important role in regulating the expression of *GmbHLHm1* in soybean nodules. Understanding the role of each GA-responsive element in the promoter region helps understand the regulation mechanism of GA in *GmbHLHm1* expression. Three GA-responsive elements were examined by editing and functional testing in soybeans (Chapter 4). None of the edited *GmbHLHm1* promoters was shown to be expressed in roots and nodules, indicating each of the GA-responsive elements was important for the *GmbHLHm1* expression. The *GmbHLHm1* promoter was mainly targeted to the infected cells and the nucleus of those cells. The GA treatment reduced the expression of the *GmbHLHm1* in the infected region and repressed *GmbHLHm1* expression in most of the outer layer cells.

GmAMF3 (Ammonium Major Facilitator 3) was suggested to behave as an NH_4^+ permeable transport protein, dominantly expressed in nodules, with *GmbHLHm1* as a potential transcription factor (TF) of *GmAMF3*. Investigating potential genes bind to the promoter of *GmbHLHm1* and *GmAMF3* initiates the study of the potential signalling cascade of the *GmbHLHm1*-AMF3 regulation model. Yeast One-Hybrid experiments were performed to investigate genes that interact with the *GmbHLHm1* and *GmAMF* promoters. Five annotated proteins were found to interact with the promoter of *GmbHLHm1*, and eleven for *GmAMF3*. These proteins include proteins related to both nodulation and symbiotic nitrogen fixation processes, membrane-localized proteins, and proteins related to important processes in plant development. Further studies are required to investigate the function of each protein and the pathway interacting with these promoters respectively.

Lotus japonicus is a well-characterized model legume. To understand the role of bHLHm1 in *L. japonicus* nodulation and nitrogen fixation, a homolog of *GmbHLHm1*, *LjbHLHm1.1*, was

identified and studied. The *LORE1* line with disrupted *LjbHLHm1.1* expression was used to investigate the function of the *LjbHLHm1.1* in nodule and plant development. With interrupted *LjbHLHm1.1* expression, plants were unable to grow healthy nodules, sterile, sensitive to nitrogen supply, had nitrogen deficiency symptoms, and a shorter lifespan, indicating the *LjbHLHm1.1* expression plays an important role in *L. japonicus* growth and nodulation.

GA-responsive elements were also discovered in the promoter region of the *LjbHLHm1.1*. Is *LjbHLHm1.1*, like its homolog *GmbHLHm1*, regulated by GA? With long-term GA treatment, the expression of the *LjbHLHm1.1* was reduced in root nodules. Long-term GA treatment promoted shoot growth (height) and inhibited the nodule size and nodule fixation rate of the matured nodules. GA could still induce shoot height in *LjbHLHm1.1* knock-out plants, indicating GA regulates the shoot height independent of the expression of *LjbHLHm1.1*. A short-term GA treatment significantly induced *LjbHLHm1.1* expression from 3h which then returned to normal levels at 48h. The GA inhibition of *LjbHLHm1.1* expression could have a long-term effect by affecting the growth and structure of nodules and roots.

In summary, the *bHLHm1* participates in the regulation of nodulation and symbiotic nitrogen fixation in legume nodules. Phytohormones such as GA and IAA have regulatory effects on the expression of *bHLHm1*, nodulation, and plant development. Further studies are required for investigating the regulation mechanism of the *bHLHm1* in symbiotic nitrogen fixation, and its interaction with GA and IAA.

II. Declaration

STATEMENT OF ORIGINALITY

I hereby declare that this thesis is my own work and to the best of my knowledge and belief, this thesis does not contain material that has been accepted for the award of any other degree or diploma in any university or other tertiary institution and does not contain material published or written previously by another person, except where due acknowledgment has been made in the text.

Signature:

Date: 28th May 2023

III. Acknowledgements

First, I would like to thank my supervisor, Professor Brent N. Kaiser, for giving me the opportunity to undergo a Ph.D. in his lab. I am grateful for his patience in teaching me.

I am thankful to the Kaiser lab members for their support and friendship (Jodie, Kamal, Sonam, and Zainab). I am also grateful to the CCWF staff and students for their comradery. I would especially thank Julie for her technical support. I wouldn't have been able to complete my Ph.D. without her.

I would like to thank my friends in Australia, Shahnoosh, Li Si, Julie, Arjina, Erin, Wenjing, and Teng, who were always present and supported me along this path. I am forever thankful for their friendship.

I appreciate the help and support from the CIMMYT. My supervisor at the CIMMYT, Dr. Kanwarpal S. Dhugga, for his supervision. I appreciate the CIMMYT lab members for their help (Mario, Evan, and Augustin). And I am particularly grateful to Lu. Her involvement in the last year of my thesis was a huge help. She took the time to assist me in my experiments.

I am thankful to my friends (Jacky, Yubo, Ying, Xuecai, and Xinyao) in Mexico for their help and friendship in my life in Mexico.

I would like to thank Charles Warren, Claudia Keitel, and Margret Barbour for their support and encouragement during my annual progress reviews.

I am grateful to the Christian Rowe Thornett Stipend Scholarship, the Thomas Lawrance Pawlett Scholarship, and the University of Sydney for funding my research.

In the end, I would like to thank my families for their love and support, especially my parents and my husband.

IV. Abbreviations

ABA	Abscisic Acid
AbA	Aureobasidin A
ADP	Adenosine Diphosphate
AM	Arbuscular Mycorrhizal
AMF	Ammonium Major Facilitator
AON	Autoregulation of Nodulation
ARA	Acetylene Reduction Assay
ATP	Adenosine Triphosphate
bHLH	Basic Helix-Loop-Helix
BLAST	Basic Local Alignments Tool
CCaMK	Calcium- and Calmodulin-Dependent Protein Kinase
CDS	Coding Sequence
CK	Cytokinin
ER	Endoplasmic Reticulum
ET	Ethylene
EV	Empty Vector
GA	Gibberellic Acid
GARE	GA Responsive Elements
GFP	Green Fluorescent Protein
GUS	Beta-Glucuronidases
HPLC	High-Performance Liquid Chromatography
IAA	Indole-3-Acetic Acid
IC	Inner Cortex
IT	Infection Threads
JA	Jasmonic Acid
LB	Luria Borth
LCOs	Lipo-chito-oligosaccharides
LORE1	Lotus Retrotransposon 1
LRR	Leucine-Rich Repeat
LTR	Long Terminal Repeat
M	Molar
MA	Methylammonium
mM	Millimolar
mRNA	Messenger RNA
N	Nitrogen
N ₂	Nitrogen Gas
NCBI	National Centre for Biotechnology Information

NF	Nod Factor
ng	Nanogram
NIN	Nodule Inception
NUE	Nitrogen Use Efficiency
OC	Outer Cortex
OD	Optical Density
OEX	Over-Expression
PCR	Polymerase Chain Reaction
PM	Plasma Membrane
ppm	Parts-Per-Million
qPCR	Quantitative PCR
RNAi	RNA Interference
Rnase A	Ribonuclease A
RT-PCR	Reverse Transcription Polymerase Chain Reaction
SD medium	Synthetic Defined Medium
SM	Symbiosome Membrane
TF	Transcription Factor
TM	Transmembrane Domain
TML	Too Much Love
UPLC	Ultra-Performance Liquid Chromatography
UTR	Un Translated Region
v/v	Volume/Volume
VB	Vascular Bundles
YEM	Yeast Extract Manitol Medium
μg	Microgram
μM	Micromolar

Chapter 1 Literature Review

1.1 Introduction

1.1.1 Nitrogen use efficiency is important for agriculture.

Nitrogen (N) is a macro element required for plant growth and development. Its availability in the soil is essential to achieving high yields and quality for most crops. In most monoculture growing systems, soil N is often depleted, necessitating the use of inorganic N fertilisers to support growth. However, the efficiency of N fertilizer use by crop plants is often not optimal. In cereals, only 33% of nitrogen fertilizer was estimated to be recovered by the crop (Raun and Johnson, 1999). This NUE value is calculated on the quantity of applied N that contributes to the harvested product. Unassimilated N is a source of economic loss to the grower and a contributor to increased environmental problems through the pollution of water bodies and the eutrophication of freshwater bodies and oceans (Giles, 2005). N escape from the agricultural sector also enters the atmosphere as a significant greenhouse gas through nitrous oxide emissions (Stulen et al., 1998). The improvement of agricultural NUE is a global challenge and will be the basis of developing more sustainable approaches to expand the agricultural crop sector.

1.1.2 Legumes are improving NUE.

Legumes are important crops for their ability to produce highly valued protein-rich seeds in a nitrogen-self-sufficient manner. Most legumes form an N₂-fixing symbiosis with soil-borne bacteria called rhizobia. After entry into the root, differentiated rhizobia, called bacteroids, are

housed in specialized root organs called nodules. Within the nodule, bacteroids receive carbohydrates from the plant, and in return, the bacteroids fix N_2 in the atmosphere to NH_3 that can be used by the plant. There is a long history of rotating and mixing cropping legume plants with other crops to capitalise on the nitrogen fixation process to add nitrogen compounds into the soil (Fujita et al., 1992). The decomposition of the legume plant and its nodules provides organic nitrogen to the soil system, a N resource that other plants can use instead of N fertilisers (Peoples et al., 1995). Hence, biological N_2 -fixation provides a renewable N resource to supplement or even replace N fertilisers for sustainable agricultural production practices (Peoples et al., 1995).

1.1.3 Soybean is an important legume crop for the economy.

Soybean (*Glycine max (L.) Merr.*) is one of the most important crops in the world economy. Soybean is used in the production of plant oil, animal feed, chemical products, food and biofuels. N_2 -fixation in soybeans is widely studied. Alves (2003) reported that symbiotic fixation could supply 70–85% of the N required for the growth and development of soybean crops in well-managed fields. The symbiosis formed between soybean and *Bradyrhizobium japonicum* can fix up to 337 kg N ha^{-1} (Herridge, 1982). However, as a complicated process, nodulation involves in series of interactions, signalling and regulation processes between the host plant and rhizobium and lots of the regulatory mechanisms remain unclear. For example, drought stress, soil pH, soil N, phosphorus level, and temperature are all factors that can change the N_2 -fixation rate of soybean symbiosis (Patterson and LaRue, 1983; Chaudhary et al., 2008; Salvagiotti et al., 2008). Understanding the factors that impact the nodulation and N_2 -fixation process is of vital importance for soybean productivity and NUE improvements.

1.2 Nodulation

The development of nitrogen-fixing nodules is a complex process traditionally divided into three major stages: pre-infection, root colonisation/nodule morphogenesis, and nitrogen fixation (Sergeevich et al., 2015). The interaction between plants and microbes involves different physical and chemical cross-talking events across the rhizosphere. The process is governed by symbiotic

nitrogen fixation (SNF) genes present in plant and compatible rhizobia (Göttfert, 1993; Roy et al., 2019).

1.2.1 Symbiotic communication

The first stage involves plant-rhizobia communication through chemical release and reception. In N-limited soils, the host plant exudes flavonoids into the external rhizosphere which triggers the attachment of compatible rhizobia to the root hair cells (Cesco et al., 2010). The flavonoids stimulate the synthesis and secretion of Nod factor (NF) from symbiotic rhizobia bacteria. The NFs are lipochitooligosaccharides (LCOs), that are symbiosis specific. The NF is recognised by the plant as the Nod factor receptor and induces root hair deformation (Geurts and Bisseling, 2002).

This stage involves different gene regulation and communication between plants and rhizobia. Initially, Nod factor perception occurs through Nod factor receptor gene pairs. In *Lotus*, they are *LjNFR1* (NOD FACTOR RECEPTOR) and *LjNFR5* and in *Medicago*, *MtLYK3* (LysM RECEPTOR KINASE) and *MtNFP* (NOD FACTOR PERCEPTION) (Limpens et al., 2003; Radutoiu et al., 2003). These genes encode LysM-type protein domain receptor kinases and induce a calcium flux which leads to a membrane depolarisation (Limpens et al., 2003). Then a transmembrane Leucine-rich repeat (LRR) receptor-like kinases in the plasma membrane perceive the addition of the nod factor signal (Endre et al., 2002). Several minutes later the signal is processed via the action of nuclear channels, inducing a cytosolic calcium spiking, activating chimeric Ca²⁺/calmodulin (CaM)-dependent protein kinases (CCaMK) (Lévy et al., 2004; Mitra et al., 2004). Finally, nodulation initiation is achieved by activating the transcriptional networks via the nodulation signalling pathway (Oldroyd and Downie, 2004; Sergeevich et al., 2015).

1.2.2 The infection thread elongation

During the second stage, root hairs curl by changing growth direction and entrapping rhizobia bacteria within the curl (Batenburg et al., 1986). The nodulation FLOTs (flotillin-like genes), *MtFLOT4* (in *Medicago*) and *GmFLOT2/4* (in *Glycine max*), accumulated at the tips of root hairs within 24h of inoculation with rhizobia (Haney and Long, 2010; Qiao et al., 2017). The *Mtflot4* silenced mutant resulted in fewer ITs (Infection threads), indicating that this gene is responsible for IT initiation and elongation (Haney and Long, 2010; Xie et al., 2012).

NF induces the growth and elongation of the infection thread from the trapped rhizobia. This process requires plant cell wall modification and degradation, enabling the infection thread to migrate through cell layers and eventually burst through cortical cell walls and release rhizobia into the cytoplasm. The infection thread is a special structure generated by the invagination of the plant cell membrane, covered with the plant-derived cell wall, and filled with a matrix produced by both plant and bacteria. In *L. japonicus*, the *LjNPL* (NODULE PECTATE LYASE) was shown to be responsible for the degradation of pectin and polygalacturonic acids (Xie et al., 2012). The defective mutants, *npl*, produce small, non-functional nodules (Xie et al., 2012).

While the infection thread grows, NF signalling also activates the division of pericycle and cortical cells, which form the nodule primordium. Infection threads grow toward the base of the root hair cell and subsequently across the epidermis towards the nodule primordium (Perret et al., 2000).

1.2.3 The bacteria invasion and nodule organogenesis

In the third stage, rhizobia bacteria (now called bacteroids) are released from the IT inside inner cortical cells when they reach the nodule primordium. The released bacteroids are encircled by a plant-derived plasma membrane forming the symbiosome. The plant-rhizobium bacteria partnership develops into a fully functioning nodule with the capability to fix nitrogen (Mylona et al., 1995). In order to generate functional nodules, and accommodate the symbionts, infected meristematic cells in the nodule differentiate into polyploids and facilitate the development of the complete structure of the mature nodule (Roy et al., 2019). *MtCCS52A* is responsible for endoreduplication during infected cell differentiation (Vinardell et al., 2003). The KNAT3/4/5-like *class 2 KNOX* transcription factors are involved in nodule morphogenesis (Di Giacomo et al., 2017). The *NODULE ROOT* and *COCHLEATA* genes in the *M. truncatula* are essential in maintaining the root nodule identity throughout the nodule development (Couzigou et al., 2012).

1.3 Structure of mature nodules

The nodule consists of multiple cell types, including the epidermis, vascular bundles, outer cortex, and inner cortex. The inner cortex is where bacteroids reside inside symbiosomes (Oldroyd et al.,

2011). The symbiosome membrane (SM) is a plasma-membrane-derived plant membrane surrounding the bacteroid. It is an important signal and nutrient exchange membrane between plants and bacteroid (Udvardi and Poole, 2013). Mature legume nodules are classified into two different types according to their inner structures (Ferguson et al., 2010; Kohlen et al., 2017). As cell division initiates in the pericycle, the indeterminate nodules emerge from the inner cortex (Hadri et al., 1998). The mature indeterminate nodules are differentiated into four functional zones: the meristem zone, infection zone, nitrogen fixation zone, and senescence zone. The structure leads to an elongated shape and a developmental gradient (Hirsch, 1992). The persistent meristem maintains the nodule in sustainable growth, successive differentiation, and continuous nitrogen fixation status, while the inactive cells are all “pushed” to the senescence zone. *Medicago sativa* (alfalfa), *M. truncatula*, and *Pisum sativum* (pea) all develop indeterminate nodules (Gage, 2004). For determinate nodules, cell division starts from the inner cortex (Hadri et al., 1998). The mature determinate nodule consists only of the nitrogen fixation zone, which eventually becomes the senescence zone of the nodule (Hirsch, 1992). In determinate nodules, there is no developmental gradient of cell types due to the lack of persistent meristem. *Glycine max* (soybean), *Vicia faba* (bean), and *L. japonicus* are important legume materials for determinate nodule research (Hirsch, 1992; Gage, 2004; Kohlen et al., 2017).

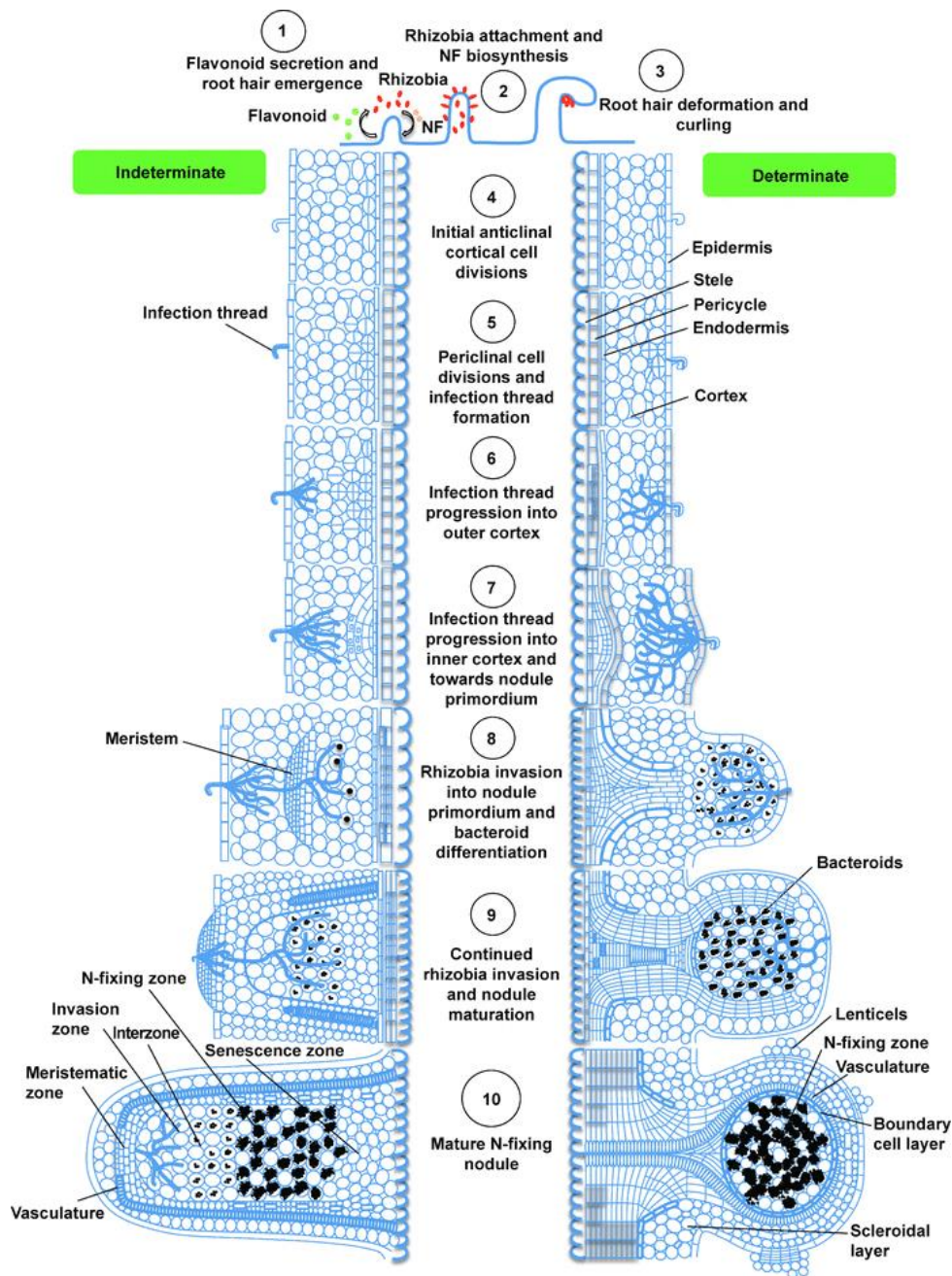


Figure 1. 1 The organogenesis of determinate and indeterminate nodules. Steps 1 and 2 illustrate the first stage, steps 3-8 illustrate the second stage, and steps 9-10 demonstrate the third stage. The structures of the determinate and indeterminate nodules are shown in the bottom part of the picture. The picture was modified from Ferguson et al. (2010).

1.4 Autoregulation of nodulation

Bacteroids fix atmospheric N_2 into NH_3 which is released and assimilated by the host legume. The delivery of NH_3 occurs through the exchange of plant-derived carbohydrates. For host plants, this is an expensive way to obtain nitrogen based on carbon allocations. The symbiotic nitrogen fixation process is tightly controlled by the levels of nitrogen in the soil environment, decreasing when soil N is sufficient for plant growth and development. The host plant optimises this process via the autoregulation of nodulation (AON). AON involves long-distance signalling between the shoot and root acting to develop the level of nodulation, inhibiting unnecessary nodule development when soil N is high. Papparozziz (1991) discovered that the removal of nodules on soybean results in the creation of newly formed nodules, which is consistent with the study from Nutman (1952). Furthermore, it was observed that the newly developed nodules are not the result of new bacteria invasion but developed from previous infections. Many infections appear to be paused at the early stages of development around the younger root hairs by previously established nodulation signals. Once the signal is interrupted, the paused infections become active and start to develop nodules (Caetano-Anollés et al., 1991). Root–shoot grafts of wild-type plants and super-nodulating mutants demonstrated that AON involves long-distance signalling between root and shoot. Grafting a super-nodulation mutant (*nts382*) shoot with a wild-type root results in a super-nodulating phenotype, while the opposite graft results in a wild-type phenotype (Olsson et al., 1989; Caetano-Anollés et al., 1991).

AON is accomplished by complicated regulating mechanisms involving different genes and regulatory factors in plants. Studies have revealed some modules of AON at the molecular level. In 2013, Takahara et al. (2013b) demonstrated that a root regulator, *TOO MUCH LOVE (TML)*, is a repressor of nodulation. Tsikou et al. (2018) revealed that a microRNA *miR2111* translocates from shoot bud to root, negatively regulating the expression of the *TML*. Gautrat et al. (2020) discovered a CEP/CRA2 pathway positively regulating the nodulation via *miR2111*. In nitrogen starving condition, root-derived CEP (C-terminally Encoded Peptide) signalling peptides is produced, interacting with the CRA2 (Compact Root Architecture 2) receptor from shoot, then promoting the expression of the *miR2111* (Mohd-Radzman et al., 2016; Gautrat et al., 2020).

The CEP/CRA2 pathway positively regulates the nodulation, while the CLE/SUNN (Super Numeric Nodule) pathway negatively regulates the nodulation via *miR2111/TML* interaction module as well. Nodule inception (NIN) transcription factor (TF) was reported to regulate rhizobial infection (Schauser et al., 1999). After the perception of the NF, the expression of NIN is activated, where NIN directly binds to the promoter and activates the expression of nodulation-related CLE (Clavata3/Embryo surrounding region) peptides in nodulated roots, including MtCLE12, MtCLE13, MtCLE35 in *M. truncatula*, LjCLE-RS1, LjCLE-RS2, LjCLE-RS3 (CLE-ROOT SIGNAL) in *L. japonicus*, PsCLE13 and PsCLE12 in *Pisum sativum* and GmRIC1, GmRIC2 (RHIZOBIUM INDUCED CLE), GmNIC1 (NITRATE INDUCED CLE 1), GmNIC2 in soybean (Krusell et al., 2002; Schnabel et al., 2005; Reid et al., 2011a; Reid et al., 2011b; Lim et al., 2014; Mens et al., 2021). CLE peptides are then transported via xylem, and recognised by the LRR receptor-like kinases, MtSUNN/GmNARK/LjHAR1/ PsCLV2 in shoot (Kinkema et al., 2006; Okamoto et al., 2009; Krusell et al., 2011; Lim et al., 2011; Reid et al., 2011b). The CLE/SUNN complex suppressed *miR2111* expression, negatively regulating the nodulation in roots via *miR2111/TML* interaction module (Gautrat et al., 2020).

Moreover, NIN/*miR172*/NNC1 was also found to be regulators of the AON (Wang et al., 2019). The *miR172c* in soybean roots is induced by infection (Wang et al., 2014). The *miR172c* and the NNC1 (Nodule Number Control1) are negative regulators of each other. Induced *miR172* suppressed the NNC1. NNC1 competitively binds to the NIN, which is important for nodule initiation, leading to the suppression of the subsequent transcriptional function of the NIN (Soyano et al., 2014). Reduced NNC1 increased functional NIN, leading to improved nodulation. This mechanism might benefit legume by avoiding over-suppression on nodulation and maintaining bistable switch of the AON (Wang et al., 2019).

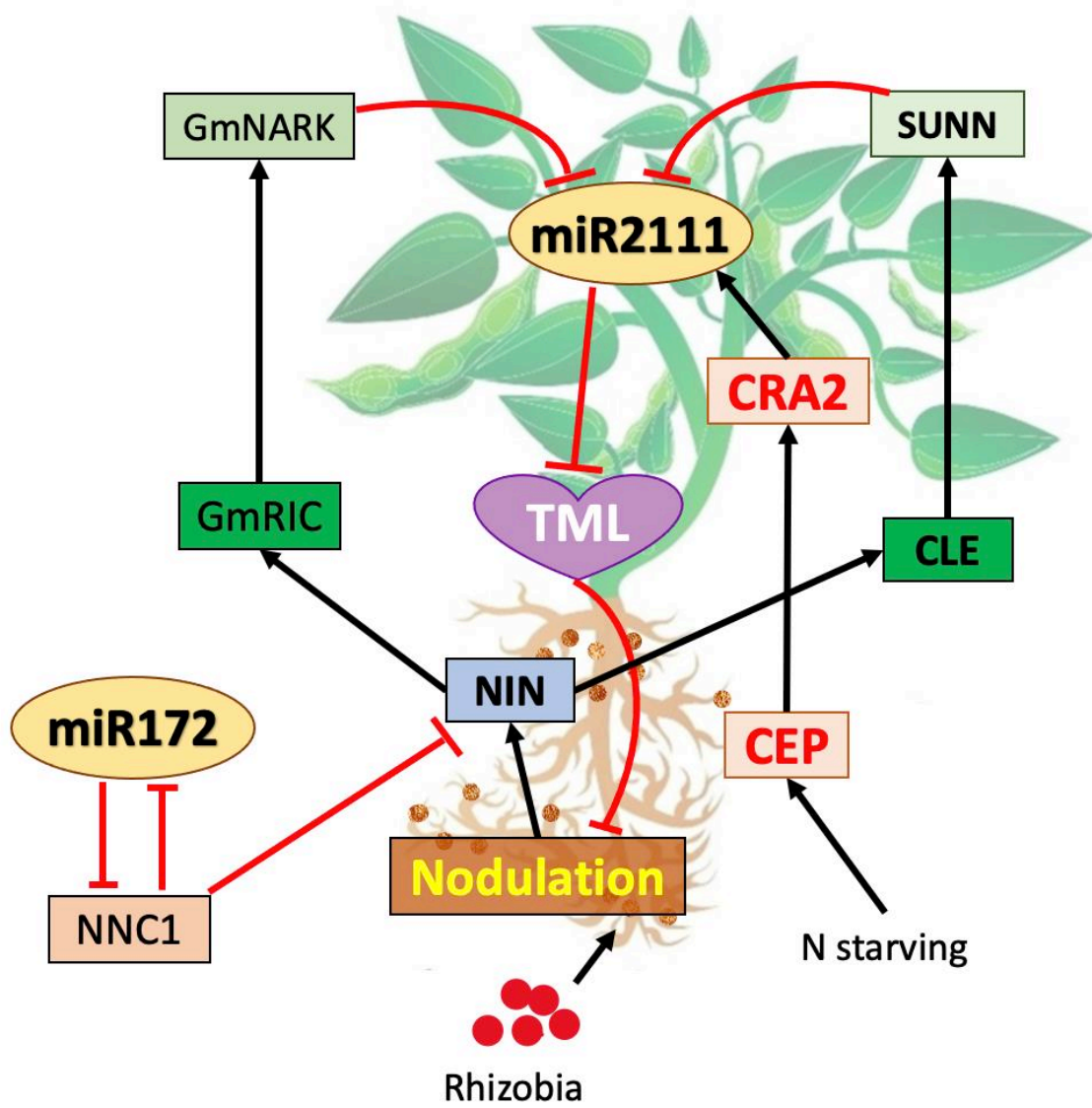


Figure 1. 2 The CEP/CRA2, NIN/CLE/SUNN and NIN/miR172/NNC1 pathway models for Autoregulation of nodulation

1.5 Phytohormone regulation of nodulation

1.5.1 Gibberellins

Gibberellins (GAs) are plant hormones that regulate cell and tissue growth and influence various developmental processes. During the “green revolution” in the mid-1960s, bioactive GAs were found to be responsible for promoting internode elongation and increased shoot height (Sasaki et al., 2002). A disruption in GA₃ synthesis and signalling resulted in dwarf, lodging-resistant, and high-yielding phenotypes (Khush, 1999; Peng et al., 1999). GA₃ synthesis and signalling are regulated via the DELLA protein, the key repressor of GA-mediated growth and development. In wheat, *Rht-B1* and *Rht-D1* alleles encode DELLA proteins and the *Rht-B1b* and *Rht-D1b* mutations are thought to confer dwarfism by producing constitutively active forms of these growth repressors (Peng et al., 1999). However, the dwarf phenotype can be overcome by the addition of an exogenous GA (Sasaki et al., 2002). A key GA regulatory module for plant growth and development, GA-GID1-DELLA pathway, is established (Xue et al., 2022). Binding of biologically active GA induces a conformational switch of the GID1 receptor, which facilitates the interaction with DELLA proteins (Ueguchi-Tanaka et al., 2007). The GID1-GA-DELLA complex stimulates polyubiquitination of DELLA by the SCF (SLY1/GID2) E3 ubiquitin ligase and then degrades by the 26s proteasome (Sasaki et al., 2003). Reduced DELLA level promotes the GA synthesis and improves plant growth (Figure 1.3).

GA₃ also affects nodulation and nodulation-related genes. The optimum level promoting nodulation varies depending on the species, stage of nodule development, and growing conditions. Exogenous GA₃ application before rhizobia inoculation inhibited nodulation in *L. japonicus* by inhibiting infection thread formation, leading to a reduced nodulation phenotype (Maekawa et al., 2009). Similarly, treatment with various GA biosynthesis inhibitors, chlormequat chloride and uniconazole-P, reduced lateral root-based nodulation in *Sesbania rostrata*, same as the application of a high level of bioactive GA (Lievens et al., 2005). A GA-deficient mutant of pea showed decreased nodulation levels. The application of 10⁻⁶ M GA₃ restored the nodulation level compared to the wild-type (Ferguson et al., 2005). Moreover, 10⁻⁹ to 10⁻⁶ M GA₃ application increased the

nodule number in wild type, while increased GA₃ level, up to 10⁻³ M decreased nodule number in both wildtype and GA deficient mutant peas (Ferguson et al., 2005).

Studies reported that the gibberellic acid 20-oxidase (GA20ox), which is crucial for bioactive GA synthesis, is upregulated during the lateral root-base nodulation (Lievens et al., 2005). Several GA biosynthesis genes, *GmGA20ox* and *GmGA3ox1*, are also reported to be upregulated during the early nodulation stage in soybean roots (Hayashi et al., 2012). Measurements of endogenous GA levels are achieved using high-performance liquid chromatography (HPLC) or ultra-performance liquid chromatography (UPLC) complemented with mass spectrometry (MS) (Dobert et al., 1992a; Dobert et al., 1992b; Satomi et al., 2014). Endogenous bioactive GA levels are found to be increased in the zone of nodulation of soybean roots, after USDA110 inoculation (Potten, 2015). High abundance of gibberellins A1, A3, A19, A20, and A44 were identified in nodules of cowpea (*Vigna unguiculata* L. Walp) and Lima Bean (*Phaseolus lunatus* L.), suggesting the early 13-hydroxylation pathway, a unique GA synthesis pathway in higher plants, predominately happens in the tissue where these compounds are synthesized (Dobert et al., 1992a; Dobert et al., 1992b; Spray et al., 1996). The study also quantified the endogenous concentration of GAs in lima bean and cowpea nodules inoculated with different rhizobia strains (Dobert et al., 1992b). The total GA content ranged from 5 to 132 ng/g dry weight for lima bean nodules, and 29 to 104 ng/g dry weight for cowpea (Dobert et al., 1992b). Akamatsu et al. (2021) reported that GA biosynthesis is activated during nodule formation, in and around the vascular bundle of nodules by constructing a pGA20ox1: GUS expressing plant. Levels of GA20, GA19, and GA44 in lima bean and cowpea nodules varied greatly with two different rhizobial strains, 127E14 and 127E15 (Dobert et al., 1992b). This result suggests that the level of bioactive GA's varies between legume species and symbiotic rhizobium (Maekawa et al., 2009). However, a mutation study revealed that both GA signalling and GA biosynthesis deficiency mutants in pea (*na*, *ls*, *lh*) and a constitutive GA signalling mutant (*NA la cry-s*) result in suppression in the number of nodules formed (Ferguson et al., 2005; Ferguson et al., 2011). It was also reported that a GA-responsive cis-acting region was discovered on the NIN promoter, indicating that endogenous GA also plays a role in optimising the rhizobial symbiosis (Akamatsu et al., 2021).

A double mutant (GA deficient and super-nodulation) pea resulted in an aberrant nodule phenotype, indicating that low GA doesn't inhibit nodule initiation but a higher GA level is required for nodule organogenesis and maturity (Ferguson et al., 2011). McAdam et al. (2018) reported consistent results in peas, that biosynthesised GA suppresses infection thread formation. Moreover, study suggested that biosynthesised GA promotes nodule organogenesis into nitrogen-fixing organs via the activity of DELLA protein. In *M. truncatula*, GA signalling mediated by DELLA1 decreases the amount of bioactive cytokinin (CK) in roots and negatively regulates the Cytokinin Response1 (CRE1)-dependent NF activation, including CK-signalling genes as well as the CK-regulated early nodulation genes (Nodulation Signalling Pathway2 and Ethylene Response Factor Required for Nodulation1). GmNMHC5, confirmed to promote the growth of soybean lateral roots and root nodules, was reported to interact with GmGAI (DELLA), and inhibit *GmGA3ox* GA biosynthesis gene through feedback-regulation, to keep GA₃ homeostasis in plants (Figure 1.3). Outcomes suggest a positive role for GAs in nodule organogenesis via DELLA protein with an appropriate concentration, too low, or too high, which are both inhibitory to the process.

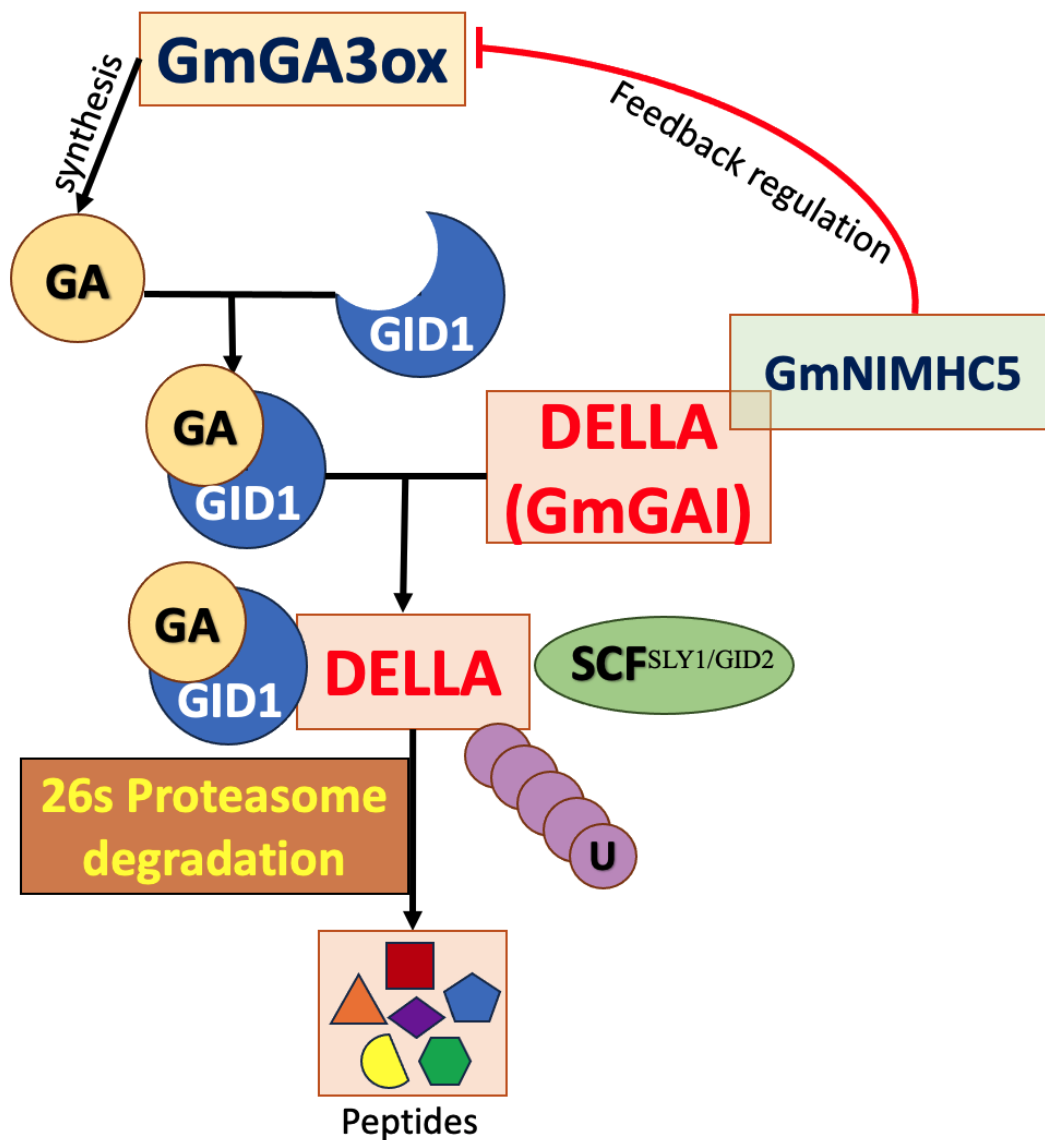


Figure 1. 3 The molecular regulation of GA signalling via DELLA

1.5.2 Auxin

Auxin is a plant hormone involved in many stages of plant development (Zhao, 2010). Indole-3-acetic acid (IAA), is the main form of natural auxins, produced by plants (Zhao, 2010). As a prerequisite for cell division competence, auxin is an important regulator of cell proliferation. The auxin also regulates embryo development, shoot apex growth, reproductive organ development, and root growth (Zažímalová et al., 2014). It was reported that an auxin gradient at the root tip

maintains the structure of the apical meristem (Grieneisen et al., 2007). This originates from the pericycle cells, where lateral root development requires the pericycle cells to maintain a capacity for division. The auxin induces cell cycle reactivation and specification in the pericycle, thus regulating lateral root initiation (Zažímalová et al., 2014).

The nodulation process is also regulated by the auxin by controlling cell cycle reactivation, vascular tissue differentiation, and rhizobial infection (Kohlen et al., 2017). The auxin positively regulates the IT (infection thread) elongation (Step 3 in Figure 1.4), which is opposite to the effect of GA, via an AUXIN RESPONSE FACTOR (MtARF16a) in *M. truncatula* (Breakspear et al., 2014). During nodule organogenesis (step 4 Figure 1.2), auxin promotes cell division via interacting with the CELL DIVISION CYCLE16 (CDC16), thus increasing nodule number (Kuppusamy et al., 2009). The acropetal auxin transport inhibition of auxin is reported important in maturation of indeterminate nodules, but not determinate nodules (Ng and Mathesius, 2018). A recent study also demonstrated that the methylation of auxin, by an IAA carboxyl methyltransferase 1 (IAMT1), promotes nodule development in *L. japonicus* (Goto et al., 2022).

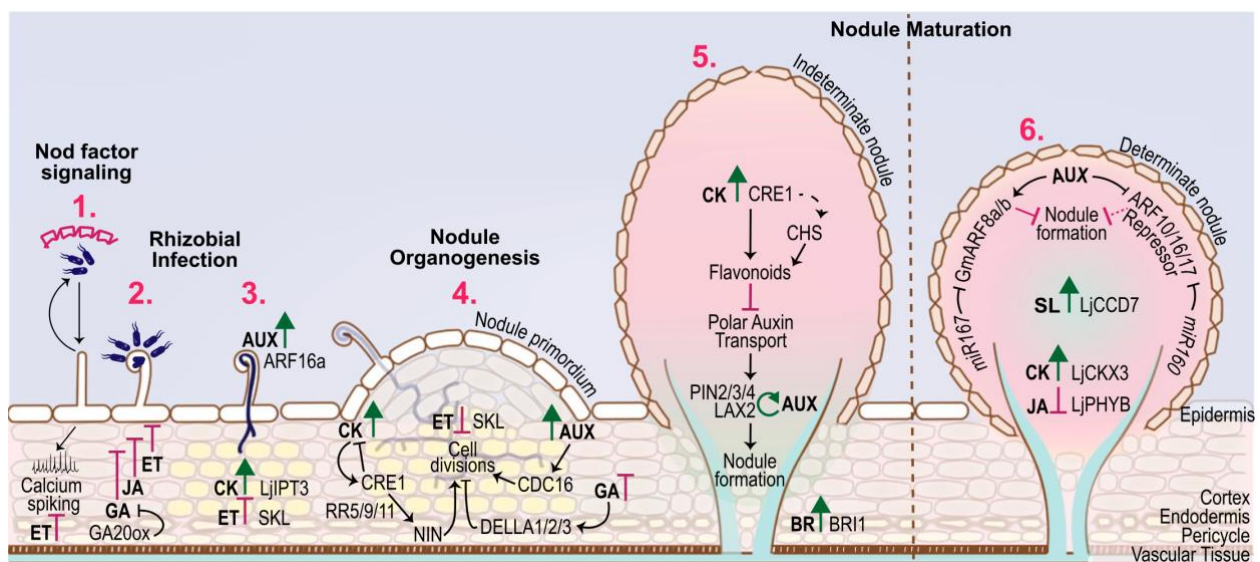
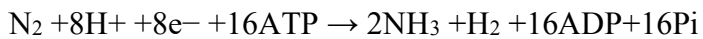


Figure 1. 4 Hormone regulation of nodulation in different stages. ET: ethylene; JA: jasmonic acid; GA: gibberellic acid; CK: cytokinin; AUX: auxin.(Roy et al., 2019)

1.6 Nitrogen fixation and N transport in the nodule

A mature nodule fixes atmospheric N₂ through the activity of the bacteroid enzyme, nitrogenase (Roberts and Tyerman, 2002; Udvardi and Poole, 2013). The chemical reaction catalysed by the nitrogenase enzyme complex is:



This reaction is oxygen liable at atmospheric concentrations (21% v/v). On the other hand, the growth and development of bacteroids require oxygen for respiration and energy metabolism. To be oxygen responsive, an oxygen diffusion barrier in the outer cortex of the nodule limits oxygen diffusion into the infected region of the nodule. This structure creates a microaerobic environment in the infected region. The reduction in oxygen concentrations results in the expression of plant-derived leghemoglobin, which assists the binding and transfer of oxygen at a high flux rate (low concentration) to symbiosomes and the enclosed bacteroids. The consistent supply of low concentrations of oxygen provides the perfect microaerobic environment to support bacteroid respiration and the generation of ATP to support the reduction of N₂ to NH₃ by nitrogenase (Udvardi and Poole, 2013).

After N₂ is reduced to NH₃ in the bacteroid, it is assumed to be protonated and released into the symbiosome space. The delivery of NH₄⁺ to the plant must involve transport across the symbiosome membrane. Biophysical studies with soybean symbiosomes have identified an NH₄⁺ transport activity (channel and/or transporter) on the symbiosome membrane (SM). The identified current is voltage-dependent, calcium rectified and specific to univalent cations, with high specificity to NH₄⁺ (Tyerman et al., 1995; Whitehead et al., 1995). There is also evidence of NH₃ transport across the symbiosome membrane (Niemietz and Tyerman, 2000).

1.6.1 The AMT family

AMT (Ammonium transporter) is a large family that exists in all plants. AMT1 and AMT2 are two main subgroups of the family. In *L. japonicus*, *LjAMT1;1* is found expressed in the leaf, flower,

and root (Rogato et al., 2008). Subcellular localization studies showed LjAMT1;1 is localised to the PM of the infected zone and vascular tissues in root cells (Rogato et al., 2008). Inhibition of *LjAMT1;1* expression resulted in a partially impaired nitrogen fixation activity (Rogato et al., 2008). LjAMT1;2 and LjAMT1;3 are found expressed in the roots and flowers (Rogato et al., 2008). Additionally, LjAMT1;3 was also characterized as an NH_4^+ sensor, which is required for root development in potentially toxic external NH_4^+ concentrations (Rogato et al., 2010). LjAMT2;1 was found targeted to the plasma membrane (Simon-Rosin et al., 2003). Yeast mutant functional complementation experiments indicate that LjAMT2.1 functioned as an NH_4^+ transporter in the possible recovery of NH_4^+ that is lost from nodule cells by efflux (Simon-Rosin et al., 2003). LjAMT2;2 is upregulated in mycorrhizal colonised roots but not in the nodule. The yeast mutant complementation experiment indicated that LjAMT2;2 functions as an NH_4^+ transporter, that is more active under acidic pH (Guether et al., 2009). LjAMT2;3 is also expressed in the mycorrhizal roots and is required for root premature arbuscular degeneration suppression (Breuillin-Sessoms et al., 2015; Hao et al., 2020).

1.6.2 The AMF family

AMF transport proteins are a recently identified low-affinity NH_4^+ transport proteins, homologous to the DHA2 drug H^+ /antiporter family, in bacterial and fungal systems (Chiasson et al., 2014). ScAMF1 and a soybean homolog (GmAMF3) were shown to transport NH_4^+ and methylammonium (MA) (Chiasson et al., 2014). Soybean contains five AMF homologous but only GmAMF3 and to a limited extent GmAMF4 and GmAMF5 have been studied. Experiments using the *GUS* reporter gene indicated that *GmAMF3* is expressed in parenchyma cells and the enveloping vascular tissue and is nodule-enhanced relative to root cells. *GmAMF4* shares high sequence similarities with *GmAMF3* (Chiasson thesis 2012) and is expressed in nodule and flower tissues. In *Arabidopsis thaliana*, three homologs exist, AtAMF1, AtAMF2 and AtAMF3, which are characterized as low-affinity ammonium transporters (Apriadi Situmorang thesis, unpublished result). AtAMF1 is localised to the ER, AtAMF2 is targeted to the tonoplast and AtAMF3 is localised to the plasma membrane. All three influence the transfer of nitrogen to developing seeds and when deleted initiate early senescence and poor N delivery to developing seeds.

1.7 GmbHLHm1 and GmAMF3

Within the infected cells of nodules, N₂-fixing bacteroids are enclosed by the symbiosome membrane, a plant-derived membrane that segregates the bacteroids from the plant cytosol and controls nutrient exchange between the symbionts. The AMFs (Ammonium Facilitators) are a group of NH₄⁺ permeable transport proteins located plasma membrane which facilitates NH₄⁺ transport. Previous results have indicated that a membrane-localised basic helix–loop–helix membrane 1 (GmbHLHm1) DNA-binding transcription factor directly binds to the ScAMF1 promoter, and plays a significant role in enhancing the function of ScAMF1 in yeast (Chiasson et al., 2014). Five AMF1 homologs are identified in soybean, and GmAMF3 is up-regulated in nodules relative to roots, which is similar to GmbHLHm1. (Chiasson et al., 2014). Loss of GmbHLHm1 expression with RNAi technology in soybean results in a reduction of nodule fitness and growth and ultimately N transfer to the shoots (Chiasson et al., 2014). The GmbHLHm1 gene encodes a DNA-binding transcription factor that is present in legumes and most other plant species where sequence data exists. The relationship between GmbHLHm1 and AMFs suggests these two proteins are important in how nodules function and ultimately their effectiveness as a plant organ to generate symbiotically fixed N. Further study is required on how GmbHLHm1 is regulated and how effective it is in nodule N₂-fixation and in maximising N₂-fixation activity in legumes of interest to Australian growers. As a nutrient-dense food and an important economic crop in Australia, the relationship between GmbHLHm1 and its role in the nodule activity of important Australian legumes such as soybean require further study.

Transcription factors (TFs) are the most important class of regulatory factors in plants and can maintain growth and development of plants. The basic/helix-loop-helix (bHLH) proteins are the second largest superfamily of transcription factors that have been well characterized in plants (Feller et al., 2011). Members of bHLH family are generally involved in aspects of plant growth and metabolism, at the same time, play an important role in plant responses to stress (Sun et al., 2018). Most transcription factors are located in the cytoplasm (Schwechheimer et al., 1998). After receiving a signal from development or stress, transcription factors are activated and then translocated into the nucleus where they interact with the corresponding DNA (Liu et al., 2018). Membrane-bound transcription factors (MTFs) are TFs that are anchored to membranes in a

dormant state and function as a TF after being translocated into the nucleus (Hoppe et al., 2001; Seo, 2014). MTFs are synthesized in the cytoplasm and are rapidly transported to the cellular membrane (Seo, 2014; Liu et al., 2018). PM proteins can be transported directly into the nucleus or via Golgi to ER retrograde trafficking, then protein fragments finally enter the nucleus (Senoo et al., 2013). *GmbHLHm1* has been confirmed as a membrane-localised DNA-binding transcription factor expressed in soybean root nodules and to a lesser extent non-nodulated roots (Chiasson et al., 2014). Immunogold labelling also revealed a signal in PM, ER, Golgi and nucleus indicating the translocation route from PM to the nucleus.

In nodules (focus on species that use root hair infection), it is localised in the nucleus as well as cellular membranes, including the symbiosome membrane, which encircles nitrogen-fixing bacteroids (Kaiser et al., 1998). In roots, *GmbHLHm1* is predominantly located in the vascular system increasing in expression when starved of nitrogen. The functional role of *GmbHLHm1* is still evolving. At present, results indicate *GmbHLHm1* may be involved in a membrane-based transcriptional network linked to a transport pathway, *ScAMF1* facilitating low-affinity ammonium (NH_4^+) transport (Chiasson et al., 2014). The genetic linkage between *GmAMFs* and *GmbHLHm1* is further emphasized by their close physical chromosomal association within 5-20 Kb of each other across most sequenced dicot species.

A link between *GmbHLHm1* expression and plant responsiveness to N has been established. Loss of *GmbHLHm1* using RNAi (*GmbHLHm1*-silenced soybean which silences both *GmbHLHm1* and *GmbHLHm2*) suppresses nodulation, nodule growth and nitrogen fixation. The loss of *GmbHLHm1* expression in non-nodulated roots results in a repression of a core set of N transporters (*AMT2*, *NRT1.7*, *NRT2.4*, *NRT2.5*, *DUR3*) each of which is often stimulated in plants under N deficiency. In contrast, loss of *GmbHLHm1* results in the overexpression of known nitrate-responsive genes (*NRT1;1*, *NI1*). This suggests a potential link between *GmbHLHm1* expression and N homeostatic responses in soybean roots, conditions which are favourable for either: 1) N scavenging, 2) nodulation and symbiotic N_2 -fixation or alternatively 3) the uptake and assimilation of nitrate by roots.

Interestingly, previous research found that (Figure 1.4) the loss of *GmbHLHm1* expression in non-nodulated soybean roots grown on NH_4NO_3 resulted in a significant increase in plant height, a

response that is similar to a nodulated wildtype soybean receiving exogenous GA₃ supply (Dehcheshmeh, 2013, unpublished result). This significant increase in plant height growth response was lost when *GmbHLHm1* expression was increased in soybean roots or when exposed to rhizobia (Dehcheshmeh, 2013, unpublished result). These observations indicate that *GmbHLHm1* and rhizobia together may influence legume development and in particular the nature by which roots respond to external N. Exposure to GA₃ reduces nodule number and growth but also causes a reduction in *GmbHLHm1* expression in nodules (Dehcheshmeh, 2013, unpublished result). GA₃ responsive elements have been identified on the promoter of *GmbHLHm1* and GA supply to soybean roots expressing a *GmbHLHm1: GUS* construct results in a reduction in GUS activity and a reduction in the native *GmbHLHm1* transcript pool (Dehcheshmeh, 2013, unpublished result). It would appear GA may act as a repressor of *GmbHLHm1*. Is there any link between GA and N signalling through the activity of *GmbHLHm1*? The question deserves further investigation.

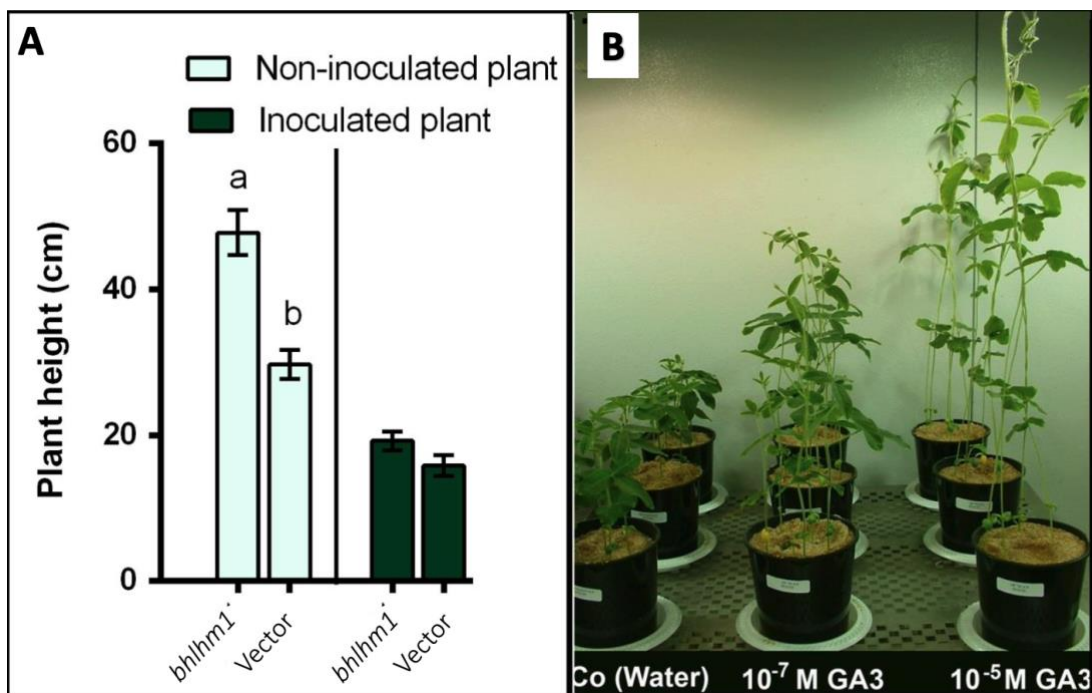


Figure 1. 5 N and GA treatment affect soybean shoot height (A) The effects of *GmbHLHm1* silencing on shoot height of inoculated plants and non-inoculated plants (supplemented with 2.5mM NH₄NO₃) (B) GA treatments significantly induced shoot height. (Dehcheshmeh, 2013, unpublished result).

Chapter 2 Functional analysis of *GmbHLHm1* in soybean roots through silencing and overexpression.

2.1 Introduction

GmbHLHm1 is characterized as a basic helix-loop-helix membrane (bHLHm) localised DNA-binding transcription factor (Chiasson et al., 2014). The intercellular localization of *GmbHLHm1* is identified on the plasma membrane (PM), endoplasmic reticulum (ER), Golgi, and symbiosome membrane (SM) and in the nucleus of infected nodule and root cells (Chiasson et al., 2014). It has a circadian expression pattern and is highly expressed during the night (Chiasson et al., 2014). The expression level of *GmbHLHm1* is enhanced in N₂-fixing nodules relative to the root (Chiasson et al., 2014). A *GmbHLHm1*-RNAi soybean mutant was found to have fewer and smaller nodules with impaired symbiosome development, indicating the function of *GmbHLHm1* to both nodulation and nodule activity (Chiasson et al., 2014). The transcriptional regulatory roles of *GmbHLHm1* suggest it behaves as a transcription factor that positively regulates the expression of the low-affinity NH₄⁺ transport protein (AMF) that is involved in NH₄⁺ transport in plant cells (Chiasson et al., 2014).

How *GmbHLHm1* affects soybean nodulation and N₂ fixation remains unclear. In this chapter, RNAi silencing and overexpression of *GmbHLHm1* were used to study the role of this gene on nodule growth and development, N₂-fixation, and overall plant growth in soybean.

2.2 Results

2.2.1 *GmbHLHm1* RNAi-silencing

To verify the expression level of *GmbHLHm1* in the RNAi mutant (*bhlhm1*) qPCR was performed on extracted total RNA from harvested roots and nodules. The results indicated that *GmbHLHm1* was more highly expressed in nodules than in roots in wild-type soybean tissues (Figure 2.2 A). *GmbHLHm1* expression levels in the transformed pK7GWIWG2D(II) empty vector (Vector) control nodules (Figure 2.2 B) showed no significant difference from that of the wild-type tissues. *GmbHLHm1* expression was significantly reduced in the *bhlhm1* nodules, compared to the Vector control, indicating that the *GmbHLHm1*-RNAi construct effectively downregulated the expression of *GmbHLHm1* in nodules (Figure 2.2 B). The pK7GWIWG2D(II) transformed plants allowed for eGFP (enhanced green fluorescent protein) expression analysis using fluorescence microscopy. Fluorescence was observed in both the transformed nodules and roots under UV light (Figure 2.3).

To study the impact of *GmbHLHm1* on soybean growth and nodulation, quantitative data on soybean development and N₂-fixation activities (acetylene reduction assay) were tested. With reduced *GmbHLHm1* expression (*bhlhm1*), the shoot height, nodule number, nodule dry weight, and N₂-fixation rate (Figure 2.4 A, B, C and D) were significantly suppressed in the *bhlhm1* plants compared to the Vector controls. Images were collected to analyse the effect of *GmbHLHm1* on the overall soybean phenotype. The leaves of *bhlhm1* plants were yellow (Figure 2.5 A). The plants growing on *bhlhm1* hairy roots tended to be short and contained fewer leaves compared to wild-type and empty *Vector* plants (Figure 2.5 A). The *bhlhm1* plants had reduced nodule numbers, nodule size (Figure 2.5 B), and a reduced effective N₂-fixation area (pink area; Figure 2.5 C) compared to wild-type and empty vector groups. These results indicate that a reduction of *GmbHLHm1* expression affects both nodulation and nodule activities which would appear to influence shoot development at this harvested stage of growth.

A previous study showed that without the *GmbHLHm1* expression, exogenous nitrogen sources significantly induced the soybean shoot height in non-nodulated soybeans (Mohammadi

Dehcheshmeh, unpublished result). To investigate soybean growth on different nitrogen sources when *GmbHLHm1* is silenced, 5mM KNO₃ or rhizobium inoculant was applied to the *bhlhm1* group, Vector group, and wild type respectively. When soybeans developed nodules while no KNO₃ was applied (Figure 2.6 A), the only nitrogen source was from the biological nitrogen fixation. The *bhlhm1* group was short and unhealthy, with less leave, compared to the Vector group and wild-type group (Figure 2.6 A), which is consistent with the result in Figure 2.5. When soybean did not develop nodules and absorbed exogenous KNO₃, the *bhlhm1* group had larger plants than the Vector and wild-type groups (Figure 2.6 B), showing a significant increase in plant shoot dry weight (Figure 2.6 D). However, inconsistent with the previous study, the shoot height of the non-nodulated *bhlhm1* group was not significantly induced with the exogenous nitrogen (Figure 2.6 C). In the wild-type group and Vector group, the non-nodulated soybean grown in 5mM KNO₃ (Figure 2.6 A) were bigger, with significantly increased shoot dry weight compared to that of the nodulated Vector group and Wild-type group (Figure 2.6 B).

2.2.2 *GmbHLHm1* Overexpression

To verify the expression level of *GmbHLHm1* in the overexpressed mutant (*GmbHLHm1* OEX) lines, qPCR was performed on total RNA extracted from root and nodule tissues. *GmbHLHm1* expression was significantly induced in *GmbHLHm1*-overexpressed nodules (Figure 2.8A). To study the effect of overexpressed *GmbHLHm1* on soybean growth and nodulation, quantitative data on soybean development and N₂-fixation rate capacity were collected. Shoot height and nodule number per plant were not affected by the higher levels of *GmbHLHm1* expression in the nodules and root tissues (Figure 2.8 B and C). However, nodule DW, N₂-fixation rates measured through acetylene reduction assays and the ultimate %N in leaves were significantly increased in the *GmbHLHm1*-overexpressed plants compared to the vector control (Figure 2.8 D-F). These results indicate that the expression of *GmbHLHm1* does not influence the nodulation performance of the roots but improves nodule growth and development, promoting higher rates of nodule N₂-fixation while at the same time facilitating a higher level of N accumulation in aerial shoot tissues.

Representative images were collected to qualify the effect of *GmbHLHm1* overexpression on soybean growth. In general, the shoots were taller, and the leaves of *GmbHLHm1*-overexpression plants were bigger in appearance compared to wild-type and empty vector groups (Figure 2.9 A). The *GmbHLHm1* overexpression increased nodule size and effective N₂-fixation area (pink area) compared to wild-type and empty vector controls (Figure 2.9 B and C).

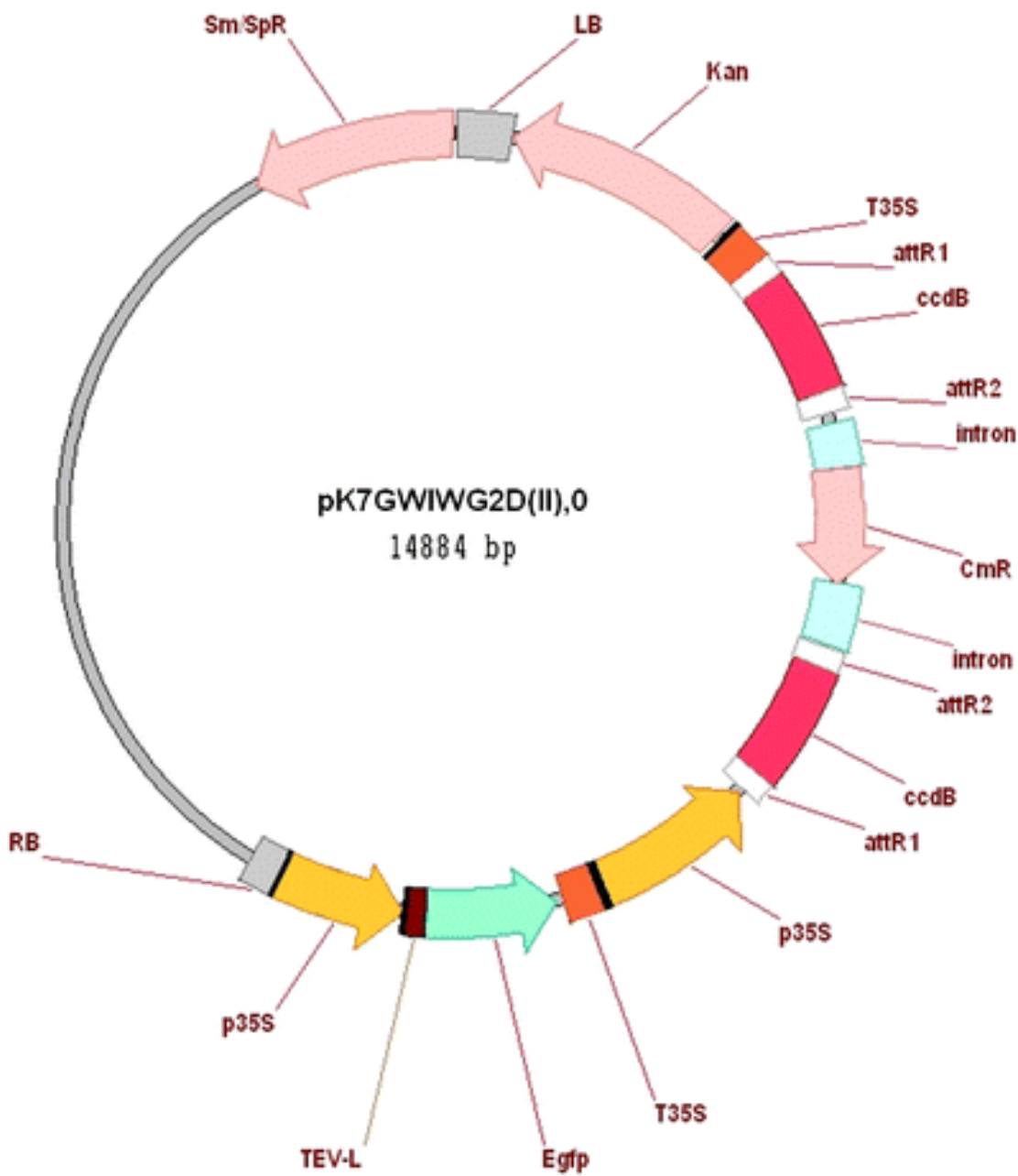


Figure 2. 1 Map of pK7GWIWG2D(II) vector used for RNAi silencing of *GmbHLHm1*. pK7GWIWG2D(II) was used in *Agrobacterium rhizogenes* K599 hairy root transformation of soybean hypocotyls (Mohammadi-Dehcheshmeh et al., 2014). The vector contains the selectable marker, *nptII*, which encodes neomycin phosphotransferase for kanamycin resistance, an enhanced green fluorescent protein (Egfp) driven by the 35S promoter (p35S) and streptomycin-spectinomycin resistance (Sm/SpR) for plasmid selection (Karimi et al., 2002).

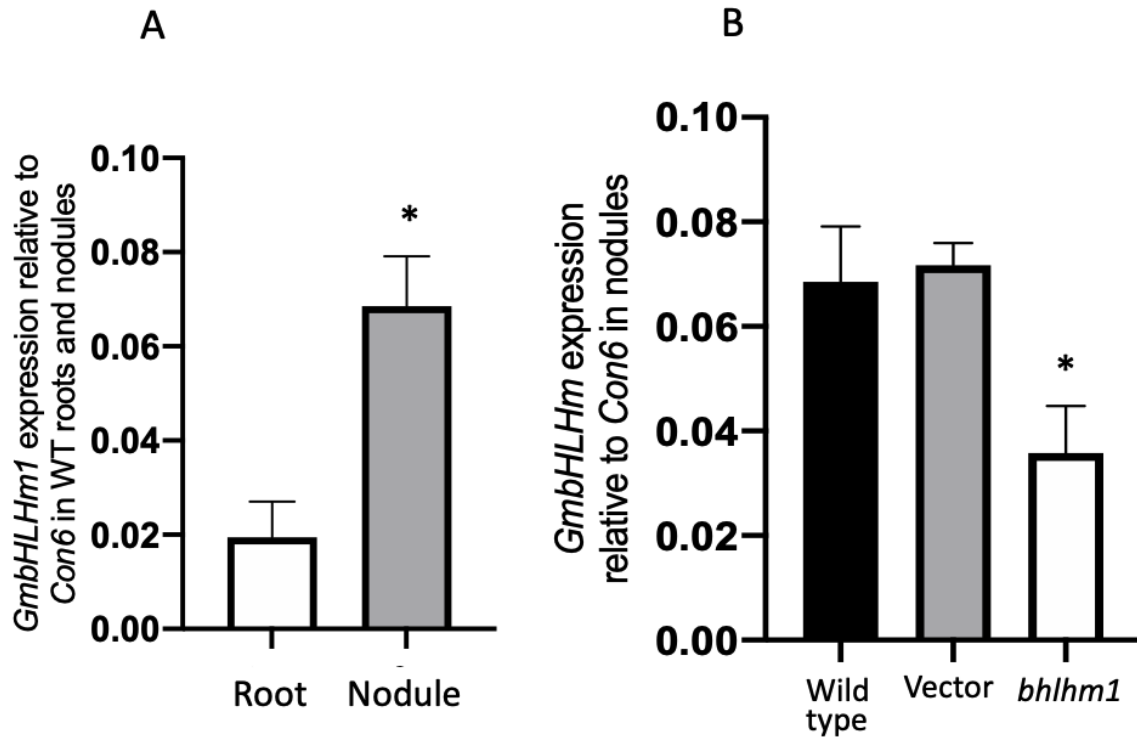


Figure 2. 2 *GmbHLHm1* expression in wild-type, empty vector (Vector), and *GmbHLHm1*RNAi-silenced mutant (*bhlhm1*) nodules and roots. Comparison of *GmbHLHm1* expression in 28 d (A) Wild-type nodules and roots. The * indicates the significant differences between groups based on the Student T-test ($P < 0.05$). (B) wild-type and transgenic nodules. The expression of *GmbHLHm1* was normalized with *Con6* as a reference gene and was calculated using the $2^{-\Delta\Delta Ct}$ method (Libault et al., 2008). Values were means \pm SE (n=4) biological replicates. The * indicate the significant differences compared to the Wild-type based on the Student T-test ($P < 0.05$).

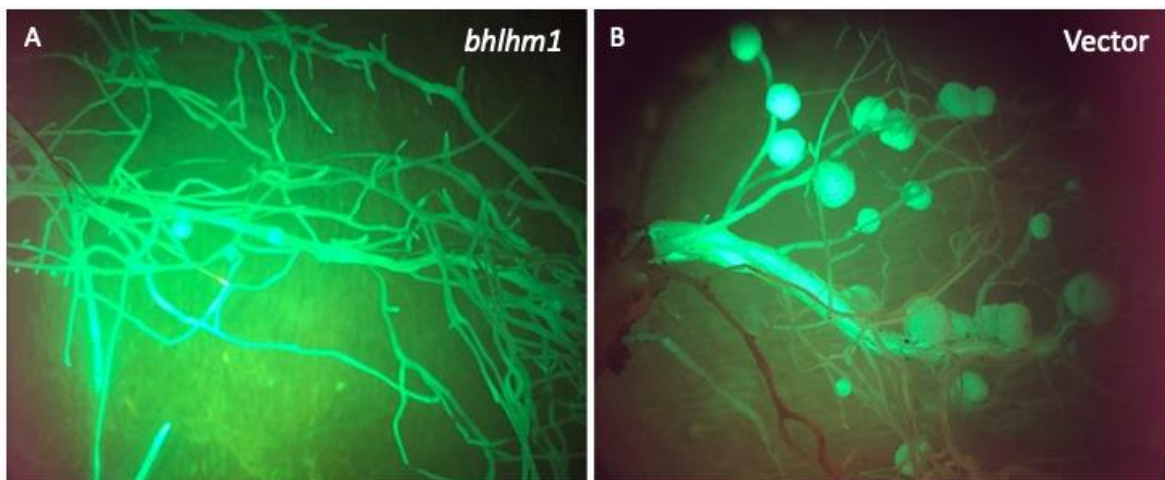


Figure 2. 3 Egfp expression in pK7GWIWG2D(II) identified in transformed hairy roots and nodules. (A) The pK7GWIWG2D(II)-*GmbHLHm1* transformed hairy roots and nodules. (B) pK7GWIWG2D(II) empty vector transformed hairy roots and nodules. Transgenic hairy roots were made according to the protocol of (Mohammadi-Dehcheshmeh et al., 2014). Soybeans were grown in a mixed matrix of quartz sand and turface (1:1 ratio). B&D nutrient solution (Broughton and Dilworth, 1971) was applied twice a day using a semi-hydroponic growing system. 28 d nodules on wild-type roots and transgenic hairy roots were harvested for experiments and for **Egfp** detection.

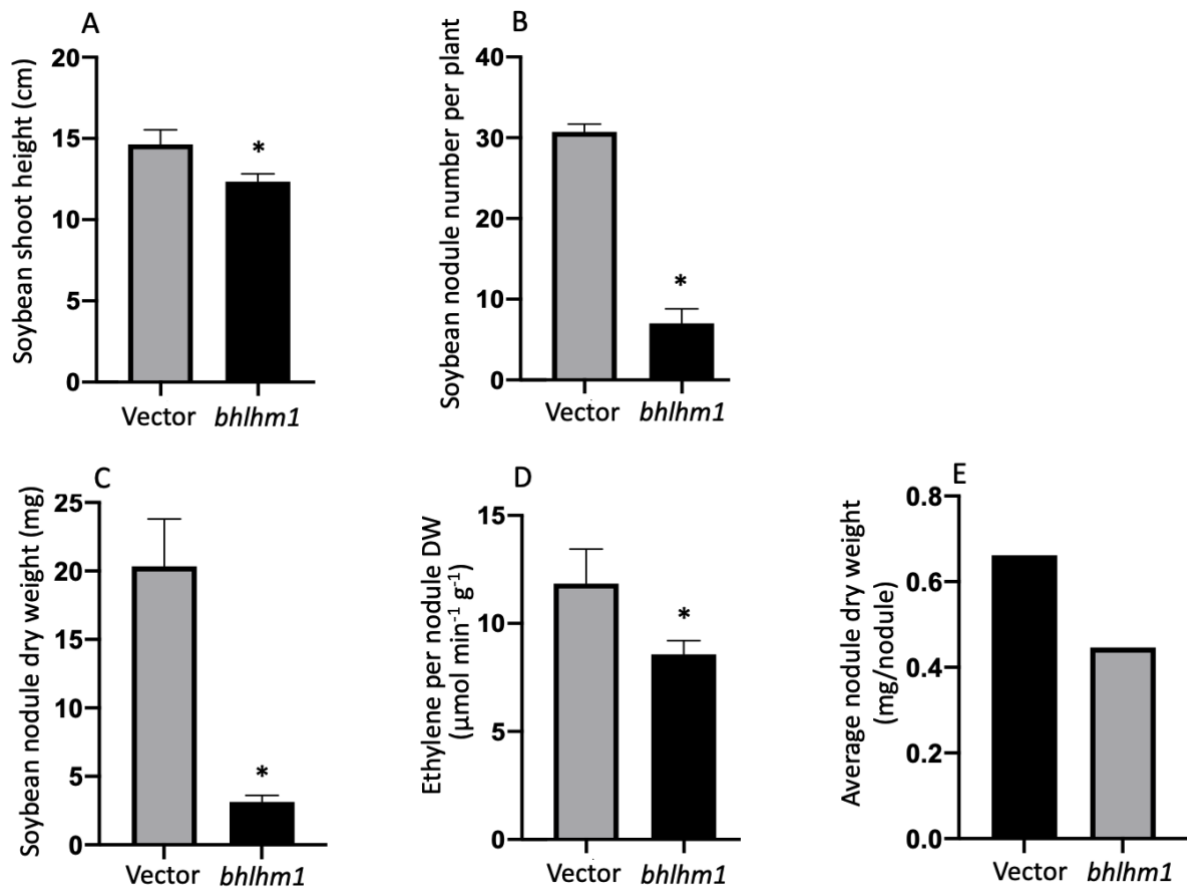


Figure 2. 4 The effects of *GmbHLHm1* silencing on shoot height, nodulation, nodule growth and nodule N₂-fixation activity. (A) Shoot height, (B) nodule number, (C) nodule DW plant⁻¹, and (D) N₂-fixation rate (Acetylene Reduction Assay) (E) Average nodule dry weight (average nodule dry weight per plant /Average nodule number per plant) of *GmbHLHm1*RNAi-silenced and empty vector (Vector) plants. Plant tissues were analyzed 28 d after inoculation with rhizobia. Values are means ± SE (n=5). Values with * indicate significant differences compared to Vector based on the Student T-test (P < 0.05).



Figure 2. 5 The effects of *GmbHLHm1* silencing on soybean growth. (A) Shoot and root phenotypes of 28-day-old empty vector, *GmbHLHm1* RNAi transformed hairy roots and untransformed wild-type plants. Representative nodules on roots (B) and nodule cross-sections (C) of wild-type, empty vector control, and *GmbHLHm1* RNAi (*bhlhm1*) soybean plants.

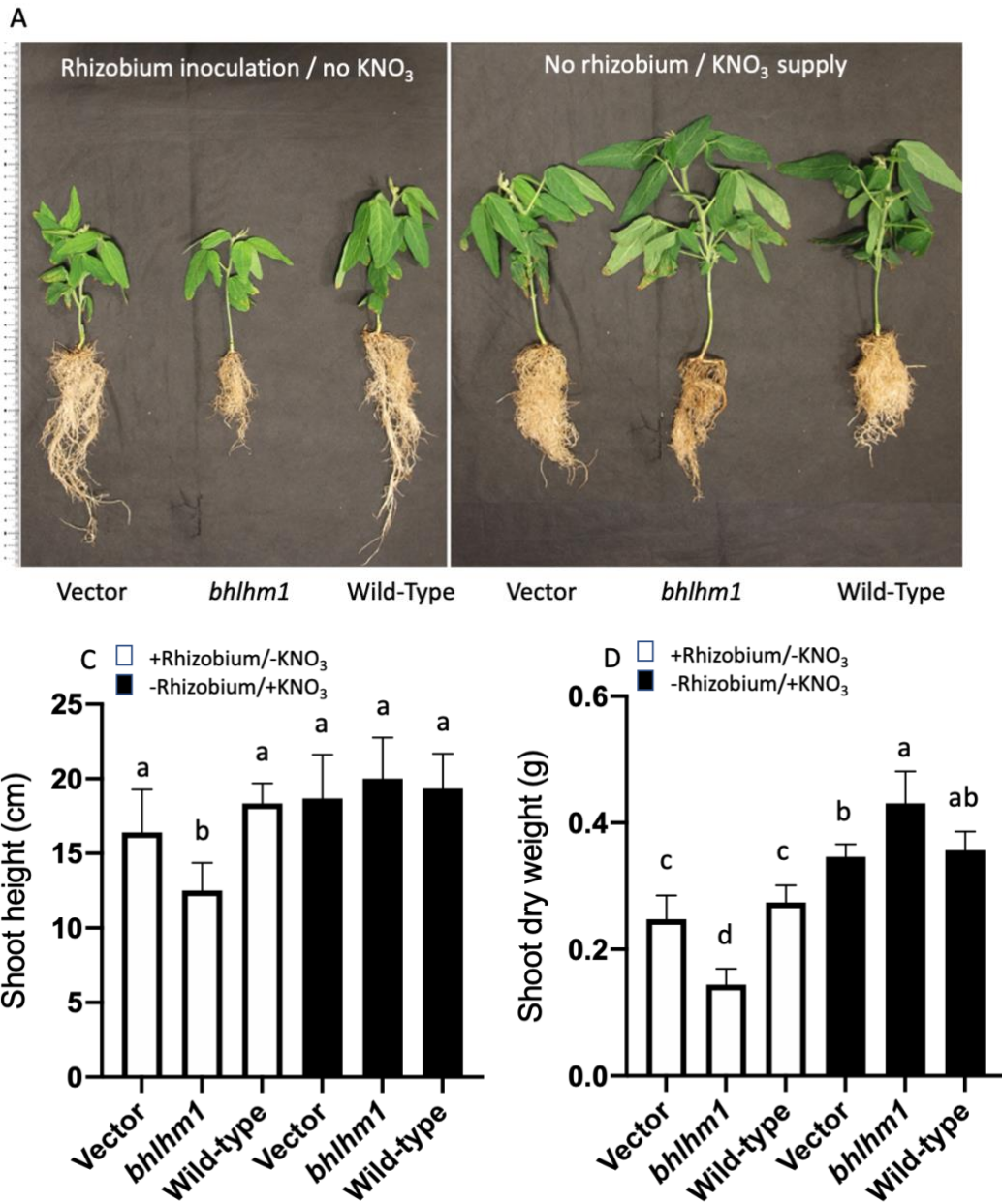


Figure 2. 6 Soybean shoot growth with/without rhizobium inoculation and exogenous nitrate. (A) Plant growth was reliant on nodule biological N₂-fixation (no supplied KNO₃) versus (B) non-inoculated plants grown solely on 5 mM KNO₃. Shoot height (C), shoot dry weight (D) of empty vector control, GmbHLHm1RNAi, and wild-type control plants supplied inoculum plus nitrate and no inoculum with nitrate. B&D nutrient solutions (Broughton and Dilworth, 1971) containing ± 5 mM KNO₃ were supplied twice a day using a semi-hydroponic system. Twenty-eight-day-old plants were harvested for all experiments. Values are means ± SE (n=5 plants). Values with different letters above each bar indicate significant differences between the treatments based on a one-way ANOVA (P < 0.05).

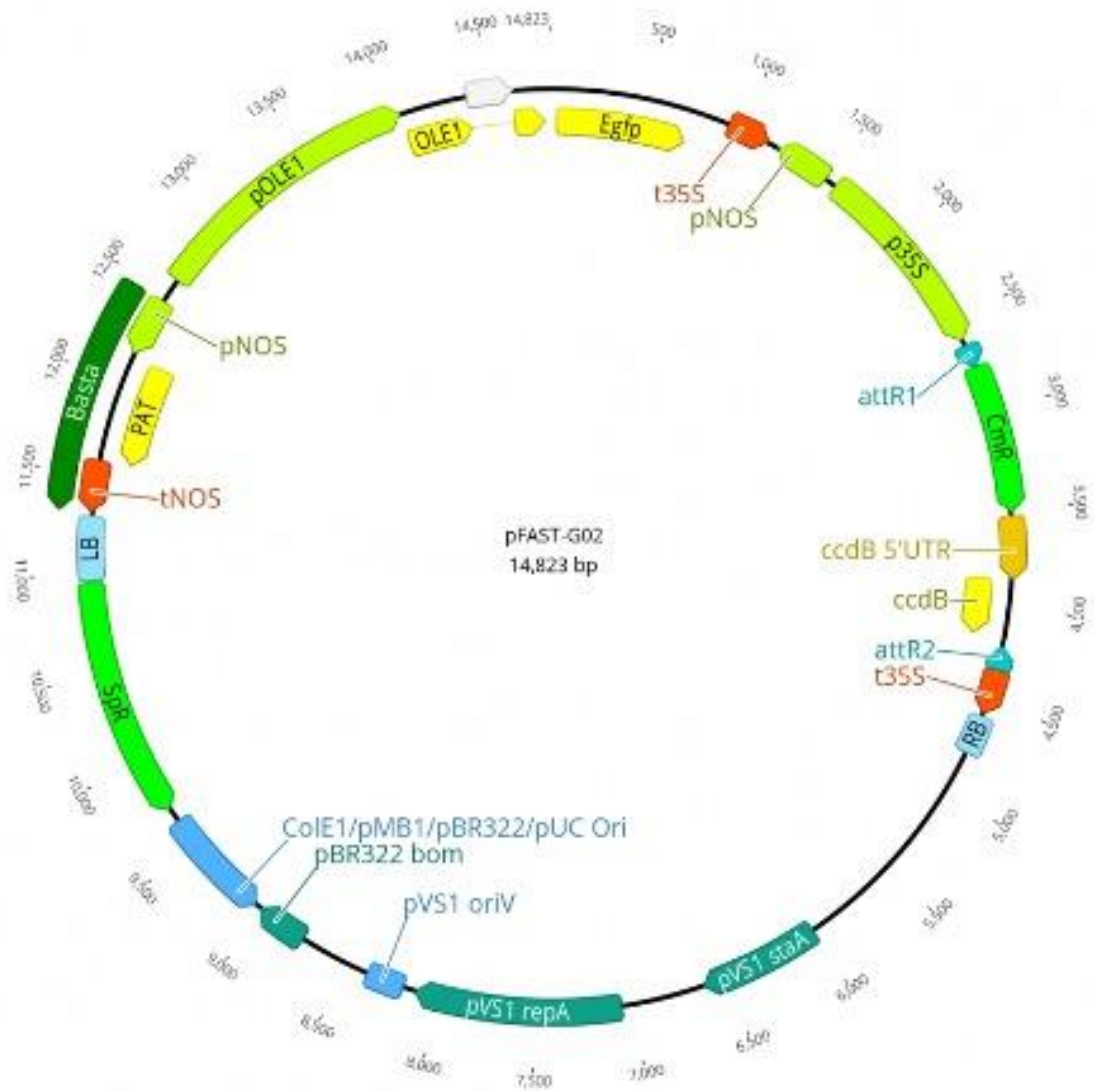


Figure 2. 7 Map of pFAST-G02 vector for gene overexpression. pFAST-G02 was used in *Agrobacterium rhizogenes* K599 hairy root transformation of soybean hypocotyls (Shimada et al., 2010). The vector contains a fusion gene encoding either GFP or RFP with an oil body membrane protein that is prominent in seeds and a marker gene for streptomycin-spectinomycin resistance (Sm/SpR) in *A. rhizogenes* (Shimada et al., 2010). Target genes of interest rely on the p35S promoter for gene transcription in planta.

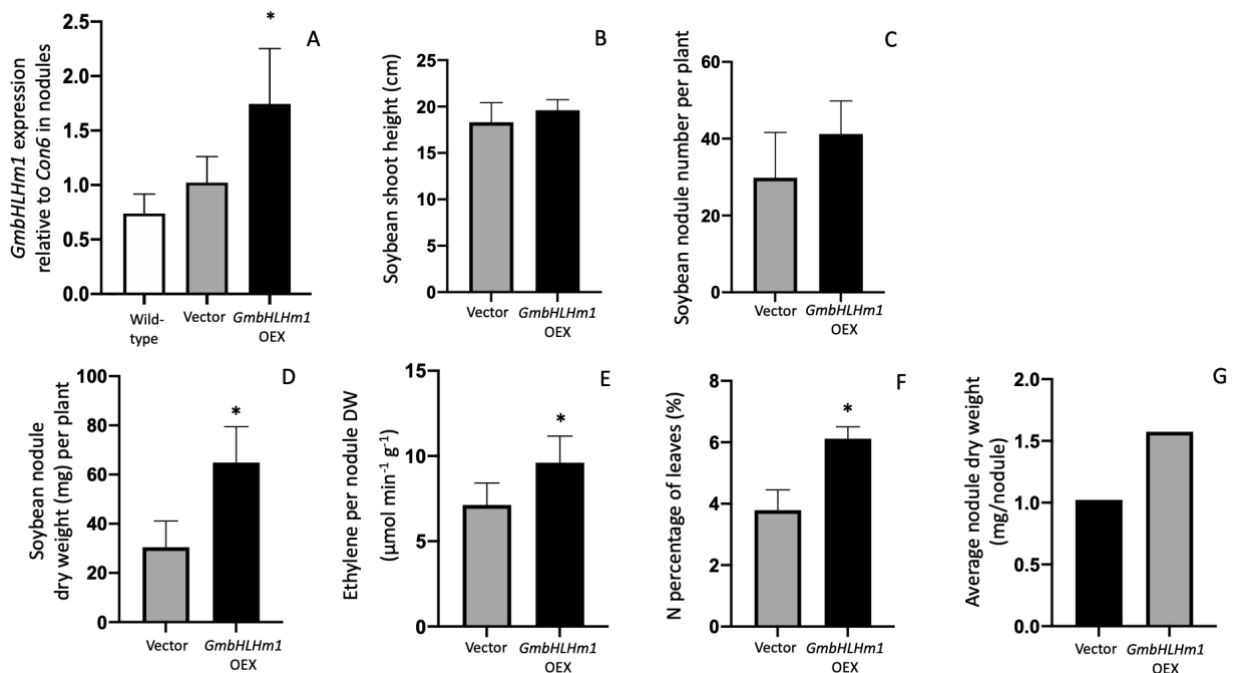


Figure 2. 8 *GmbHLHm1* expression in wild-type, empty vector (Vector), and *GmbHLHm1*-overexpressed (*GmbHLHm1* OEX) nodules. (A) Comparison of *GmbHLHm1* expression in wild-type, empty vector, and *GmbHLHm1*-overexpressed nodules. (B) Shoot height, (C) nodule number per plant, (D) nodule dry weight per plant, (E) nitrogenase activity per nodule dry weight, and (F) %N in leaves (G) Average nodule dry weight (average nodule dry weight per plant /Average nodule number per plant) of *GmbHLHm1*-overexpressed plants and the empty vector control. Transgenic hairy roots were made according to Mohammadi-Dehcheshmeh et al. (2014). Soybeans were grown in a mixed matrix of quartz sand and turface (1:1 ratio). B&D nutrient solution (Broughton and Dilworth, 1971) was supplied twice a day using a semi-hydroponic system. Twenty-eight-day-old nodules on wild-type or transgenic hairy roots were harvested for experiments. The expression of *GmbHLHm1* levels was normalized with *Con6* as a reference gene and was calculated using the $2^{-\Delta\Delta C_t}$ method (Libault et al., 2008). Values were means \pm SE (n = 4) of four biological plant replicates. The * above bars indicate the significant difference compared to wild-type (A) and /or Vector (B) to (F) based on the Student T-test ($P < 0.05$).

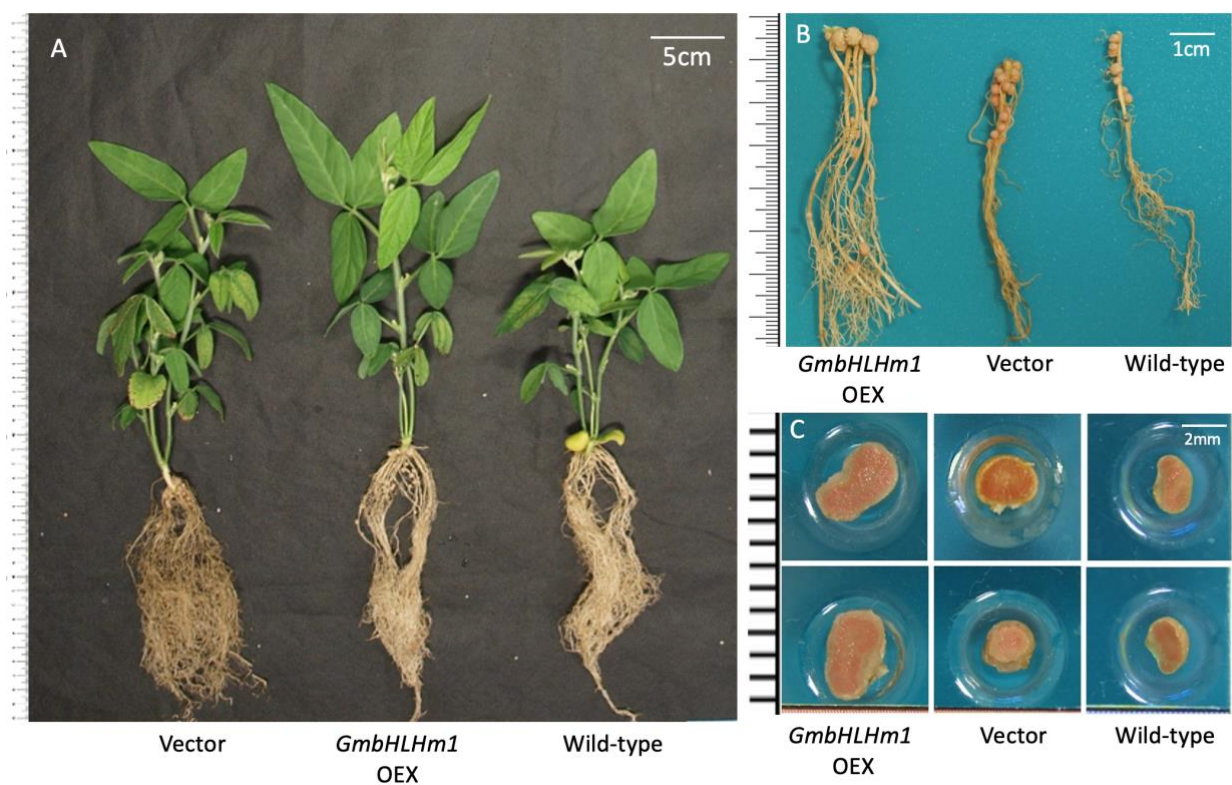


Figure 2.9 The effect of *GmbHLHm1* OEX on soybean growth. (A) Shoot and root phenotypes of 28-day-old empty vector, *GmbHLHm1* OEX transformed hairy roots and untransformed wild-type plants. Nodules on roots (B) and nodule cross-sections (C) of wild-type, empty vector control, and *GmbHLHm1* OEX.

2.3 Discussion

These results indicate that *GmbHLLHm1* is linked to nodule growth and development, promoting N₂-fixation activity in nodules, at the same time potentially facilitating increased nitrogen accumulation in aerial tissues. The root system plays two roles: N₂-fixation in the nodule and nitrogen transport from the root to the shoot. Loss of *GmbHLLHm1* in the root system leads to undeveloped nodules and reduced N₂-fixation activity (Figure 2.4 and 2.5). As a result, plants grown solely on nodule N showed nitrogen deficiency symptoms, such as short stature, yellowing of the leaves, and stunted growth (Figure 2.5 and 2.6 A). The nitrogen-deficiency phenotype observed in plants with a reduction in *GmbHLLHm1* expression could be recovered with the supply of exogenous nitrate. This result has been previously observed by Chiasson et al. (2014). This result further supports that *GmbHLLHm1* plays an important role in nodule development and N₂-fixation and the ability of the plant to be N self-sufficient.

Interestingly, in non-nodulated *bhlhm1* plants, the response to exogenous N (KNO₃) was found to be strong with an increase in shoot growth relative to the empty vector control. From the expression profiles between nodules and roots (Figure 2.2), *GmbHLLHm1* was found to be upregulated in the *bhlhm1* root but repressed in nodules as expected (Figure 2.2C). The mechanism for the difference in expression levels of endogenous *bHLLHm1* between root and nodule tissue is unclear, but it has previously been shown that in non-nodulated roots, *bHLLHm1* expression is high but in inoculated roots is strongly repressed (Chiasson et al., 2014). This could be related to an N-linked expression by exogenous KNO₃. Select N-linked gene signalling pathways have been previously identified that correspond with *bHLLHm1* expression including the ammonium transport protein GmAMF3 and other nitrogen transporters, including NRT1.7, NRT2.4 and AMT2 (Chiasson et al., 2014; Mohammadi Dehcheshmeh, 2014).

In the symbiotic N₂-fixation relationship, plants provide carbohydrates to nodule bacteroids in exchange for bacteroid-derived reduced nitrogen (NH₃). Symbiotic nitrogen fixation is biologically expensive for plants because plants are required to synthesize carbohydrates to support plant growth (nodule development) and bacteroid metabolism at the same time. In many legumes, a nodulation control system (AON, autoregulation of nodulation) is active to control the

number of nodules that can develop on the root system, effectively optimizing both nodulation and nodule growth (Reid et al., 2011b). AON is responsive to exogenous N decreasing both nodulation and nodule growth and N₂-fixing activities when excess N is available in the rhizosphere (Caetano-Anollés and Gresshoff, 1991; Okamoto et al., 2009). Soybean responded positively to external N when grown in 5mM KNO₃ (Figure 2.6 A). Plants were bigger, with significantly increased shoot dry weights compared to that of the minus nitrogen grown nodulated Vector and Wild-type controls (Figure 2.6 B).

In the *GmbHLHm1* OEX group, nodule numbers per plant did not change significantly (Figure 2.8 C), but the nodule DW per plant (Figure 2.8 D), and the effective N₂-fixation capacity of the nodules increased (Figure 2.9 C). It would appear that overexpression of *bHLHm1* supports greater nodule development and enhanced N₂-fixation capacity (Figure 2.8E), with more nitrogen being made available in the shoots to support growth (Figure 2.8F, 2.9A) compared to the Vector group and Wild-type group.

The presence of the nodules along the root system suggested that AON may have been active to control nodule development in the overexpressing *bHLHm1* root systems. The larger nodules mostly developed at the crown of the root, while smaller nodules were found in the middle area of the roots (Figure 2.9 B). This is contrasted by the wider distribution of nodules in the empty vector and WT controls, where nodules developed further from the crown. The plants were inoculated at the beginning of the hairy root development, therefore the nodulation started from the top area of the roots. As the root grew, more nodules were generated in the lower area of the roots. However, the nodules in the crown of the roots were fully developed and fixed sufficient nitrogen to support the plant growth, while nodules in the lower area of the roots were slower to develop. It is possible that the elevated levels of shoot-based N signals from the active crown-based nodules may have evoked a strong AON response and limited nodule development further along the root systems, similar to the response when exogenous N is applied. More studies required focusing on how *GmbHLHm1* regulates the activity of nitrate or ammonium transporter and why de-regulation has such a positive response to plant growth and N₂-fixation capacities.

2.4 Materials and Methods

2.4.1 Plant material cultivation

Soybean (*Glycine max* L. cv. snowy) seeds were soaked in 1:2 water diluted bleach for 2 min and rinsed 3 times with autoclaved water. Surface-sterilized seeds were transferred to plates with autoclaved wet surface media. Plates were covered with cling wrap to prevent contamination and maintain humidity. Plates were transferred to an incubator with a 14/10hr day/night regime. Seeds were germinated in a day/night temperature cycle of 28-25 °C for 7-10 days. Germinated seedlings about 3-5cm in length were selected for *Agrobacterium*-mediated hairy root transformation.

The hairy-root transformation, with *Agrobacterium rhizogenes* K599, was performed according to the Mohammadi-Dehcheshmeh et al. (2014). After the hairy root induction and cultivation, plants were inspected. The wild-type hairy roots were removed from the plants for the optimal experiment result for the experimental groups. Similar amounts of hairy roots were removed in the wild-type groups. Processed plants were transferred to pots with a mixed matrix of quartz sand and surface (1:1 ratio). 50ml NoduleN™ Legume Inoculant peat was diluted into 1L water, and 20ml inoculant solution was applied to each seedling with a syringe, the day plant was transferred to the mixed matrix for nodulation. B&D nutrient solution (Broughton and Dilworth, 1971) was applied twice a day with a semi-hydroponic system. 5mM KNO₃ was added to the B&D nutrient solution in the +N group. Plants were grown in a controlled growth chamber with a 14/10hr day/night regime, 25/22°C day/night temperature cycle, and 60% humidity for 28 days. 28-day-old nodules on wild-type roots or transgenic hairy roots were harvested for experiments.

2.4.2 RNAi silencing

The pK7GWIWG2D(II) vector was used for RNAi silencing of *GmbHLHm1* (Figure 2.1). The constructed *GmbHLHm1*- pK7GWIWG2D(II) vector was obtained from Mohammadi-Dehcheshmeh (2014). The *Agrobacterium rhizogenes* K599 was transformed with the *GmbHLHm1*-RNAi construct for *Agrobacterium*-mediated hairy root transformation. Transgenic hairy roots and nodules were inspected for GFP fluorescence and positive plants were used for further experiments.

2.4.3 Overexpression

The pFAST-G02 vector was used for overexpression of *GmbHLHm1* (Figure 2.7). The full-length *GmbHLHm1* CDs (1048bp) was amplified from the soybean genome with forward primer GTCCGCGGATGAGGAGTTCTCATATGGAGA and reverse primer TGGCGCGCCTCACACGAAATATGAAAAAGCT with *Sac*II restriction site on 5' end and *Asc*I restriction digestion site on 3' end. The full CDs was inserted into the pEntr by double digestion (*Sac*II NEB and *Asc*I NEB) and T4 ligation (ThermoFisher Scientific™). The full *GmbHLHm1* CDs was then inserted into the pFAST-G02 with the Gateway™ system. The *Agrobacterium*-mediated hairy root transformation was performed the same as RNAi silencing protocol above, according to Mohammadi-Dehcheshmeh (2014). The vector contains a fusion gene encoding eGFP with an oil body membrane protein that is prominent in seeds. Because the eGFP expression is not highly expressed in roots and nodules, hairy roots were first inspected for GFP fluorescence under UV light. Then, PCR was performed with forward primer AGGGCATCGACTTCAAGGAG, reverse primer CGATGTTGTGGCGGATCTTG and DNA of each hairy roots with eGFP fluorescence to confirm the eGFP expression. Once confirmed, the main root and non-transgenic hairy roots were all removed with scissors. The processed plants were transferred into pots with turface and sand till harvest.

2.4.4 RNA extraction and quantitative polymerase chain reaction (qPCR) analysis

Plant samples were harvested around 11 am. Nodules were detached from the transgenic hairy roots and different tissue were kept in separated centrifuge tubes in liquid nitrogen before transfer to the -80°C freezer. RNA extraction was performed using the PureZOL™ total RNA extraction reagent. First-strand cDNA synthesis was performed using iScript cDNA Synthesis Kits. Primers for *GmbHLHm1* expression (forward primer: GCTCGGTGATAACAGCTGGA; reverse primer: CACGCCATCTCCACCTTAGG) were designed using Geneious software. Primer efficiency was tested with SYBR Green Real-Time PCR Master Mix and 1, 1/5, 1/25, 1/125, 1/625 dilution of cDNA synthesized. The primer efficiency was between 90%-110%. 2µl of 1/5 dilution cDNA was used as the qPCR templates. The SYBR Green Real-Time PCR Master Mix was used for qPCR. Results were normalized against *Cons6* as the reference gene and calculated using the $2^{-\Delta\Delta Ct}$

method (Libault et al., 2008). Values were means \pm SE (n=4) biological replicates. The significant differences between groups are based on the T-test ($P < 0.05$).

2.4.5 Acetylene reduction assay (ARA)

Samples of the intact root system (transgenic roots and nodules attached) were harvested and placed in 40ml McCartney vial sealed with a rubber stopper respectively around 11 am. A 5ml gas seal syringe was used to draw out 4ml of air from the sealed vial, and 4ml of pure acetylene gas was injected into the air with another gas-sealed syringe. The starting acetylene-ethylene levels in the vial were measured with GC-2010 Plus gas chromatography (SHIMADZU, Japan). Vials were then incubated in a 28°C incubator for 1 hr. The acetylene-ethylene levels in the vial were measured with GC-2010 Plus gas chromatograph. The difference in ethylene starting levels and final levels were calculated by subtraction. The samples were removed from the vials, nodules were removed from the roots and placed in a 60 °C oven to dry overnight. Dry nodules were weighed, and dry weight data were used for ARA calculations. The data were processed according to Unkovich M. (2008).

Chapter 3 The interaction between *GmbHLHm1* and the plant hormones GA₃ and IAA

3.1 Introduction

Gibberellins (GAs) are plant hormones that regulate cell and tissue growth and influence various developmental processes. Endogenous GA is also tightly involved in the regulation of nodulation in legumes. GA-deficient *Pisum sativum* mutants, *na-1*, *ls-1*, and *lh-2*, developed significantly fewer and more aberrant nodules (Ferguson et al., 2005; Ferguson et al., 2011). Wild-type phenotypes could be restored by exogenous GA₃ application (Ferguson et al., 2005; Ferguson et al., 2011). McAdam et al. (2018) reported that biosynthesized GA suppresses infection thread (IT) formation and promotes nodule organogenesis into nitrogen-fixing organs via the activity of the DELLA protein. GA biosynthesis genes, *GmGA20ox* and *GmGA3ox1*, are also reported to be upregulated during the early nodulation stage in soybean roots (Hayashi et al., 2012). DELLA is a key repressor of GA-mediated growth and development of nodules, where it interacts with transcriptional complexes such as CCaMK–IPD3 and NSP2–NSP1 to regulate nod-factor inducible genes (Jin et al., 2016). Nett et al. (2022) reported that rhizobia in soybean nodules produces the penultimate intermediate GA₉, which could be converted to bioactive GA₄. This rhizobial-derived GA promotes nodule size and nodule number in soybean. Results indicate that GA synthesis and signalling are required for nodulation and optimizing the rhizobial symbiosis.

GA can modulate root nodule formation through exogenous application (McAdam et al., 2018). Application of GA to roots before inoculation negatively regulates calcium spiking and IT formation in *L. japonicus* (Ferguson et al., 2019). In soybeans, GA applied to post-infection (at 10 or 100 nM GA₃) nodules showed increased nodulation (Roy Choudhury et al., 2019). High concentrations of GA₃ beyond its threshold level could inhibit nodulation and could further inhibit nodule formation in GA-deficient mutants of pea (Ferguson et al., 2005). Different GA-biosynthesis enzymes are upregulated in different parts of nodulated soybeans. *GmGA20ox1a* was predominately expressed in the transient meristem of the developing nodules until the area no longer has meristematic activity in mature nodules (Chu et al., 2022), whereas *GmGA3ox1a* is upregulated throughout the nodulated root system (Chu et al., 2022). Editing *GmGA20ox1a* and *GmGA3ox1a* in soybeans results in a reduced nodule number emphasizing the function of endogenous GA in nodulation (Chu et al., 2022). These studies suggest nodulation requires an optimal level of GAs to be expressed and spatiotemporally distributed to optimize the legume nodule symbiosis.

Auxin is a plant hormone that plays a significant role in regulating plant growth and development. The function of auxin in nodulation and symbiotic nitrogen fixation includes controlling cell cycle reactivation, vascular tissue differentiation, and rhizobial infection (Kohlen et al., 2017). After the rhizobial infection, the IT elongation was positively regulated via an Auxin Response Factor (MtARF16a) in *M. truncatula* (Breakspear et al., 2014). During nodule organogenesis, an auxin maximum is established by the nod factor signalling, during the initiation of nodule primordium, promoting cell division (inner cortex and pericycle for indeterminate nodules and middle or outer cortex for determinate nodules) and increasing nodule numbers (Hirsch, 1992; Kuppusamy et al., 2009; Suzaki et al., 2012; Xiao et al., 2014; Ng et al., 2015). The Auxin accumulation involves multiple changes in auxin transport. PIN proteins are a family of auxin efflux carriers. The MtPIN2 was reported to be involved in basipetal auxin transport, but not necessary for nodulation (Ng et al., 2019). The down-regulation of *MtPIN9* expression in roots in the initial response to Nod factors indicates a possible role of MtPIN9 in establishing an auxin maximum prior to the formation of nodule primordia (Plet et al., 2011). A family of high-affinity auxin influx carriers (AUX1/LAX) is also involved in auxin transport (Kohlen et al., 2017). In *M. truncatula*, *MtLAX2* is expressed during nodule organogenesis suggesting the auxin influx might contribute to the auxin

accumulation (Roy et al., 2017). However, more evidence is required for the role of the PIN and AUX1/LAX contributing to auxin maximum in nodule initiation. Moreover, some microRNA are also reported to involve in auxin perception and auxin/cytokinin balance during rhizobial infection and nodule maturation (Wang et al., 2015; Tiwari et al., 2021).

Auxin not only regulates the early nodulation process but is also involved in the autoregulation of nodulation response (AON). During AON, a family of peptides, CLAVATA3/endosperm-surrounding region-related (CLE), are induced, transported into shoot via xylem and interact with leucine-rich repeat receptor-like kinases (LRR-RLKs) in leaves (Tsikou et al., 2018; Ferguson et al., 2019). The perception of the CLE peptide produces a shoot-derived signal (miR2111) that is transported to the root and inhibits the formation of additional nodules by regulating an F-box containing protein, Too Much Love (TML), which is a symbiosis suppressor (Kohlen et al., 2017; Tsikou et al., 2018; Ferguson et al., 2019).

The NIN, a central regulator of nodulation, positively regulates the accumulation of auxin in dividing cortical cells during *Lotus japonicus* nodulation (Saur et al., 2011; Suzaki et al., 2012). Additionally, the activation of AON signalling, including LjCLE-RS (belongs to CLE family) and HAR1 (encoding LRR-RLK) genes, controls further cortical cell division, through inhibiting auxin accumulation (Suzaki et al., 2012). The *SUNN* (*Super Numeric Nodules*), encoding CLV1-like LRR-RLK regulates nodule numbers via decreasing the shoot-to-root auxin transport, after inoculation of roots by rhizobia on *M. truncatula* (Van Noorden et al., 2006a; Jin et al., 2012). This evidence suggests a role of auxin in the AON.

A previous study discovered that three GA-responsive elements and two auxin-responsive elements are located in the promoter of *GmbHLHm1* (Mohammadi Dehcheshmeh, 2014). Exogenous GA applications were shown to inhibit *GmbHLHm1* expression in soybean nodules, while the effect of auxin on *GmbHLHm1* expression was not clear. GA₃ is a bioactive form of gibberellic acid most frequently used in the horticulture (Gupta and Chakrabarty, 2013). Indole-3-acetic acid (IAA) is a form of bioactive auxin commonly found in plants (Duca et al., 2014).

GmbHLHm1 has a significant impact on nodulation and nodule development in soybean (Chapter 2). Loss of *GmbHLHm1* expression (*bhlhm1*) compromises both nodule development (DW) and

activity (ARA and %N in aerial tissues), while overexpression increases nodule growth, measured ARA and the %N in aerial leaves. However, the regulation of *GmbHLHm1* expression remains unclear. The identification of multiple DNA binding motifs for GA and auxin in the *GmbHLHm1* promoter suggests its expression could involve phytohormones. It is also unclear if *GmbHLHm1* operates as a GA and/or auxin-dependent TF and how fast the *GmbHLHm1* responds to GA and Auxin treatment. In this chapter, short and long-term GA₃ and IAA applications were tested for their impact on *GmbHLHm1* expression and the general impact on plant growth and root nodule development.

3.2 Results

3.2.1 GA affects the expression of nodulation genes and alters the activity of *GmbHLHm1* in nodules and roots.

In a previous study, a microarray experiment was performed on RNAi *Gmbhlhm1* silenced nodules. A few gibberellin-responsive genes, including *MTO3* (Glyma17g04330), *GASA6* (Glyma19g31480), and *GAMMA-TIP* (Glyma03g34310) were found to be significantly induced in nodules with the loss of *GmbHLHm1* expression (Chiasson et al., 2014; Mohammadi Dehcheshmeh, 2014). *MTO3* is a S-adenosylmethionine synthetase family protein that is stimulated by GA₃ in wheat (Mathur et al., 1993). The S-adenosylmethionine synthetase was reported to be up-regulated during early nodulation in soybean, which is related to the pathogen defence. *GASA6* is known as a GA inducible gene involved in cell elongation (Lin et al., 2011; Ahmad et al., 2019). *GAMMA-TIP* (gamma tonoplast intrinsic protein) is interpreted as glycine max nodulin-26 and aquaporin in root nodules, which is responsible for water transportation in symbiosome membranes (Rivers et al., 1997). In this chapter, the expression of *MTO3*, *GASA6*, *GAMMA-TIP*, and *GmbHLHm1* was further examined in nodules and roots of nodule or nitrate-grown plants exposed to short-term GA treatments. The exogenous supply of nitrate promoted plant growth and suppressed rhizobial nodulation (Xia et al., 2017). An extended exposure (10 d) to nitrate inhibited *GmbHLHm1* expression further (Figure 3.1A). Previous microarray data showed that the GA-responsive genes *MTO3*, *GASA6*, and *GAMMA-TIP* were negatively related

to *GmbHLHm1* expression (Mohammadi Dehcheshmeh, 2014). In this study, only *GASA6* expression increased similarly to the previous microarray result (Figure 3.1C), while *MTO3* and *GAMMA-TIP* failed to show any significant increases in expression in the nitrate-grown plants (Figure 3.1B and D) when *GmbHLHm1* was suppressed by exogenous N.

Short-term GA treatments (4 ppm = 10^{-5} M, Gibberellic acid potassium salt, G1025, Sigma-Aldrich®) were applied to the soil of nodulated wild-type plants treated with or without exogenous nitrate for 10 d. Without nitrate (N₂-fixing plants with healthy nodules), *GmbHLHm1* expression (Figure 3.2A) was significantly reduced relative to the controls after 1 h of GA treatment, then becoming undetectable 24 h later. The expression of *MTO3*, *GASA6*, and *GAMMA-TIP* also changed with short-term GA treatment (Figure 3.2B-D). The expression of *MTO3* increased after GA supply (1 h) but returned to base levels by 24 h (Figure 3.2 B), while *GASA6* was not affected (Figure 3.2 C). *GAMMA-TIP* expression only increased after 24 h (Figure 3.2D). In the presence of 5 mM KNO₃ (Figure 3.2 +N groups), nodulation was inhibited, and there was a minimal impact of GA treatment on gene expression relative to the -N controls (Figure 3.2 -N groups). However, at 24 h, *GAMMA-TIP* expression remained significantly higher than without GA treatment, both in -N and +N groups, indicating the induced expression of *GAMMA-TIP* by GA, is independent of the function of nodules and the presence of KNO₃.

The impact of GA on nitrogenase activity in wild-type nodules was also investigated. As a proxy to actual nitrogenase activity rates, ammonium levels in detached nodules did not significantly change after a 48 h GA treatment (Figure 3.3 A). 48 h after GA addition, nitrogen fixation rates (measured using the acetylene reduction assay) decreased relative to the controls (Figure 3.3B). The results showed that GA has a long-term impact on nitrogen fixation in soybeans.

3.2.2 Long-term GA treatment on *GmbHLHm1* expression in *bhlhm1*

Longer exposure times to GA were tested for its impact on *bHLHm1* expression and for downstream impacts on nitrogen partitioning to the shoots and nodule nitrogenase activity measured using the acetylene reduction assay. 5-day-old nodulated roots were treated with 4 ppm GA₃ over 23 days. Without GA, *GmbHLHm1* expression in wild-type and empty vector control plants were similar, while *bhlhm1* showed a reduced expression of the gene (Figure 3.4 A).

The %N measured in the leaves and nodule nitrogen fixation were suppressed in the *bhlhm1* compared to the control (Figure 3.4 B and C). In the presence of GA, *GmbHLHm1* expression in the empty vector control was suppressed (Figure 3.4 A). This treatment also resulted in a decline in the rate of nodule nitrogen fixation but not the %N measured in the leaves (Figure 3.4 B and C). In *bhlhm1*s, the GA treatment further suppressed nitrogenase activity (Figure 3.4 C), but not the expression of *GmbHLHm1* or the %N measured in leaves (Figure 3.4 A and B).

The phenotypes of empty vector and *bhlhm1* plants revealed notable changes in plant tissue presentation with GA. In the empty vector group, the GA treatment significantly enhanced nodule dry weight (Figure 3.4 D), nodule number (Figure 3.4 E), and shoot height (length of the main stem, Figure 3.4 H). The shoot and root dry weight (Figure 3.4 F and G) were not impacted by GA treatment. The loss of *GmbHLHm1* expression (*bhlhm1*) reduced all the phenotypic data measured (Figure 3.4). The results demonstrate that *GmbHLHm1* plays an important role in soybean growth and nodulation. In the *bhlhm1*, GA enhanced the shoot height (Figure 3.4 H) and had no impact on the other phenotypic measurements (Figure 3.4 D-G).

Representative images of treated plants show that the *bhlhm1* was generally small with yellow leaves (Figure 3.5 A) and had small nonfunctional nodules (Figure 3.5 B and C). The long-term GA treatments increased shoot length in both the empty vector and the *bhlhm1* (Figure 3.5 A), and further reduced nodule size and effective nitrogen-fixing area of the *bhlhm1* nodule (Figure 3.5 B and C).

3.2.3 Long-term GA treatment on *GmbHLHm1*-overexpressed (Overexpression) soybeans

Plant hairy roots with overexpression of *GmbHLHm1* (Overexpression) were created to reveal the impact unregulated expression of *GmbHLHm1* has on nodule activity (Figure 3.6). Without GA treatment (control), the overexpression of *GmbHLHm1* predictably increased the expression levels of *GmbHLHm1* relative to the empty vector control (Figure 3.6 A). At the same time, this increased shoot %N, nitrogenase activities, nodule dry weight, nodule number, and shoot dry weight (Figure 3.6 B-F).

Application of GA resulted in a collective decrease in *GmbHLHm1* expression, shoot %N and nitrogenase activities in the overexpression line and Empty Vector control (Figure 3.6 A-C). In the

Empty Vector, GA treatment significantly enhanced shoot height (Figure 3.6 G), but had no impact on nodule dry weight, nodule number, or shoot dry weight (Figures D, E and F, respectively), compared to water controls (controls). GA treatment had a similar impact on the *GmbHLHm1-overexpressed* (Overexpression) plants, compared to the Empty Vector plants, with reduced *GmbHLHm1* expression and nitrogenase activities (Figure 3.6 A and C), increased shoot dry weight and shoot height (Figure 3.6 F and G).

Visually, the overexpression of *GmbHLHm1* resulted in plants with better shoot development and more developed nodules and roots (Figure 3.7). GA, as expected, resulted in shoot elongation but reduced infected nodule size and nitrogen fixation area both in Empty Vector and Overexpression plants, as presented in Figure 3.7.

3.2.4 *GmbHLHm1* expression in nodules and roots after a short-term IAA treatment.

The nodulation process is also regulated by auxin (Kohlen et al., 2017). Breakspear et al. (2014) reported that auxin positively regulates infection thread elongation, which is opposite to the effect of GA. The expression of *GmbHLHm1* in wild-type roots and nodules after a short-term (6 h) IAA treatment with 1 ppm IAA (5×10^{-6} M, Indole-3-acetic acid sodium salt, I5148, Sigma-Aldrich®), did not change *GmbHLHm1* expression in either roots or nodules (Figure 3.8).

3.2.5 Long-term IAA treatment on *GmbHLHm1* expression in *bhlhm1*

Longer exposure times to IAA were also tested for its impact on *GmbHLHm1* expression and for downstream impacts on nitrogen partitioning to the shoots and nodule nitrogenase activity measured using the acetylene reduction assay. 5-day-old nodulated roots were treated with 1 ppm IAA over 23 days. In Empty Vector plants, IAA treatment enhanced *GmbHLHm1* expression in nodules (Figure 3.9 A). There was no impact of IAA on %N delivery to the leaves (Figure 3.9 B). IAA treatment increased root dry weight and shoot dry weight (Figure 3.9 E and F) and reduced the nodule number (Figure 3.9 D). The nodule dry weight (Figure 3.9 C) and shoot height (Figure 3.9 G) were not affected by IAA treatment.

From the visual images of the plants in Figure 3.10, IAA treatment improved the shoot growth, root size, and nodule size in the empty vector control (Figure 3.10). The effect of long-term IAA

treatments is most visible in the *bhlhm1*, which produced bigger nodules; however, the nitrogen fixation area remained white and probably non-functional.

3.2.6 Long-term IAA treatment on *GmbHLLHm1*-overexpressed (Overexpression) soybeans

Treatments with IAA didn't enhance *GmbHLLHm1* expression in nodules, relative to the overexpression line supplied water (Figure 3.11 A). In overexpression plants, IAA further increased shoot dry weights (Figure 3.11 F) but had no impact on any of the other parameters tested compared to water control groups (Figure 3.11 B-E and G). From the visual image of the IAA treatments, both the Overexpression and Empty Vector plants (Figure 3.12), had a larger infected nodule size and an effective nitrogen fixation area (Figure 3.12 C).

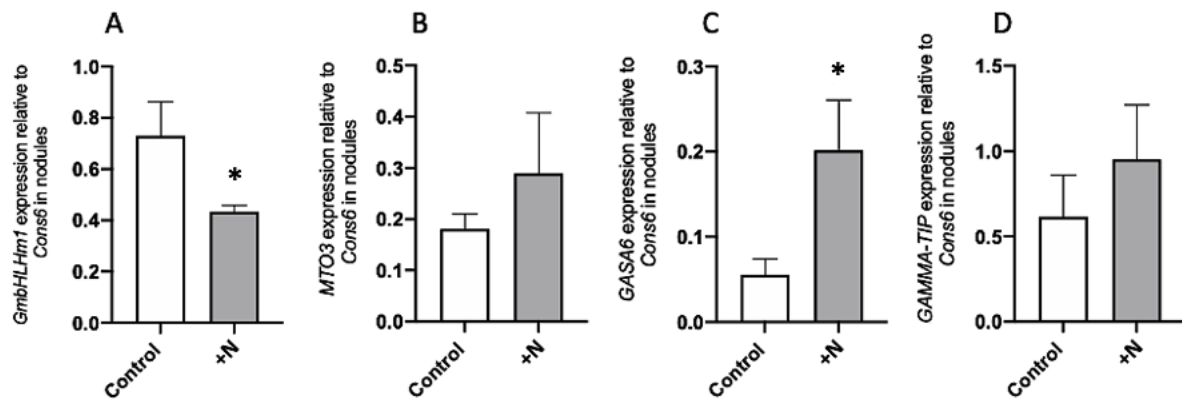


Figure 3. 1 *GmbHLHm1*, *GASA6*, *MTO3* and *GAMMA-TIP* expression in nodules with/without long-term KNO_3 treatment. Nodulated plants were supplied \pm 5 mM KNO_3 in the nutrient solution for 10 days after an initial 18 days of growth in a minus N nutrient solution. The expression levels of (A) *GmbHLHm1*, (B) *MTO3*, (C) *GASA6*, and (D) *GAMMA-TIP* in nodules were determined. The expression of gene levels was normalized with *Con56* as a reference gene and was calculated using the $2^{-\Delta\Delta C_t}$ method (Libault et al., 2008). Values were means \pm SE (n=5) of five biological replicates. The * above bars indicate the significant difference compared to Control based on the T-test ($P < 0.05$).

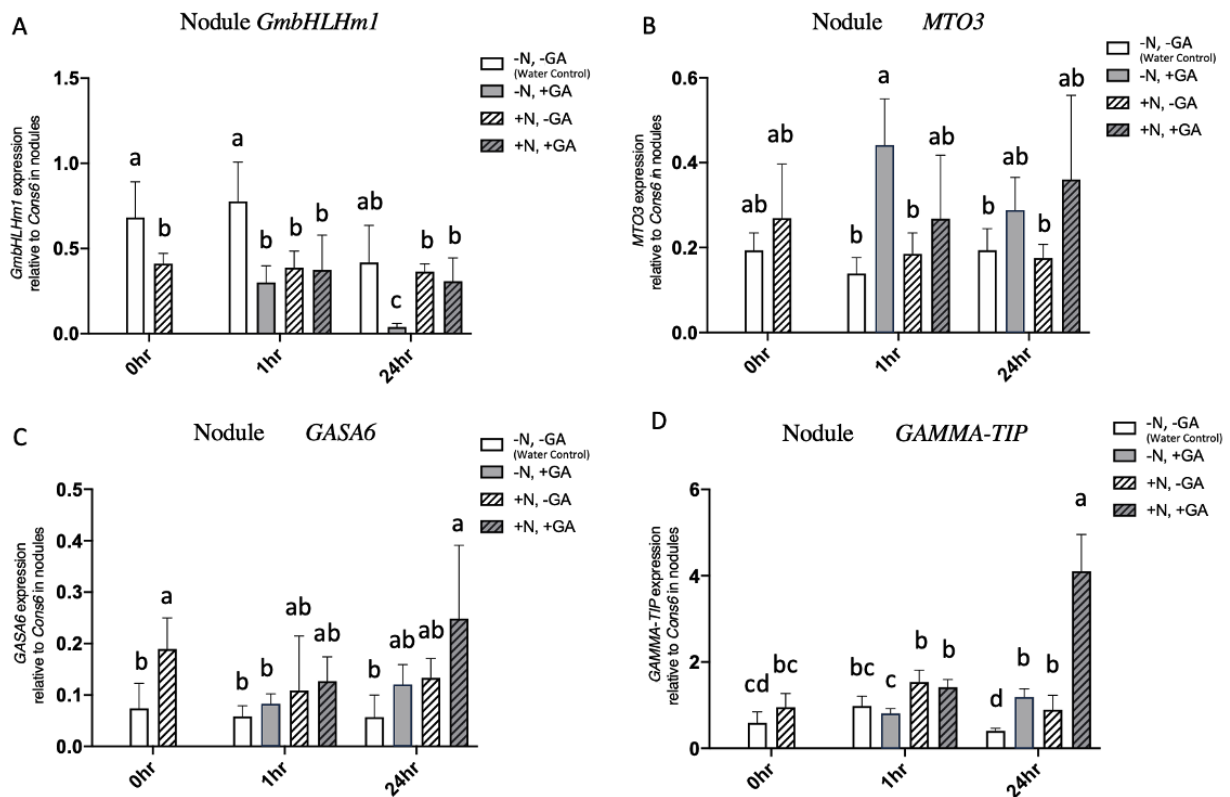


Figure 3.2 *GmbHLHm1*, *GASA6*, *MTO3*, and *GAMMA-TIP* expression in nodules with short-term GA treatment \pm KNO₃ in the nutrient solution. Nodulated plants were grown without N (-N) or with 5 mM KNO₃ for 18 days post-inoculation with rhizobia. (A) *GmbHLHm1*, (B) *MTO3*, (C) *GASA6*, and (D) *GAMMA-TIP* expression levels in nodules after 1 h and 24 hrs of GA₃ treatment. The expressions of gene levels were normalized with *Con6* as a reference gene and were calculated using the $2^{-\Delta\Delta C_t}$ method (Libault et al., 2008). Values were means \pm SE (n=5) of five biological replicates. The letters above each bar indicate the significant differences between groups based on the one-way ANOVA ($P < 0.05$).

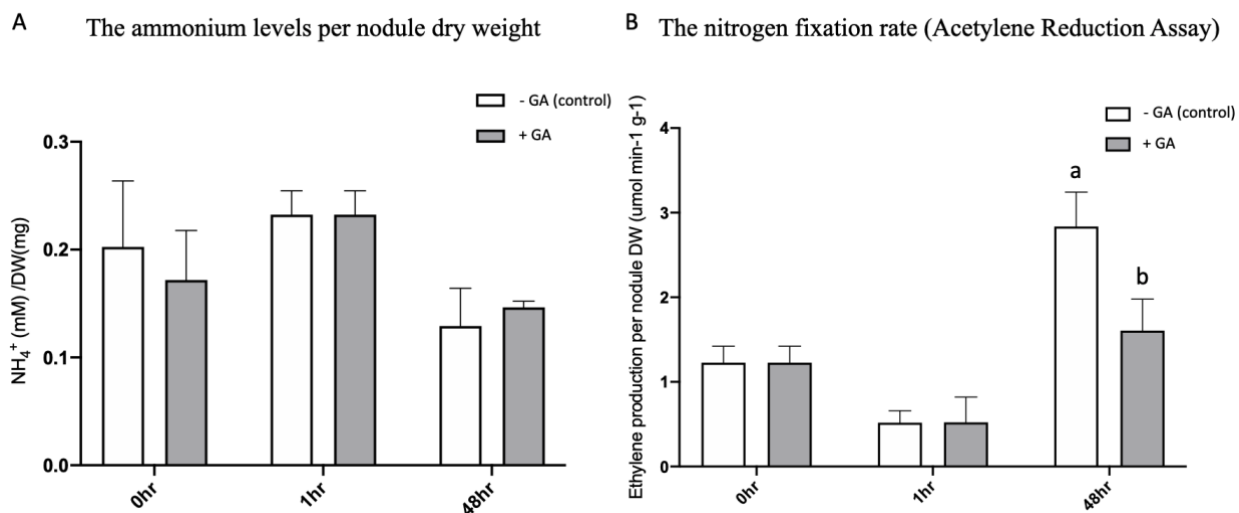


Figure 3.3 The nitrogenase activity in the wild-type nodules after short-term GA treatments (0-48 h). (A) The ammonium levels per nodule dry weight and (B) nitrogen fixation rate (Acetylene Reduction Assay) after a short-term GA treatment. 4ppm GA₃ was applied to the soil for a 48-h period. Values were means \pm SE (n=6) of six biological replicates. The letters above each bar indicate the significant differences between groups based on the one-way ANOVA ($P < 0.05$).

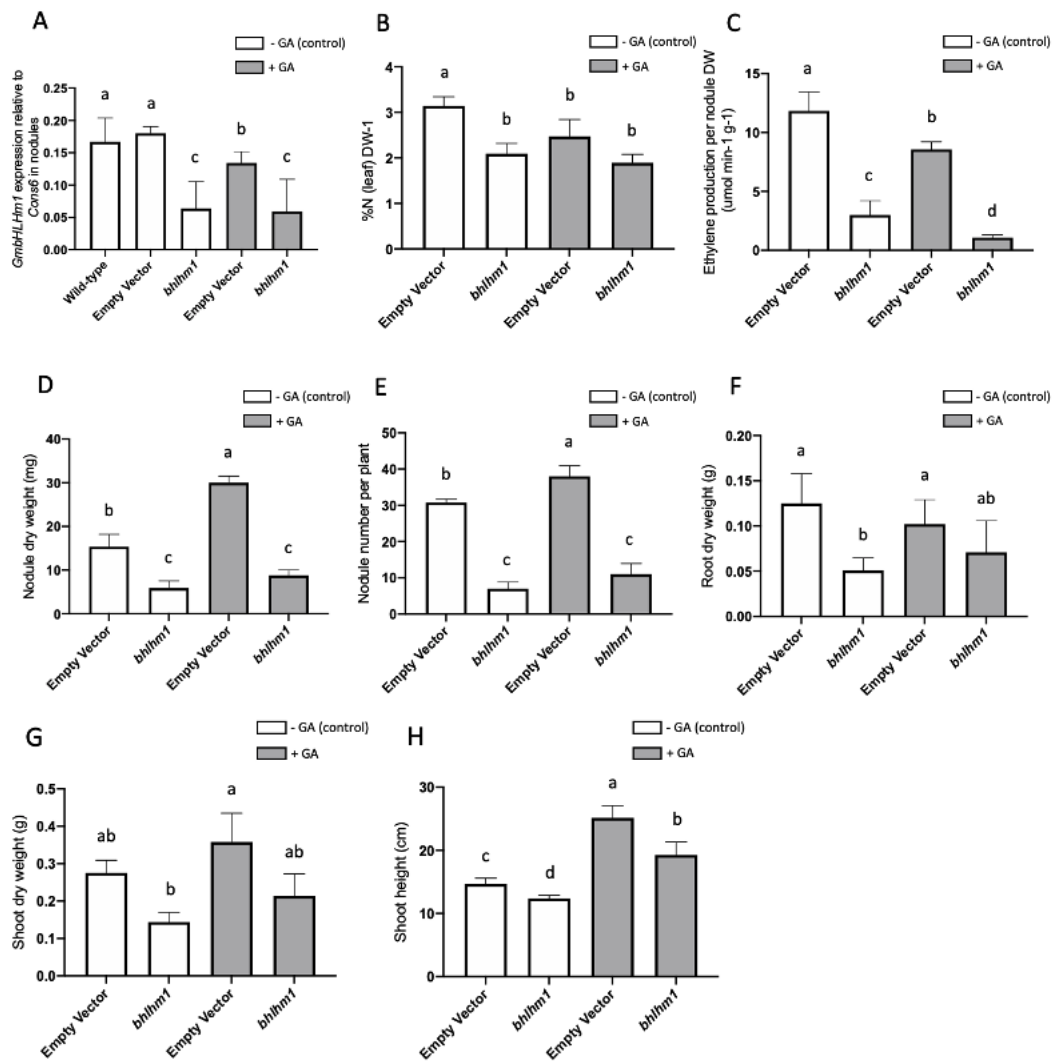


Figure 3. 4 The effect of long-term GA treatment on *GmbHLHm1* expression in nodules. From the 5th day after inoculation, 4ppm of GA₃ solution was applied directly to the soil twice a week. 28-day-old plants were harvested and analyzed. (A) Expression levels of *GmbHLHm1* in wild-type, empty vector, and *bhlhm1* plants. (B) The nitrogen percentage of the leaves, (C) nitrogen fixation rate (ARA), (D) nodule dry weight, (E) nodule number, (F) root dry weight, (G) shoot dry weight, and (H) shoot height of empty vector (EV) and *bhlhm1* with GA treatment. The expression of *GmbHLHm1* levels was normalized with *Con6* as a reference gene and was calculated using the $2^{-\Delta\Delta Ct}$ method (Libault et al., 2008). Values were means \pm SE (n=4) of four biological replicates. The letters above each bar indicate the significant differences between groups based on the two-way ANOVA ($P < 0.05$).

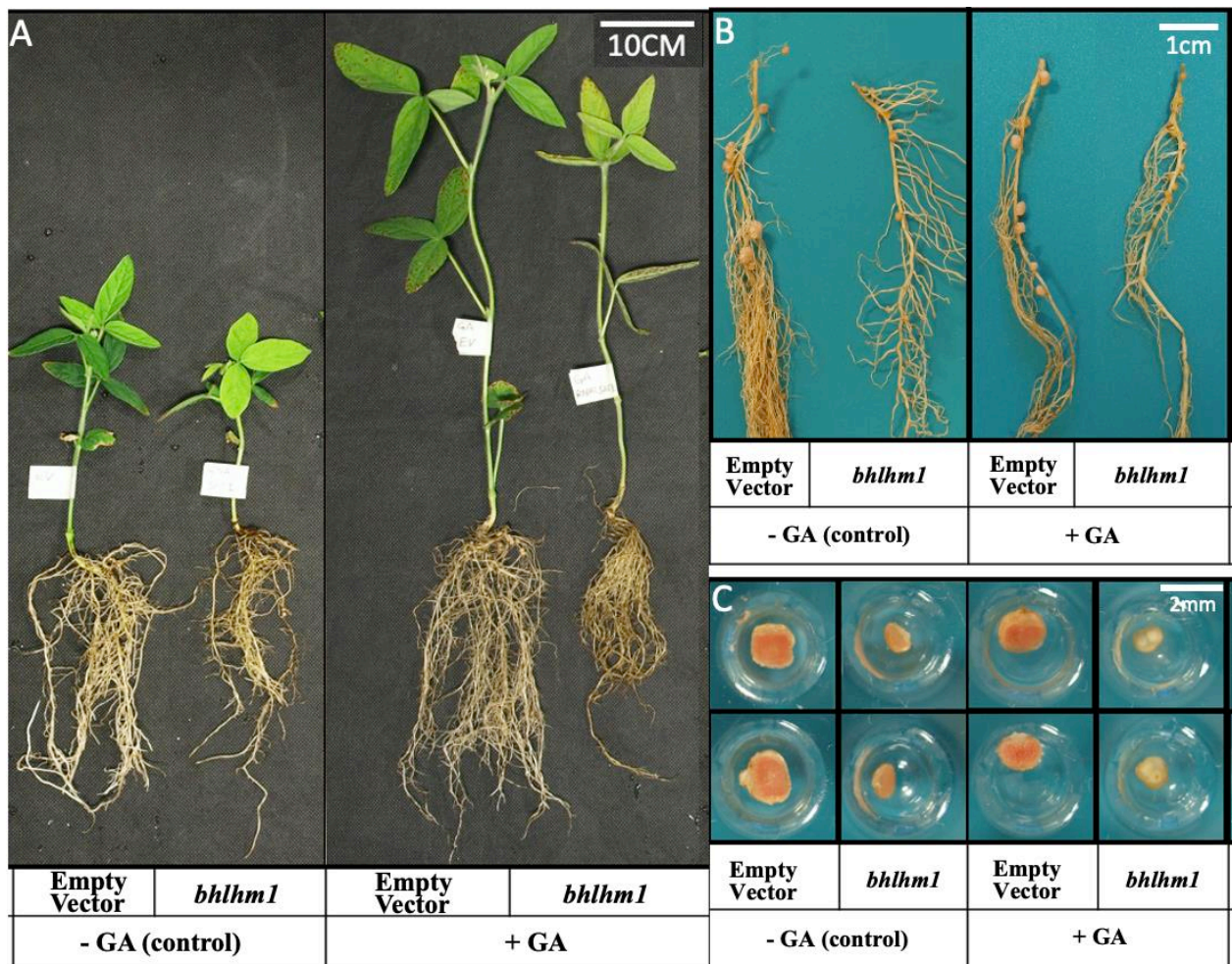


Figure 3. 5 Visual images of (A)whole plant, (B) nodules on roots, and (C) nodule cross-section of empty vector and *bhlhm1* with GA treatment.

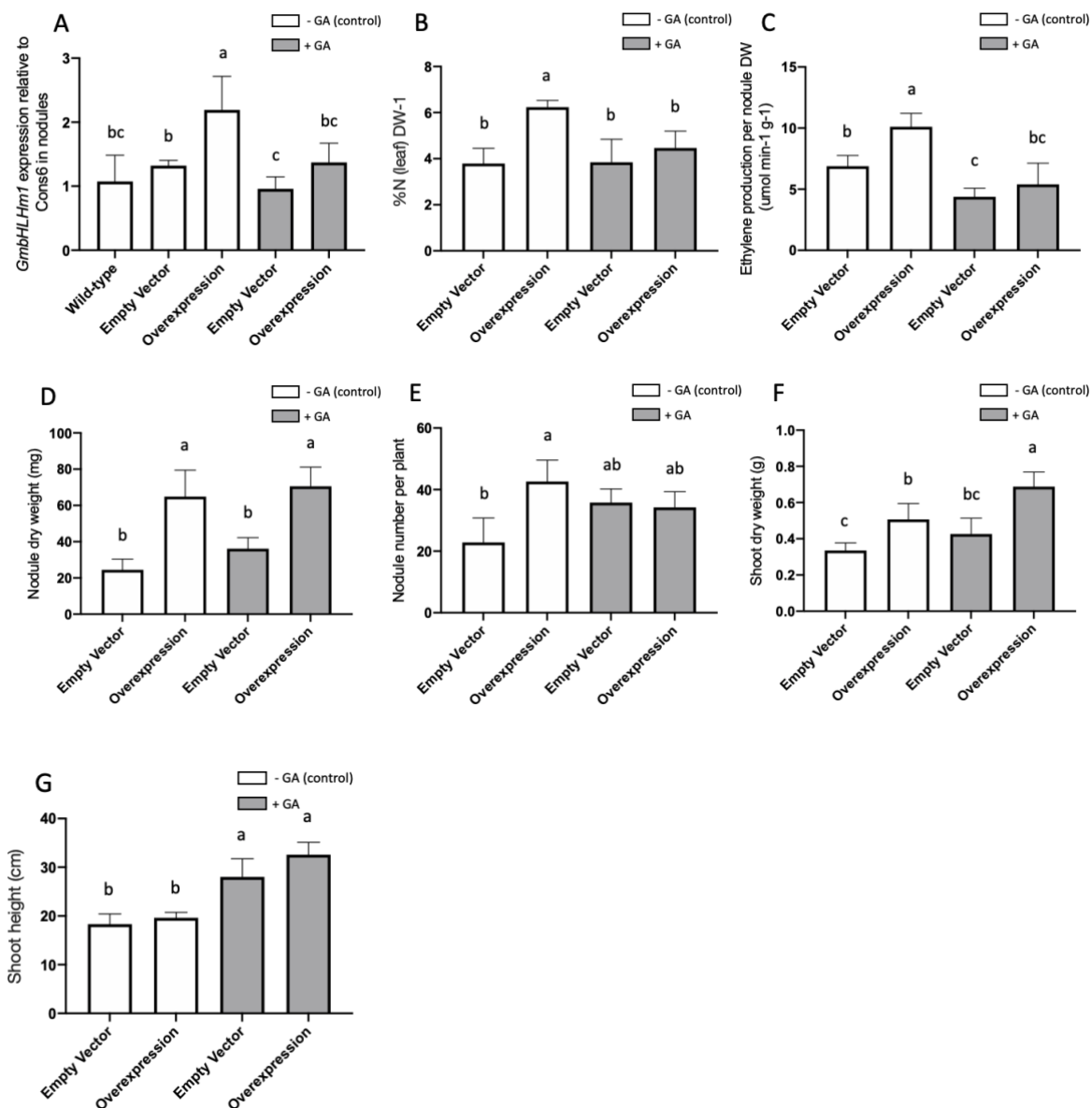


Figure 3. 6 The effect of long-term GA treatment on *GmbHLHm1* expression in nodules. From the 5th day after inoculation, 4ppm of GA₃ solution was applied directly to the soil twice a week. 28-day-old plants on wild-type, empty vector, and *GmbHLHm1* overexpression hairy roots were harvested and analyzed. (A) Expression levels of *GmbHLHm1* in nodules. (B) The nitrogen percentage of the leaves, (C) nitrogen fixation rate (ARA), (D) nodule dry weight, (E) nodule number, (F) shoot dry weight, and (G) shoot height of empty vector and overexpression plants with GA treatment. The expression of *GmbHLHm1* levels was normalized with *Con6* as a reference gene and was calculated using the $2^{-\Delta\Delta C_t}$ method (Libault et al., 2008). Values were means \pm SE (n=6) of six biological replicates. The letters above each bar indicate the significant differences between groups based on the two-way ANOVA (P < 0.05).

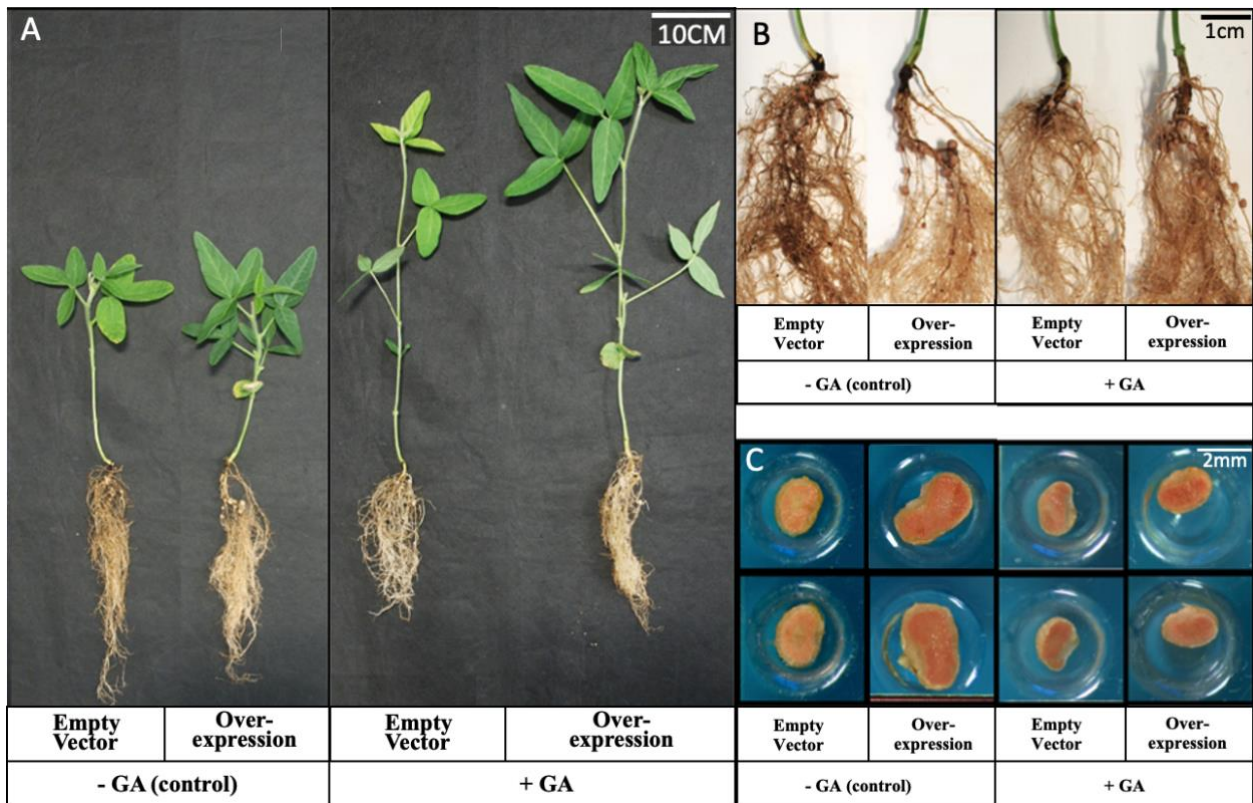


Figure 3. 7 Visual images of (A)whole plant, (B) nodules on roots, and (C) nodule cross-section of plants on empty vector and *GmbHLHm1* overexpression hairy roots with GA treatment.

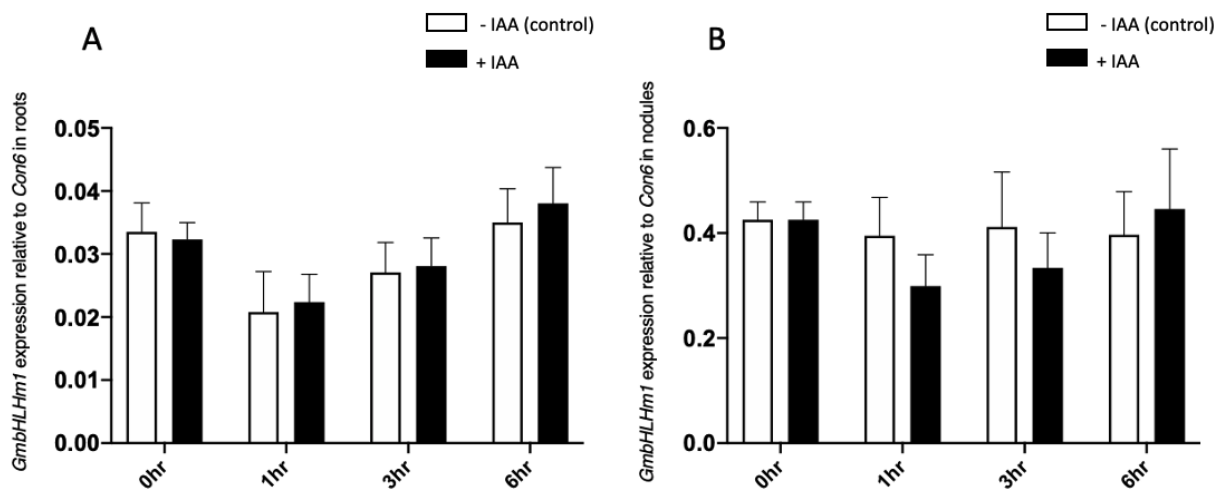


Figure 3. 8 *GmbHLHm1* expression in nodules and roots after a short-term IAA (1 ppm) treatment. *GmbHLHm1* expression in roots (A) and nodules (B) showed no response with a short-term IAA treatment applied directly to the soil. The expression of *GmbHLHm1* levels was normalized with *Con6* as a reference gene and was calculated using the $2^{-\Delta\Delta C_t}$ method (Libault et al., 2008). Values were means \pm SE (n=5) of five biological replicates. The significant differences between groups based on the one-way ANOVA ($P < 0.05$).

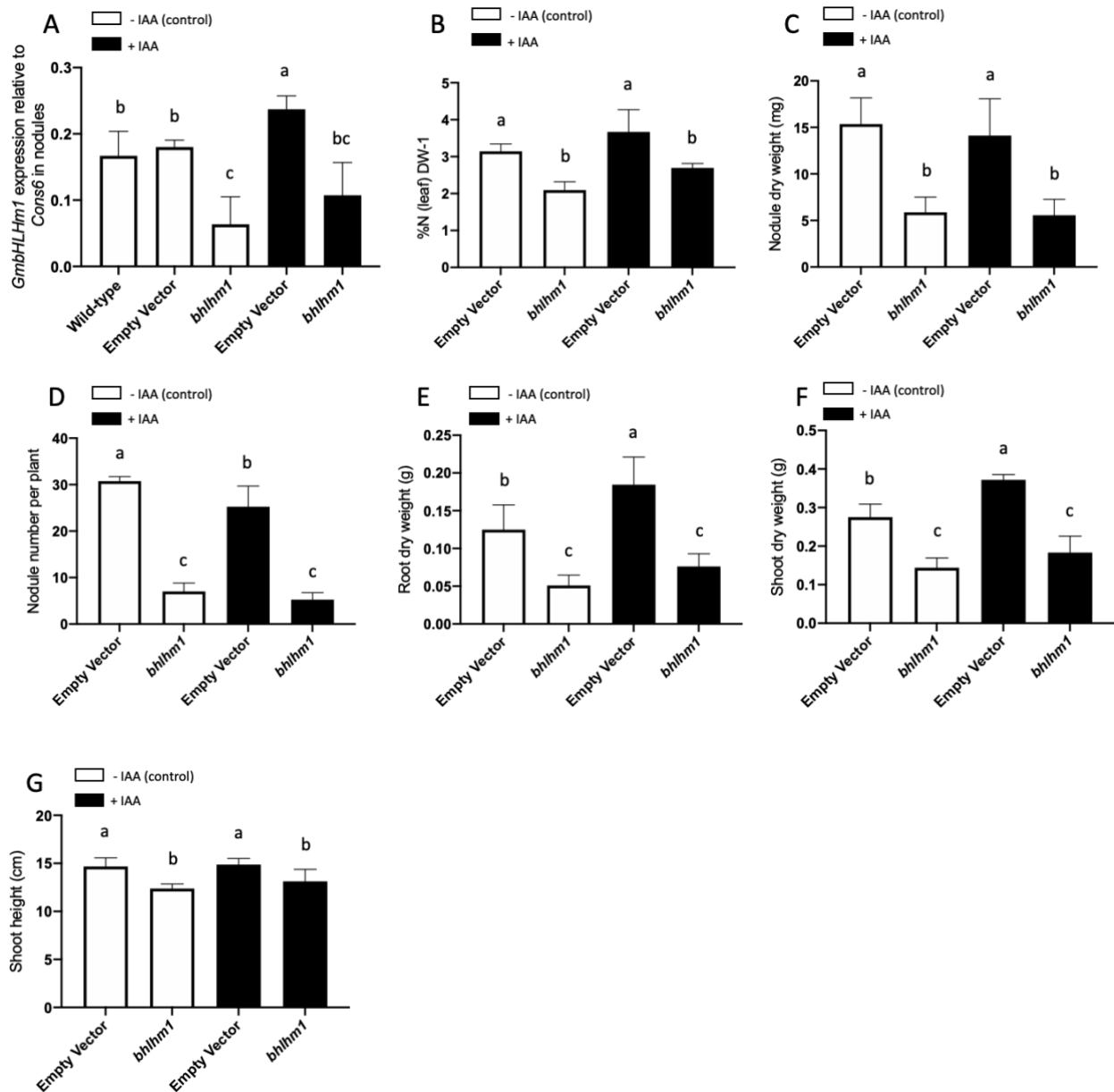


Figure 3. 9 The effect of long-term IAA treatment on *GmbHLHm1* expression in nodules. From the 5th day after inoculation, 1ppm of IAA solution was applied directly to the soil twice a week. 28-day-old plants were harvested and analyzed. (A) Expression levels of *GmbHLHm1* in wild-type, empty vector, and *bhlhm1* plants. (B) The nitrogen percentage of the leaves, (C) nodule dry weight, (D) nodule number, (E) root dry weight, (F) shoot dry weight and (G) shoot height of empty vector and *bhlhm1* with IAA treatment. The expression of *GmbHLHm1* levels was normalized with *Con6* as a reference gene and was calculated using the $2^{-\Delta\Delta C_t}$ method (Libault et al., 2008). Values were means \pm SE (n=4) of four biological replicates. The letters above each bar indicate the significant differences between groups based on the two-way ANOVA ($P < 0.05$).

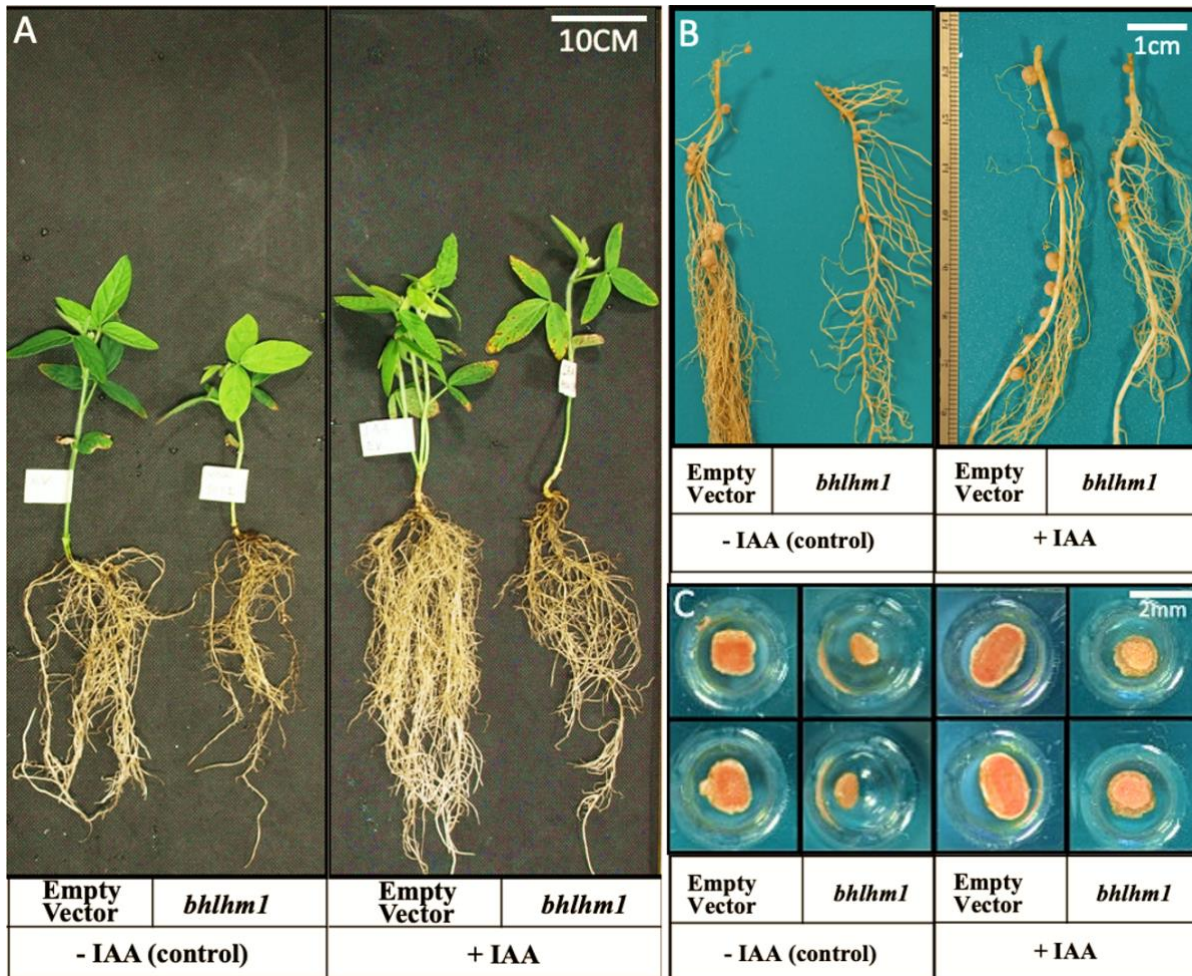


Figure 3. 10 Visual images of (A)whole plant, (B) nodules on roots, and (C) nodule cross-section of empty vector and *bhlhm1* with IAA treatment.

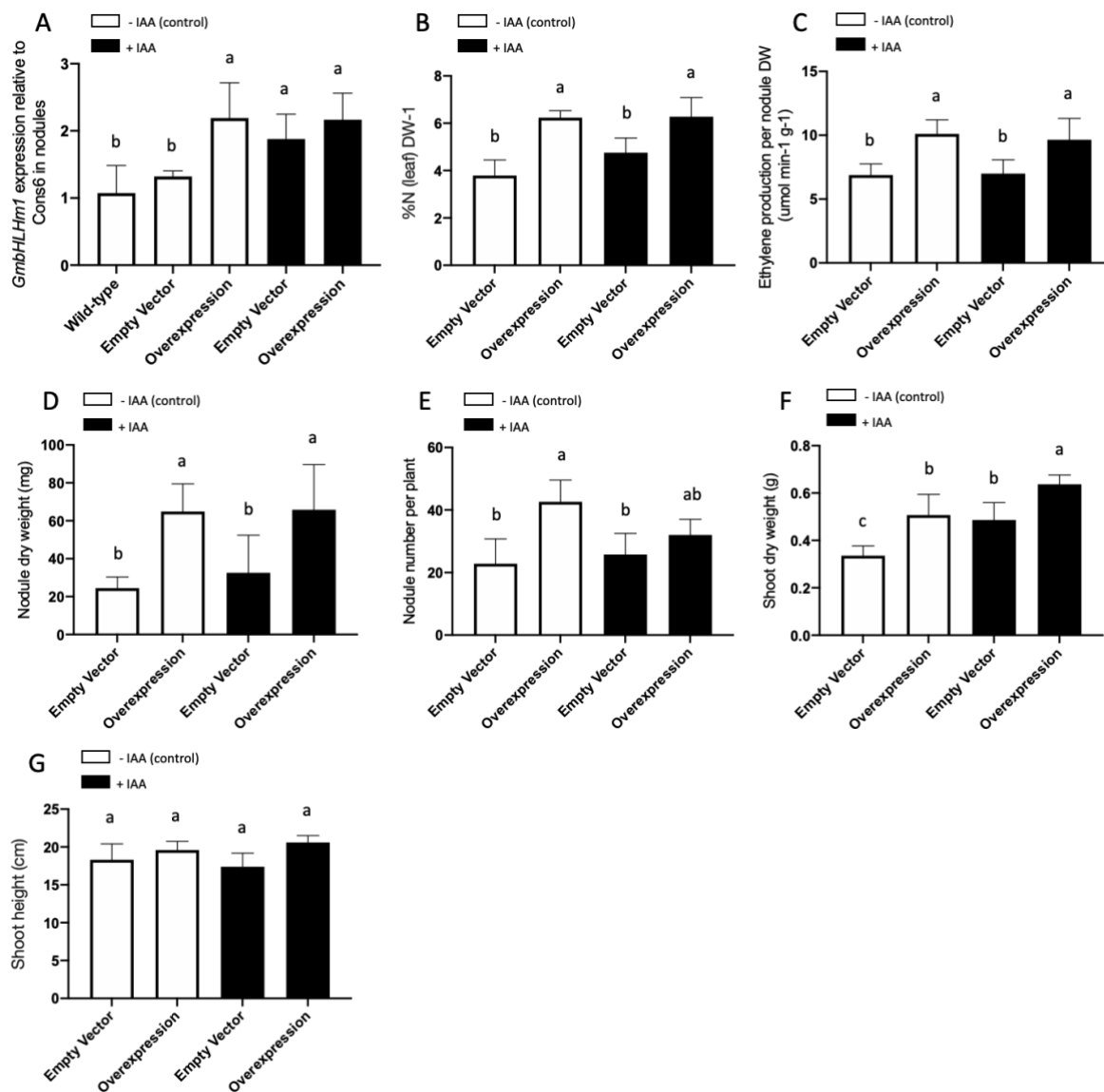


Figure 3.11 The effect of long-term IAA treatment on *GmbHLHm1* expression in nodules. From the 5th day after inoculation, 1ppm of IAA solution was applied directly to the soil twice a week. 28-day-old plants on wild-type, empty vector, and *GmbHLHm1* overexpression hairy roots were harvested and analyzed. (A) Expression levels of *GmbHLHm1* in nodules. (B) The nitrogen percentage of the leaves, (C) nitrogen fixation rate (ARA), (D) nodule dry weight, (E) nodule number, (F) shoot dry weight, and (G) shoot height of empty vector and overexpression plants with IAA treatment. The expression of *GmbHLHm1* levels was normalized with *Con6* as a reference gene and was calculated using the $2^{-\Delta\Delta C_t}$ method (Libault et al., 2008). Values were means \pm SE (n=6) of six biological replicates. The letters above each bar indicate the significant differences between groups based on the two-way ANOVA ($P < 0.05$).

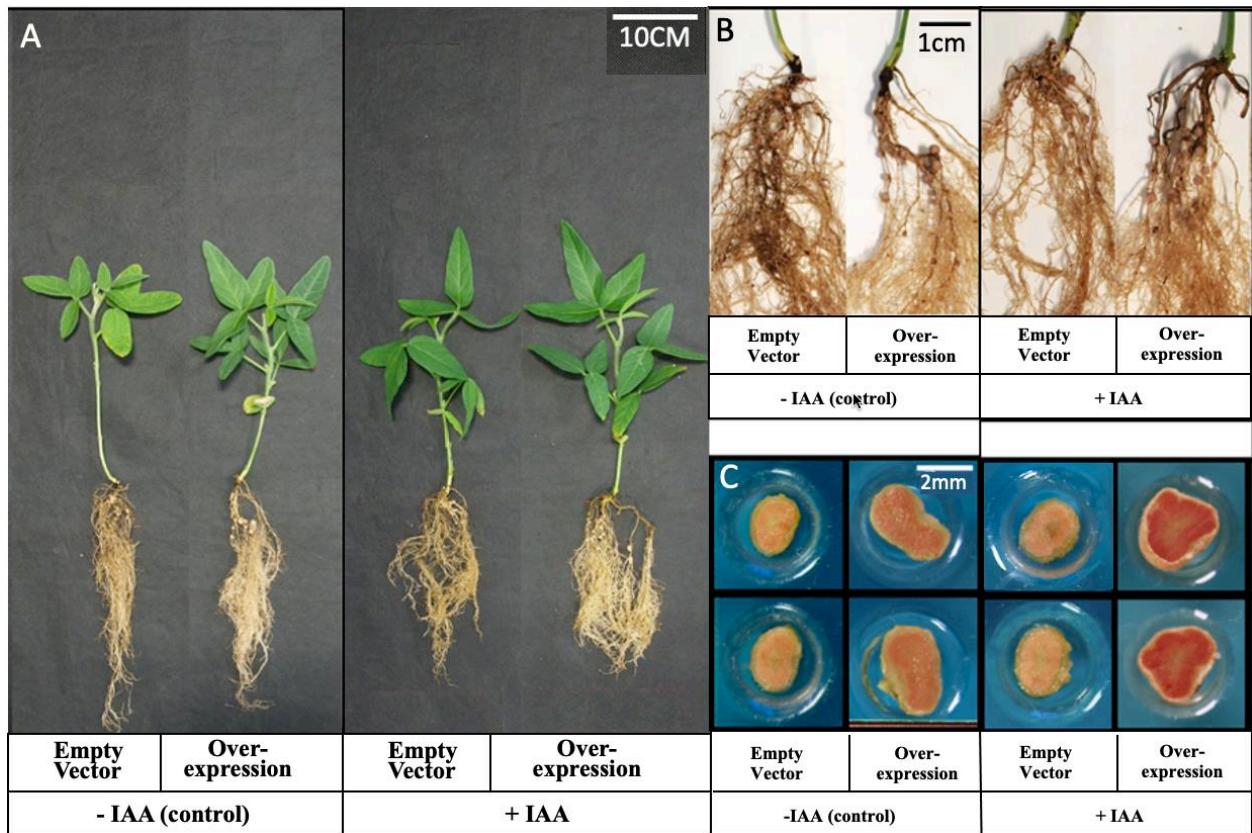


Figure 3. 12 Visual images of (A)whole plant, (B) nodules on roots, and (C) nodule cross-section of plants on empty vector and *GmbHLHm1* overexpression hairy roots with GA treatment.

3.3 Discussion

A previous microarray assay identified several differentially expressed genes when *GmbHLHm1* was silenced in both roots and nodules (Mohammadi Dehcheshmeh, 2014). Among these, the GA-regulated genes, *MTO3* (Mathur et al., 1993), *GASA6* (Lee and Kende, 2002; Lin et al., 2011), and *GAMMA-TIP* (Phillips and Huttly, 1994) were all found to be upregulated with a reduction in *GmbHLHm1* expression. We have previously shown that the nitrogen status of the plant influences *GmbHLHm1* expression (Chiasson et al., 2014). In this study, we used nitrate to reduce *GmbHLHm1* expression in nodules and to test other genes that may have a coordinated regulation pattern. Nitrate applied to nodulated soybean plants over 10 days resulted in a significant reduction in *GmbHLHm1* expression (Figure 3.1 A). However, there were no changes in the expression of *MTO3* or *GAMMA-TIP* to nitrate (Figure 3.1 B and D) while *GASA6* showed a similar response to the loss of *GmbHLHm1* expression (Figure 3.1 C). From this initial result, we assume *GmbHLHm1* is most likely not a GA-mediated transcription factor working in trans for *MTO3* or *GAMMA-TIP*.

We tested if each of these genes responded to exogenous GA supply and whether they belong to a common GA regulation module. In nitrogen-fixing nodules, short-term GA treatments significantly downregulated *GmbHLHm1* expression within 1 h of application to the roots. However, the inhibition was unstable, with expression recovering after 3 h until completely disappearing after 24 h (Figure 3.2A). *MTO3*, *GmSAS6*, and *GAMMA-TIP* showed variable responses to GA treatments over the 24 h period with no clear positive or negative response over the time periods being tested. *MTO3* showed a transient positive response to GA (up to 3 h) but then returned to control levels (Figure 3.2 B), *GASA6* was upregulated between 3-6 h (Figure 3.2 C) and *GAMMA-TIP* upregulated after 24 h (Figure 3.2 D). In the presence of exogenous nitrate, the GA interference of *GmbHLHm1* expression was overcome with expression levels returning to control levels (Figure 3.2 A). Nitrate supply kept *GmbHLHm1* expression at a low level, inhibiting the strong downregulation of *GmbHLHm1* by GA (Figure 3.2 A).

Long-term GA treatment inhibited *GmbHLHm1* expression, the nodule nitrogen fixation rate and the %N measured in aerial tissues (Figure 3.4 A, B and C, Empty Vector groups). Shoot growth (weight and height, Figure 3.4 G and H) responded positively to the extended GA treatments,

resulting in elongated shoots (Figure 3.5). Interestingly long-term exogenous GA supply stimulated the number of nodules developed and the final nodule dry weight (Figure 3.4 D and E), while reducing the nodule size (Figure 3.5 B and C). This result would suggest overall nodule development and nodulation are promoted with exogenous GA, consistent with shoot growth, independent of *GmbHLHm1* expression. When *GmbHLHm1* was inhibited by GA, the nodule size was reduced, in order to support the GA-induced shoot growth, an increased number of small nodules were established in the root, and the AON could regulate this process. Using RNAi, *GmbHLHm1* expression was reduced in nodules (Figure 3.4 A). This resulted in a significant reduction in shoot nitrogen (%N), nodule ARA, nodule DW, nodule number, root DW, shoot DW and shoot height (Figure 3.4). With the application of GA, only shoot height could be recovered in the knockdown plants. This indicates that *GmbHLHm1* activity works downstream of the GA-induced control of nodulation. With knockdown *GmbHLHm1* expression, GA treatment could not recover the overall nodulation as observed in the Empty Vector group, indicating that *GmbHLHm1* is probably involved in nodule development system AON.

Plant lines were developed where *GmbHLHm1* was overexpressed using a hairy-root transformation system. When liberated from transcriptional regulatory control, plants responded favourably with larger and more numerous nodules. N₂-fixation increased and the %N delivered to the shoots was enhanced relative to the empty vector controls (Figure 3.6). The supply of exogenous GA reduced this response with a reduction in *GmbHLHm1* expression, and a drop in nitrogen fixation (ARA activity and shoot %N levels). However, nodules continued to grow which was matched with increased shoot DW and extended shoot heights (Figure 3.6, 3.7).

It has been known for some time that soybean growth responds favorably to the supply of exogenous nitrate. This response comes at an expense of the development and activity of root nodules (Ferguson et al., 2010; Reid et al., 2011b; Udvardi and Poole, 2013; Xia et al., 2017). Nodulation and nodule development has been linked to the cell-specific generation of phytohormones, GA and cytokinin (CK). GA was reported to have an inhibitory effect while CK promotes the AON system, which controls the number of nodules that will develop on a root system when exposed to compatible rhizobia or when supplied with nitrate (Nishida et al., 2018; Akamatsu et al., 2021; Okuma and Kawaguchi, 2021; Li et al., 2022). A primary component of

the AON system is the role of the NIN and NIN-like Protein (NLP) transcription factors which influence cortical cell division in response to rhizobial signals (NIN) and nitrate signals (NLP). With NIN, rhizobia activate the endogenous synthesis of activated GA biosynthesis and accumulation, which in turn further activates its own expression through a GA-mediated binding on its promoter (Akamatsu et al., 2021). Elevated NIN and NLP activate the AON signalling network through the expression of the CLE ROOT SIGNAL (*CLE-RS1/2*) module, delivering CLE peptides to the shoots via the xylem stream and activating a CLAVATA1-like receptor-like kinase (LRR-RLKs), in soybean called NTS1/NARK (Nishimura et al., 2002; Searle et al., 2003). The signalling cascade continues with the regulation of the TOO MUCH LOVE (TML) genetic module through the expression of basipetal-delivered miR2111, which can destroy TML mRNA transcripts (Takahara et al., 2013a). Rhizobial and nitrate signals encourage miR2111 synthesis while low N enhances miR2111 synthesis (Okuma and Kawaguchi, 2021). TML is a kelch repeat-containing F-box protein that can inhibit nodulation.

GA has been shown to inhibit early nodulation events including infection thread development and elongation (Ferguson et al., 2011; McAdam et al., 2018). Bioactive GAs are recognised by the *GID1* (GA insensitive dwarf1) receptor. GA-activated *GID1* proteins can then bind to *DELLA* proteins, which are transcriptional regulators of GA-induced responses in plants. As discussed previously, the long-term application of bioactive GA₃ disrupted *GmbHLHm1* expression and decreased nodule functionality (N₂-fixation), though nodule size and final nodule numbers increased with the continued exogenous GA₃ treatment. High levels of GA would have an impact on *DELLA* protein stability and could influence a number of GA-responsive transcription factors including *GmbHLHm1*. *DELLA* has also been linked to the activation of the CK pathway through an interaction with the *NODULATION SIGNALLING PATHWAY 2* (*NSP2*) and *NUCLEAR FACTOR-Y1* (*NF-YAI*), promoting nodulation (Fonouni-Farde et al., 2016; Fonouni-Farde et al., 2019). From this data, GA acts as a negative repressor of *GmbHLHm1* expression and activity, possibly through the GA binding motif recognised in its promoter. When *GmbHLHm1* is liberated from regulatory control through overexpression, it suggests a strong positive response to nodule development akin to a reduction in AON regulatory control of nodule number and function. It will be important to understand whether GA can directly regulate *GmbHLHm1* via the promoter and

whether this regulation is essential to *GmbHLHm1* activity to encourage or negate nodule development and function.

Auxin regulates nodulation by controlling cell cycle reactivation, vascular tissue differentiation, and rhizobial infection (Kohlen et al., 2017). At the nodule primordium, high levels of endogenous IAA are found (Van Noorden et al., 2006a; Kuppusamy et al., 2009; Kohlen et al., 2017). Auxin has been linked to AON activities. In *M. truncatula*, rhizobia inoculation results in a drop of auxin flow from the shoot to the root, and increased auxin flows when either *har1* or *sun1* mutants are inoculated (van Noorden et al., 2006b). Direct signalling pathways linking auxin-managed gene transcription within nodules or at the site of nodulation remain poorly understood and described. Exogenous auxin application onto *M. truncatula* and *O sativa* roots can generate empty nodule-like structures (NLS) and result in large pools of differentially expressed genes, which include TF's, transporters, protein kinases and hormone-related genes (Hiltbrand et al., 2016).

We examined the role of the putative IAA binding motif on the promoter of *GmbHLHm1* using endogenous IAA treatments on growing nodulated soybean plants. Short-term supply of 1 ppm IAA (6 h) had no impact on *GmbHLHm1* expression in nodules or roots (Figure 3.8). However, long-term IAA application elevated *GmbHLHm1* expression, nodule size, shoot, and root dry weights (Figure 3.9 A and Figure 3.10). The addition of IAA had little impact on the presentation of the healthy nodules, which were slightly enlarged but the colour of the nitrogen fixation area remained pink, while *bhlhm1* produced bigger, non-functional nodules with IAA treatment (Figure 3.9 and Figure 3.10). The results indicate that IAA improves nodule size independent of the nitrogen fixation activity and *GmbHLHm1* expression. In line with this outcome, the IAA treatment on overexpressing *GmbHLHm1* nodules also improved the nodule size and nitrogen fixation area but did not enhance plant growth and nodulation at a whole-plant level (Figure 3.11 and 3.12). In the empty vector control groups, an increased number of large nodules were observed in the root with IAA treatment (Figure 3.10 B; Figure 3.12 B). Although the nodule number was reduced (Figure 3.9 D), the total nodule dry weight did not decline (Figure 3.9 C). Therefore, the nitrogen fixed from the whole root system was sufficient to support the larger shoot dry weight (Figure 3.9 F).

It is still unclear what the link auxin has with the expression of *GmbHLHm1*, except that long-term IAA exposure stimulates gene expression compared to water control. This would suggest IAA has a positive regulatory control of *GmbHLHm1* and that *GmbHLHm1* activity is supportive of nodulation, nodule development and increased nodule activity.

3.4 Material and Method

3.4.1 Plant material cultivation and treatment

GA₃ and IAA stock solution was prepared by dissolving 10 mg of IAA or GA₃ in a small quantity of ethanol prior to dilution with distilled water. Then distilled water was added to make the volume 0.1 liter to get 100 ppm solution (Sarkar et al., 2002). Working solution was diluted from stock with distilled water, ratio 1:100 (IAA) and 4:100 (GA₃).

Wild-type and transgenic soybean were germinated and grown as described in Chapter 2.4.1. Short-term GA/IAA treatments were applied to 28-day-old wild-type seedlings at 10 am with water (control) 4 ppm GA₃ (Mohammadi Dehcheshmeh, unpublished result) or 1 ppm IAA solution (Sudadi and Suryono, 2015) directly to the soil. The pots were covered with aluminium foil to block light from hitting the soil surface during the application of GA and IAA. Nodules and roots were harvested in separated tubes at 0, 1, 3, 6, 24 and 48h after the GA/IAA application. Long-term GA/IAA treatment was applied to wild-type soybeans seedlings with transgenic hairy roots, 5 days after inoculation. 4 ppm GA₃ or 1 ppm IAA solution was applied directly to the soil twice a week. 28-day-old plants were harvested and analyzed.

The hairy-roots transformation, qPCR, and acetylene reduction assay (ARA) were performed according to Chapter 2.4.4. The ammonium assay was performed according to Chapter 5.4.4.

Chapter 4 Genetic control of *GmbHLHm1* and *GmAMF3* promoters

4.1. Introduction

GA-responsive elements, pyrimidine box (P-BOX) and TATC-BOX (TGGGATA) and the putative auxin-responsive TGA elements (AACGAC) have been identified in the promoter region of the *GmbHLHm1* (Mohammadi Dehcheshmeh, 2014). P-BOX motifs were first characterised in the regulation of GA-responsive genes in the barley aleurone (Mena et al., 2002). Sequence analysis of the *Brassica napus* GA-insensitive dwarf mutant *NDF1*, identified a mutation in the P-BOX motif of the GA receptor, *BnGID1* promoter (Li et al., 2011). Mutation of P-BOX motif leads to the GA-insensitive phenotype of the dwarf mutant *NDF1* suggesting that P-BOX motif is related to GA-related activities in *BnGID1*. Similarly, A TATC-BOX (TGGGATA) in the promoter of 4-coumarate: coenzyme ligase (4CL) in *Pennisetum purpureum* has been shown to bind GA through deletion analysis, EMSA binding of GA and GUS promoter fusion experiments (Peng et al., 2016). This GA-responsive element is like that observed in the *GmbHLHm1* promoter. The TGA element was first reported as a protein-binding DNA sequence in an auxin-regulated gene, *GmAux28*, in soybean (Nagao et al., 1993). The SFR2 (EMBL accession number X98520), an S Gene Family Receptor-like Kinase Gene in *Brassica oleracea*, includes TGA as an auxin-

responsive element in its promotor region (Pastuglia et al., 1997). Based on these previous studies, a hypothesis can be put forward that *GmbHLLHm1* can be positively or negatively regulated by GA and Auxin. In this chapter, the expression of the *GmbHLLHm1* promoter-GUS was investigated using both GA and IAA treatments. A mutation analysis of the GA-responsive elements (P-BOX and TATC-BOX) in the promoter of *GmbHLLHm1* was then investigated to determine the functionality of these elements in both GA and IAA treatments.

The ScAMF1 is characterized as an ammonium transporter in yeast which is regulated by *GmbHLLHm1* as a transcription factor (Chiasson et al., 2014). The ScAMF1 ortholog of soybean, *GmAMF3*, is reported highly expressed in nodules relative to other organs tested, indicating its potential role in nitrogen fixation and transportation in nodules that could be regulated by *GmbHLLHm1* (Chiasson et al., 2014). N-linked gene signaling pathways have been previously identified that correspond with *bHLLHm1* expression including the ammonium transport protein *GmAMF3* and other nitrogen transporters, including NRT1.7, NRT2.4 and AMT2 (Chiasson et al., 2014; Mohammadi Dehcheshmeh, 2014). As a part of N-linked gene signaling cascade, could *GmbHLLHm1* and *GmAMF3* expression also be regulated by other proteins or signals? The Yeast One-Hybrid was performed in this chapter, looking for proteins that directly bind to promoters of *GmbHLLHm1* and *GmAMF3*. Identified proteins could be the potential regulator of these two genes.

4.2. Result

4.2.1 Promoter-GUS expression in response to GA and IAA treatment.

A full-length promoter (1926bp upstream of the start codon) of *GmbHLLHm1* was cloned from genomic DNA and inserted into the pKGWFS7 (Promoter-GUS reporter) vector (Figure 4.1). The promoter-GUS construct was transformed into the *Agrobacterium rhizogenes* strain K599. The promoter-GUS construct was then transformed into (7-day-old) *Glycine max L. (cv. Snowy)* seedlings, generating transgenic hairy roots (detail refer to method 2.4.1.). Transformed roots of intact plants were then inoculated with *Bradyrhizobium japonicum*, strain UDSA110. After 23

days, the growing plants containing transgenic roots were treated with 4ppm GA₃ or 1ppm IAA for 5 days before harvesting. The transformation was verified using PCR on selected root samples (long, nodulated hairy roots were preferred) from each explant, and successfully transformed hairy roots with nodules attached were harvested. Harvested transgenic hairy roots and nodules were stained for GUS expression (see method 4.4.1). 23 days after inoculation, roots and nodules were treated with 1ppm IAA or 4ppm GA₃ respectively for five days. As shown in Figure 4.2, the GA treatment reduced GUS expression in both nodules and roots, compared to the water control. IAA enhanced GUS expression in the root with no enhanced expression in the nodules relative to the water control (Figure 4.2 A and B). The qPCR analysis of gene expression revealed that GA significantly reduced the expression of *GmbHLHm1* promoter-GUS in both roots and nodules (Figure 4.2 C and D). The IAA treatments significantly increased *GmbHLHm1* promoter-GUS expression in the roots only (Figure 4.2 C and D). The qPCR results are consistent with the GUS staining results.

4.2.2 The role of each GA responsive element on *GmbHLHm1* expression in nodules and roots.

Three GA-responsive elements were observed in the promoter region of *GmbHLHm1* (Fig 4.3). Each of the GA-responsive elements was edited (replaced by AAAAAA) and inserted into the pKGWFS7 vector and used for hairy root transformation. As shown in Figure 4.3, no GUS expression was observed in edited constructs with/without GA, auxin, or water treatments. This result indicates that each of these three GA-responsive elements is individually important in regulating the expression of the *GmbHLHm1* regardless of the presence of GA or IAA.

4.2.3 Localization of *GmbHLHm1* expression

Cross-sections of GUS-stained nodules with/without GA treatments were fixed in resin, sectioned, and deposited onto glass microscope slides. The slides were screened with a Leica Microsystems Camera/Microscope (DFC500/DM2500). Promoter-GUS expression was mainly expressed in infected cells in the infected zone and a small amount was found expressed in the infected and uninfected cells, respectively (Figure 4.4 A and B). Localization was also observed in the nucleus of the infected cells (Figure 4.4 C and D). The GA treatment reduced the expression of the *GmbHLHm1* Promoter-GUS in the infected region and was repressed in most of the out-layer cells

and nucleus of the infected region (Figure 4.4 B and D). Under control conditions, GUS was mainly targeted to the infected cells and the nucleus of those cells (Figure 4.4 A and C).

4.2.4 Proteins bind to the promoter of *GmbHLHm1* and *GmAMF3*.

In this experiment, the *GmbHLHm1* promoter was integrated into the yeast genome, creating a *GmbHLHm1* promoter-specific yeast strain (*Saccharomyces. Cerevisiae* - Y1HGold) using the pAbAi vector (Figure 4.5 A). Target cDNAs were synthesized from total RNA purified from soybean nodules and ligated into linearised pGADT7-Rec vectors (Figure 4.5 B). The ligated cDNA vectors and empty vector controls were individually transformed into the *GmbHLHm1* promoter-specific Y1HGold strain. The following assay involved the activation of the AbA resistance gene (AbA^r) when encoded protein from the cDNA library binds to the *GmbHLHm1* promoter (Clontech Laboratories, 2012). Successful binding is determined through antibiotic selection (e.g., growth on the SD/-LEU/ AbA^{250} medium plates). A total of 43 colonies grew on the SD/-LEU/ AbA^{250} selection media after 5 days of incubation at 28°C. Identified colonies were selected, plasmid DNA purified, and cDNA size was determined by restriction digest and gel electrophoresis. PCR amplification of identified cDNAs, larger than 400 bp, was performed on 36 isolated plasmids. Each plasmid was sequenced further with the flanking primer sequence AATACGACTCACTATAGGGCGAGC. Sequence alignments were performed using Geneious software, from which, 7 unique sequences were identified by BLAST analysis within Phytozome (<https://phytozome-next.jgi.doe.gov/blast-search>).

To reduce false positive colonies, plasmids of the 7 unique sequences were re-transformed into *GmbHLHm1* promoter-specific yeast strains and grown again on the SD/-LEU/ AbA^{250} medium plates, respectively. Those which continued to show AbA resistance, similar to that of the control yeast line transformed with the positive control vector (p53-pAbAi) and p53 Control Insert, were selected and assumed positive for an interaction between the protein from the soybean nodule cDNA sequence and the *GmbHLHm1* promoter (Figure 4.6).

From the NCBI BLAST analysis of the sequenced cDNAs, five were found to have annotated transcripts in the database (Table 4.1). These included gene sequences with motifs identified as: 1) sphingomyelin synthetase-like domain; 2) translation machinery associated (*TMA7*); 3) translation

initiation factor 5A (*EIF5A*); 4) metallothionein (metallothio2) and 5) *MYB* family transcription factors (Table 4.1). The sphingomyelin synthetase-like domain is responsible for transferase activity, transferring phosphorus-containing groups, which is an integral component of the plasma membrane, vacuole, endoplasmic reticulum membrane, and the Golgi membrane in soybean (Panther, 2022). Phosphorus is very important in nodulation and symbiotic nitrogen synthesis, for it is a key element of ATP and is required for nitrogenase and leghemoglobin (Tang et al., 2001; Divito and Sadras, 2014). Expressed in nodules, *GmbHLHm1* is also a membrane-localized basic helix-loop-helix (bHLH) DNA-binding transcription factor. Both these genes are related to nodulation and located in the plasma membranes, which could preclude a possible interaction. The *MYB* family transcription factor PHOSPHATE STARVATION1 (PHR1) was reported to activate AON under Pi starvation, for direct binding to the promoter region of NIN (Isidra-Arellano et al., 2020). The translation machinery associated gene (*TMA7*), and translation initiation factor 5A (*EIF5A*) are associated with gene transcription and protein translation, respectively (Fleischer et al., 2006; Dubos et al., 2010; Tauc et al., 2021). They may bind to the *GmbHLHm1* promoter in a role linked to gene transcription and/or protein translation. Metallothioneins (MTs) are a group (types 1–4) of cysteine-rich metal-binding proteins that are involved in metal homeostasis and reactive oxygen species (ROS) response (Hassinen et al., 2011), but their roles are not fully known in the plant. MT2 is expressed in soybean roots, leaves, and seeds (Pagani et al., 2012). A study reported a synergistic effect between arbuscular mycorrhizal fungi and *Bradyrhizobium* on metallothionein-linked gene expression in soybeans grown under a zinc stress (Ibiang and Sakamoto, 2018). This may indicate the potential interaction between MTs and the *GmbHLHm1*, however, the mechanism remains to be studied.

A second parallel experiment was conducted with a promoter of the genetically linked ammonium facilitator protein, GmAMF3 (Chiasson et al., 2014). In total, 48 positive colonies were selected, confirmed, and then sequenced. Sequence alignments were performed using Geneious software, and 12 unique sequences were identified from the alignments. The growth of the 12 transformed yeast lines (another yeast transformation to eliminate false positive colonies) showed AbA resistance, indicating the stable interaction between the protein from the soybean nodule cDNA sequence and the *GmAMF3* promoter (Figure 4.7). These 12 sequences were analysed using the BLAST program against the soybean genome (assembly version Glycine max Wm82.a4.v1.) in

the Phytozome (<https://phytozome-next.jgi.doe.gov/blast-search>). From the BLAST results, 11 sequences were found to have annotated transcripts (Table 4.2). These included gene sequences with motifs identified as 1) Linoleate 9S-lipoxygenase; 2) Transcription factor GRAS domain family (GRAS); 3) Nodulin (Nodulin-22); 4) F-box containing protein; 5) Gamma-tubulin complex component; 6) Small subunit ribosomal protein S23e (RP-S23e); 7) Large subunit ribosomal protein L35e (RP-L35e); 8) G protein-coupled receptor 157-related; 9) Ubiquinol-cytochrome c reductase; 10) WW domain binding protein WBP-2, contains GRAM domain and 11) RING-type zinc finger domains.

Lipoxygenases (LOXs) are a family of non-heme, non-sulphur oxidoreductase, iron-containing dioxygenases that exist ubiquitously in eukaryotes. They catalyse the oxidation of lipids and are related to seed germination, seed nutrient storage, herbivore defence, stress, and nodule development (Gardner et al., 1996; Hayashi et al., 2008; Viswanath et al., 2020). Studies reported that LOX genes are induced at the beginning of the nodule development and enhanced in the lumen of the infection thread, while an increase of lipoxygenase activity was observed 28 DPI (Gardner et al., 1996; Junghans et al., 2004). LOX9 was identified as a potential cDNA that could activate the promoter region of the *GmAMF3*. Both genes are co-expressed in the outer parenchyma and the developing vascular bundles (Hayashi et al., 2008; Chiasson et al., 2014). RNAi silencing of *GmAMF3* results in impaired nodule formation and symbiotic (infected) cell development, indicating its importance for normal nodule formation and growth (Evgenia Ovchinnikova, 2014). However, RNAi-silenced LOX9 in transgenic hairy roots has no impact on nodule growth and plant development (Hayashi et al., 2008). Taken together, these two experiments imply that LOX9 could positively regulate the expression of *GmAMF3*, possibly through an oxylipin-induced activation of gene expression previously observed in *Arabidopsis* (Walper et al., 2016).

The transcription factor GRAS domain family (GRAS) was also identified to interact with the promoter of *GmAMF3*. GRAS proteins have been aligned with a range of functionalities including GA signalling (Hirsch and Oldroyd, 2009). An *in silico* study using the PlantCARE (<https://bioinformatics.psb.ugent.be/webtools/plantcare/html/>) identified a GA-linked GARE motif (TCTGTTG) in the promoter region (95 bp upstream of the start codon) of *GmAMF3* (Lescot et al., 2002). This could suggest a potential GA regulation of *GmAMF3* and having an impact on

nodulation and symbiotic nitrogen fixation. Further studies are required to understand if GA regulates *GmAMF3* expression.

Multiple copies of nodulin 22 (nodulin genes are organ-specific plant proteins induced during symbiotic nitrogen fixation) were identified. Rodriguez-López (2014) reported that nodulin 22 is synthesized in Rhizobium-infected roots and is thought to inhibit protein aggregation and help maintain ER homeostasis preventing the induction of cell death via the unfolded protein response during episodes of oxidative stress in common beans (Mohammad et al., 2004). Both *GmAMF3* and Nodulin-22 are located in the roots and linked to the legume-Rhizobium symbiosis. There might be undiscovered regulatory mechanisms both proteins share. Further study is required for more information.

The F-box protein is a large family that regulates a diverse range of hormone signalling and stress responses in plants. F-BOX genes display complex tissue-specific transcriptional patterns, suggesting their putative role in legume seed development and nodulation (Bellieny-Rabelo et al., 2013; Jia et al., 2017). TOO MUCH LOVE (TML), a root transcription factor functioning downstream of CLE-RS1/RS2 of the autoregulation of nodulation (AON) program, is a Kelch repeat-containing F-box protein (Takahara et al., 2013a). It is unclear which type of F-box protein in the family interacts with the *GmAMF3* promoter. A C₃HC₄-type RING-type zinc finger protein was reported to regulate rhizobial infection and nodule organogenesis in *L. japonicus* (Cai et al., 2018). However, the relations between these genes and why they could bind to the promoter of *GmAMF3* require further investigation.

The G protein-coupled receptor 157-related G-protein coupled receptors (GPCRs) are plasma membrane-spanning proteins that transduce specific physical and chemical extracellular signals into the cell (Millner and Causier, 1996). Ubiquinol-cytochrome c reductase is located in the plasma membrane and serves as the electron junction in many respiratory systems (Berry et al., 1991; Prochaska et al., 2017). GRAM domain, containing WBP-2, is a putative membrane-associated protein (Doerks et al., 2000). These three genes are plasma membrane located which is the same as *GmAMF3*. The co-localization might contribute to the promoter-binding activity.

Other proteins that interacted with the promoter region of *GmAMF3* have different functions, but the relation to the nodule, symbiotic nitrogen fixation and *GmAMF3* remain unclear. For example, Gamma-tubulin complex is involved in nuclear architecture (Batzenschlager et al., 2013). Small subunit ribosomal protein S23e (RP-S23e) is implicated in the binding of transfer RNA to messenger RNA (Thompson and Hearst, 1983; Schluenzen et al., 2000) Large subunit ribosomal protein L35e (RP-L35e) catalyses the key chemical event in protein synthesis and peptide bond formation (William E. Balch, 2017).

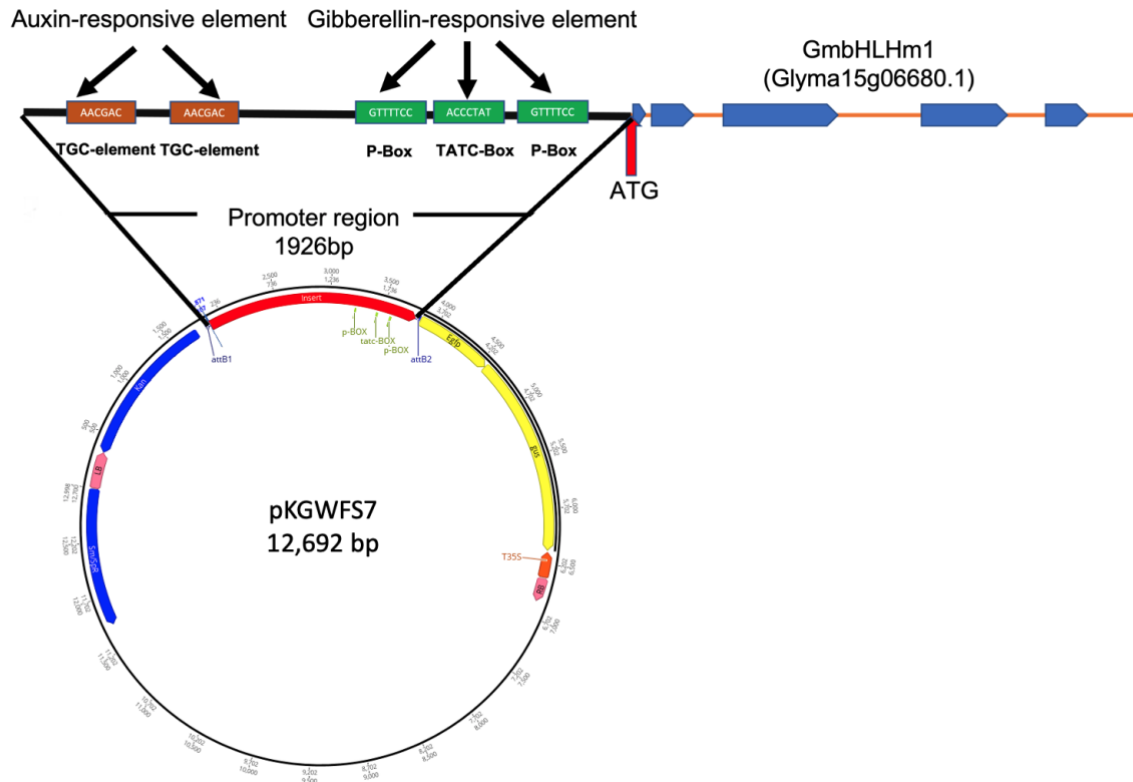


Figure 4. 1 Map of pKGWFS7 vector with inserted the *GmbHLHm1* promoter. pKGWFS7 was used in the *Agrobacterium rhizogenes* K599 hairy root transformation of soybean hypocotyls (Karimi et al., 2002; Mohammadi Dehcheshmeh, 2014). The vector contains the selectable marker, *nptII*, which encodes neomycin phosphotransferase for kanamycin resistance, an enhanced green fluorescent protein (eGFP) and a beta-glucuronidase (*gus*) driven by the *GmbHLHm1* promoter under study. Streptomycin-spectinomycin resistance (Sm/SpR) for plasmid selection (Karimi et al., 2002).

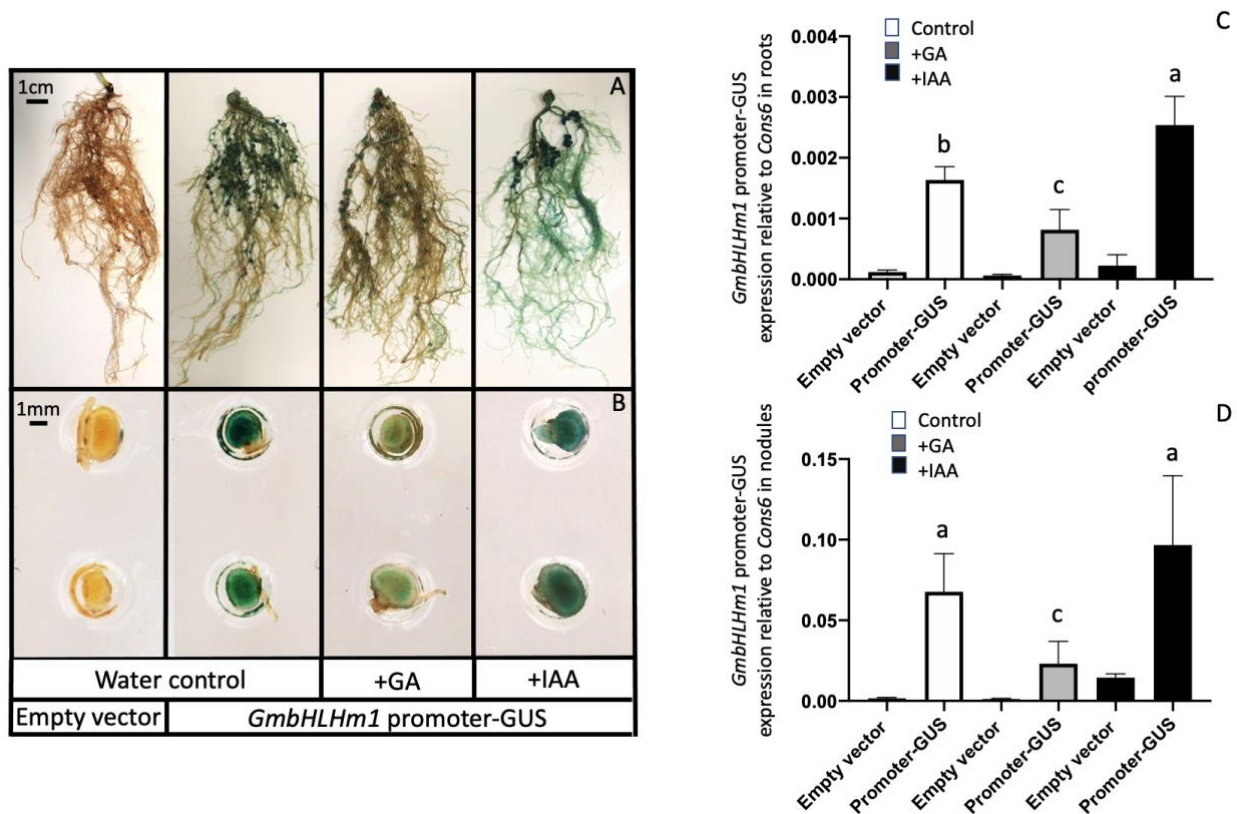


Figure 4. 2 *GmbHLHm1* promoter-driven GUS expression in nodules and roots. 28-day-old transgenic nodules were stained for GUS activity. (A) the whole root; (B) nodule cross sections after supply of either 1ppm IAA or 4ppm GA. *GmbHLHm1* gene expression levels in roots and nodules with either IAA or GA treatments; (C) and (D) GUS expression levels in roots and nodules with 1ppm IAA or 4ppm GA supply. The expression of GUS levels was normalized with *Con6* as a reference gene and was calculated using the $2^{-\Delta\Delta C_t}$ method (Libault et al., 2008). Values were means \pm SE (n=4) biological replicates. The letters indicate the significant differences between groups based on the one-way ANOVA ($P < 0.05$).

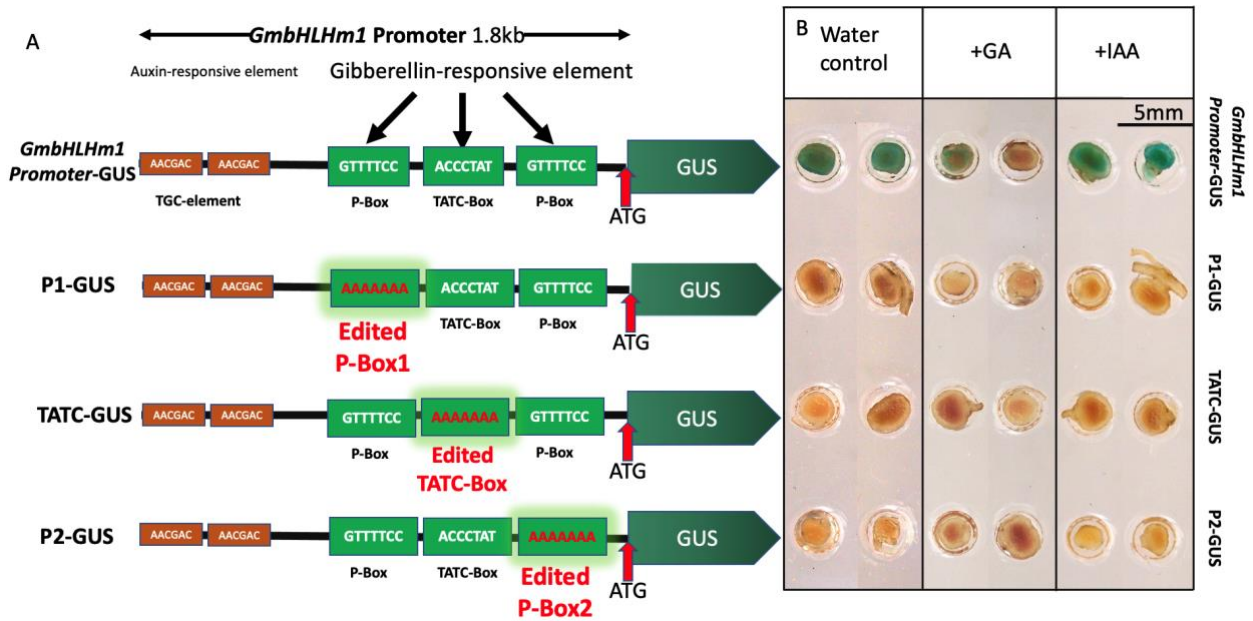


Figure 4. 3 Illustrations of edited *GmbHLHm1* promoters and their activation of GUS expression in soybean nodules. (A) Three Gibberellin-responsive elements of the *GmbHLHm1* promoter were edited respectively. Bases of each element were replaced with a similar number of adenine residues. (B) GUS expression of each edited construct in 28-day-old soybean nodules treated with water, 4ppm GA or 1ppm Auxin treatments for 5 days. GUS staining was developed over 5 hours. Images are representative samples of repeated nodule experiments.

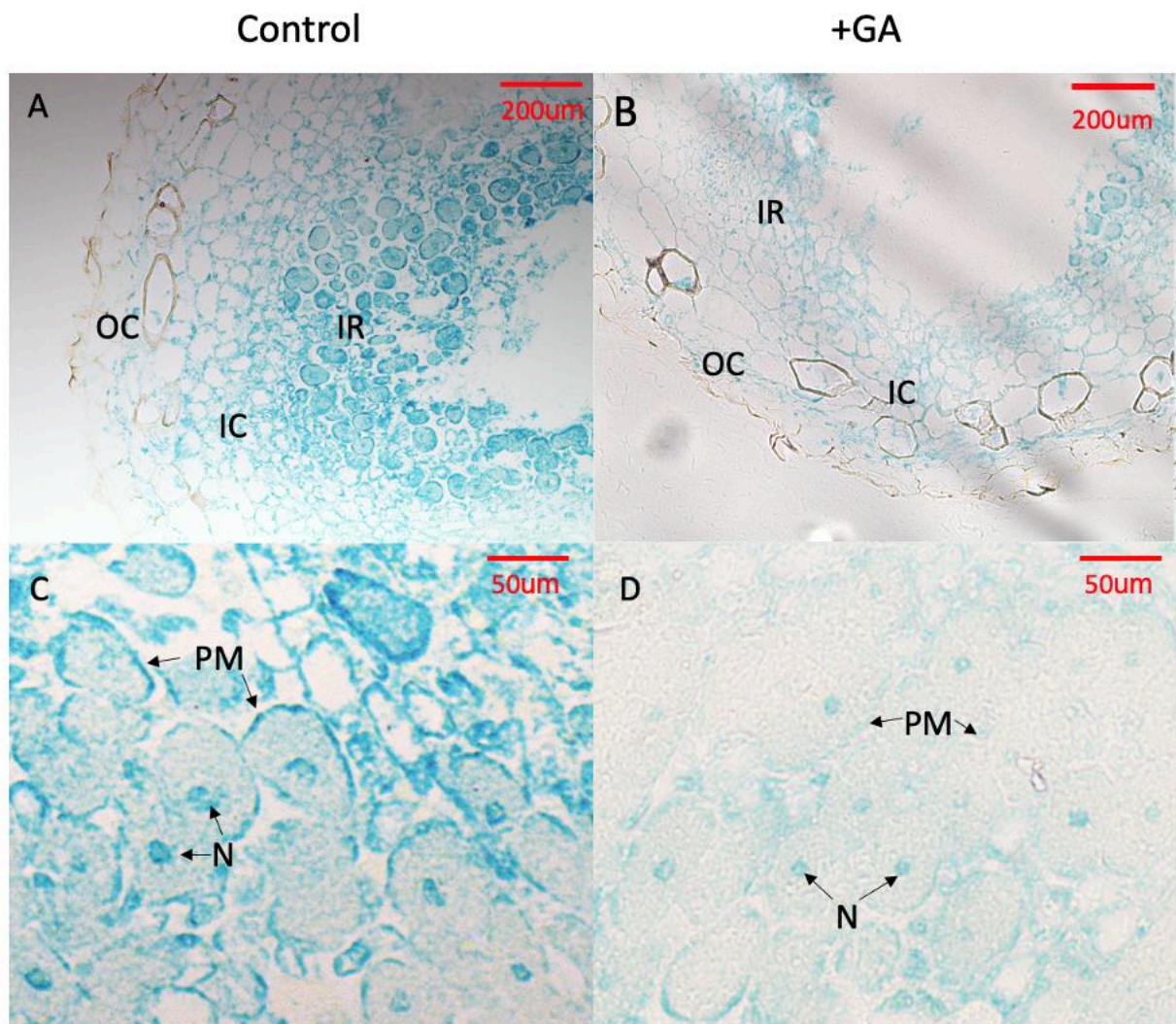


Figure 4.4 *GmbHLHm1* promoter-GUS expression with/without GA treatment. 28-day-old soybean nodules were stained for GUS analysis (see methods 4.4.1). Plants were treated with water (A, C) or 4ppm GA₃ (B, D). Nodule cross sections identify the central infected region (IR), which contains infected cells (I). The IR is surrounded by the inner cortex (IC) with vascular bundles (VB) and the outer cortex (OC). In the IR (C and D), GUS staining is observed in both infected and uninfected cells including within the enlarged infected cell nucleus (N). GUS signal was less intense in those tissues receiving a GA treatment. Images are representative of multiple nodules treated with this experiment.

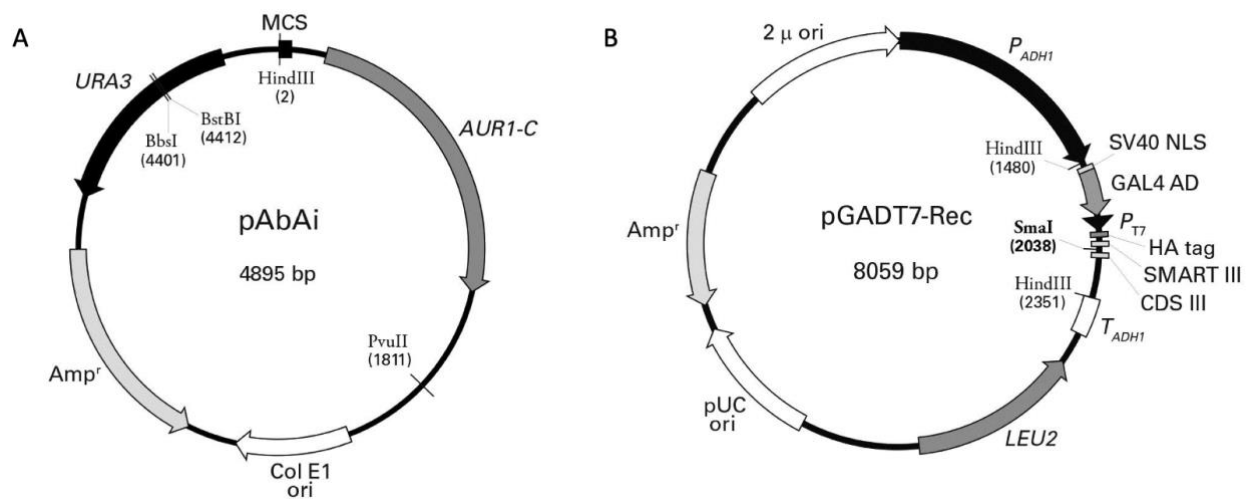


Figure 4. 5 Maps of vector pAbAi and vector pGADT7-Rec used for Yeast One-Hybrid promoter screening. (A) The pAbAi was used for constructing transgenic yeast strains with the promoter construct of interest and to provide AbA resistance. (B) The pGADT7-Rec was used for constructing the cDNA library from soybean nodules. Soybean nodule cDNA was ligated into pGADT7-Rec and the collective library of ligated cDNAs transformed in promoter:pAbAi transformed yeast.

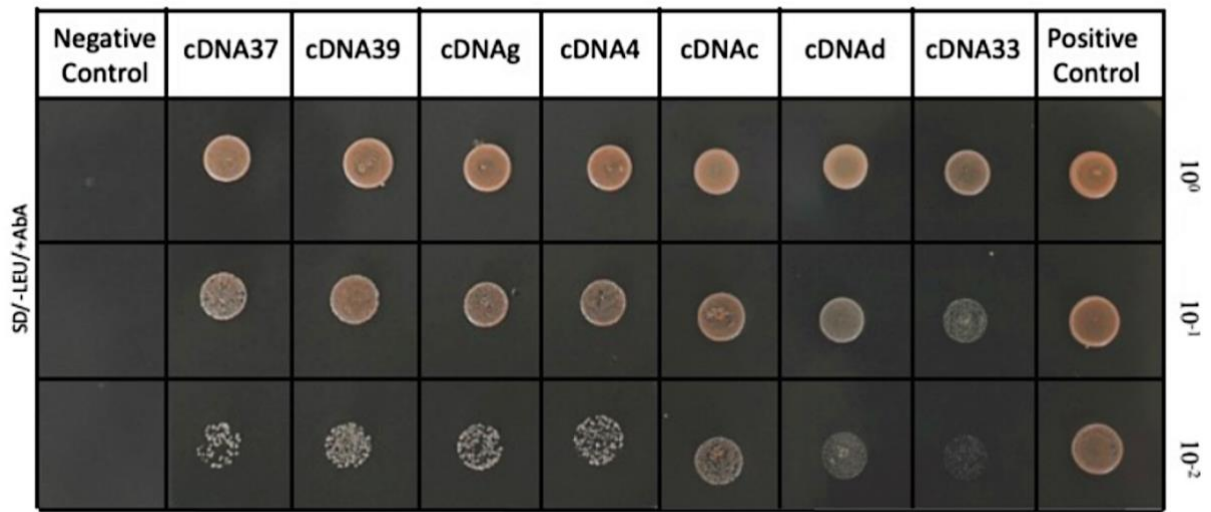


Figure 4. 6 The growth of serial-diluted cultures of AbA resistance yeast lines, with *GmbHLHm1* promoter inserted in the genome. Serial diluted cells were plated onto solid yeast media (SD, leu, AbA²⁵⁰) and grown for 5 days at 28°C.

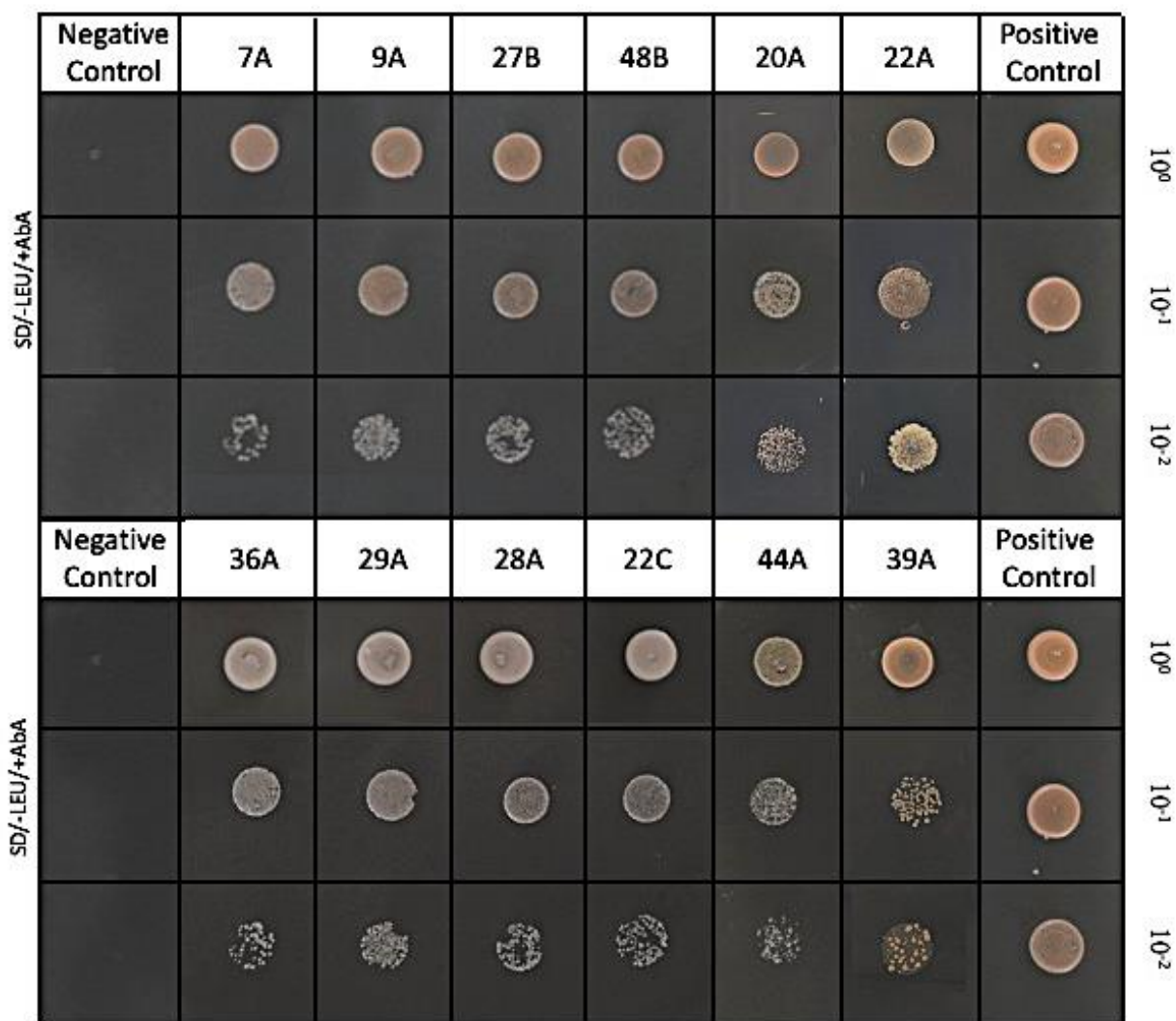


Figure 4. 7 The growth of serial-diluted cultures of AbA resistance yeast lines, with *GmAMF3* promoter inserted in the genome. Serial diluted cells were plated onto solid yeast media (SD, leu, AbA²⁵⁰) and grown for days at 28°C.

cDNA	Location	Number of colonies	Homology analysis	E-Value	Species and Accession
cDNA 37	Gm01, 03, 04, 07, 18	12	Sphingomyelinsynthetase-like domain	9.36e-40	<i>Glycine max</i> [PTHR21290]
cDNA 39	Gm03, 07, 08, 14, 20	10	Translation machinery associated (TMA7)	8.28e-47	<i>Glycine max</i> [PTHR21290]
cDNA g	Gm01, 02, 04, 05, 06, 17, 18	8	Translation initiation factor 5A (EIF5A)	1.40e-68	<i>Glycine max</i> [PTHR11673]
cDNA 4	Gm07	2	Metallothionein (Metallothio2)	2.93e-45	<i>Glycine max</i> [PF01439]
cDNA c	Gm14, 17	2	MYB family transcription factor	2.02e-66	<i>Glycine max</i> [PTHR10641]
cDNA ad	Gm05, 15	1	Uncharacterized	2.24e-2	<i>Glycine max</i> [PTHR33924]
cDNA 33	Gm13	1	Uncharacterized	1.72e-92	<i>Glycine max Lee</i> [PTHR34950]

Table 4. 1 Identified soybean nodule cDNAs isolated through interactions with the promoter of *GmbHLHm1* in transgenic yeast (*Aureobasidin A* resistant). The BLAST result was generated using Phytozome (<https://phytozome-next.jgi.doe.gov>). The assembly version is *Glycine max Wm82.a4.v1*.

cDNA	Location	Number of colonies	Homology analysis	E-Value	Species and Accession
7A	Gm01, 02, 03, 04, 05, 05, 06, 077, 08, 09, 10, 11, 12, 13, 14, 15, 16, 18, 20	8	Linoleate 9S-lipoxygenase / Linoleate 9-lipoxygenase	0	Glycine max Lee. [PTHR11771]
9A	Gm01, 02, 03, 04, 07, 08, 09, 14, 15, 16, 17, 18, 20	5	Transcription factor GRAS domain family (GRAS)	0	Glycine max Lee. [PF03514]
27B	Gm10, 13, 15, 19, 20	3	Nodulin (Nodulin-22)	0	Glycine max [PF02451]
48B	Gm03, 04, 05, 06, 11	2	F-box containing protein	3.05e-152	Glycine soja [SSF52047]
20A	Gm04, 06, 08	2	Gamma-tubulin complex component	0	Glycine max Lee [PTHR19302]
22A	Gm03, 10, 12, 13, 19	2	Small subunit ribosomal protein S23e (RP-S23e)	3.23e-143	Glycine soja; Glycine max Lee [K02973]
36A	Gm10, 13	1	Large subunit ribosomal protein L35e (RP-L35e)	5.04e-133	Glycine soja; Glycine max Lee [K02918]
29A	Gm14, 17	1	G protein-coupled receptor 157-related	3.16e-152	Glycine max [PTHR23112]
28A	Gm02, 14	1	Ubiquinol-cytochrome c reductase	1.11e-170	Phaseolus acutifolius [SSF81508]
22C	Gm8, 16	1	WW domain binding protein WBP-2, contains GRAM domain	2.04e-131	Glycine max [KOG3294]
44A	Gm5, 17	1	RING-type zinc finger domains	2.25e-91	[IPR00841]
39A	Gm10, 20	1	Uncharacterized	2.18e-125	Glycine soja [PTHR33878]

Table 4. 2 Soybean nodule cDNAs were identified to bind to the *GmAMF3* promoter. The blast result was conducted using Phytozome (<https://phytozome-next.jgi.doe.gov>). The assembly version *Glycine max Wm82.a4.v1*.

Name	Sequence
p-box1 f	aaaaaaaGTAAAAATGAGTTGGGCAAATAACCTTTG
MYBp-box1 r	TTCATTATTTTCTAAGTTCCTTTCTTAGATCCT
tatc-box f	aaaaaaaAGTCTATTATCCTTGGTTGAAAATAGGC
tatc-box r	TTTTATATTTTAGAGACCCCTTCATGCTG
p-box2 f	aaaaaaaAATTACAACAACGAAATATATAATCATCAGCTTC
p-box2 r	TATACTCTACCCCACTGTATTACAGCATATAAC

Table 4.3 List of Primers for *GmbHLH1* promoter-GUS construct editing.

4.3 Discussion

Three GA-responsive elements and two Auxin-responsive elements were identified in the promoter region of the *GmbHLHm1* (Mohammadi Dehcheshmeh, 2014). To investigate the effect of GA and IAA on *GmbHLHm1* expression, a soybean transgenic hairy root system was used to create transgenic roots and nodules containing a *GmbHLHm1* promoter-GUS construct. Plants were treated with water, GA, or IAA over successive days. GUS-stained nodules cross sections were screened for GUS activity. *GmbHLHm1* GUS expression was mainly found in infected cells in the infected zone and to a lesser extent in the inner and outer cortex region (Figure 4.4 A and B). Localization was also observed in the enlarged nucleus of the infected cells (Figure 4.4 C and D). GUS expression was repressed in both root and nodule tissues with the GA treatment, while there was no decrease observed with the application of Auxin (Figure 4.2 A and B). Similar tissues were tested for gene expression in response to water, GA, or Auxin treatments using qPCR. Auxin enhanced *GmbHLHm1* promoter activity (GUS signal) and enhanced the expression of associated mRNA in roots but not significantly in nodules (Fig 4.12 C, D). No GUS expression was observed in each of the three edited constructs (Figure 4.3) indicating that each of the GA-responsive elements is individually important in regulating the expression of the *GmbHLHm1*. Although we found that there are three GA-responsive elements on the promoter of *GmbHLHm1* and have shown through experiments that GA has a regulatory effect on the expression of *GmbHLHm1*, we don't know whether this regulation is via direct binding of GA to these GA-associated elements or indirectly through other regulatory pathways. The positive response to auxin supply suggests the two untested auxin elements may have a more dominant impact on *GmbHLHm1* activity, while GA is a collective repressor of *GmbHLHm1* or other networks in the nodule.

GmAMF3 was previously identified in soybean nodules (Chiasson et al., 2014). Gene expression was primarily localized to nodule parenchyma cells and the enveloping vascular tissues (Chiasson et al., 2014). In yeast and *Xenopus laevis* oocytes, GmAMF3 was suggested to behave as an NH₄⁺ permeable transport protein and *GmbHLHm1* is a potential TF of *GmAMF3* and other *AMF* homologs in yeast (*ScAMF1*) (Chiasson et al., 2014). In soybean, RNAi silencing of the *GmAMF3*

results in hampered nodule formation and symbiotic (infected) cell development, indicating that the AMF3 presence is important for normal nodule formation and growth (Evgenia Ovchinnikova, 2014). However, in the *bhlhm1* nodules, no significant change in *GmAMF3* expression was observed in the *GmbHLLHm1* silenced soybean nodules (Chiasson et al., 2014). As AMF3 is an ammonium channel, it most likely has an important functional role in the mediation of ammonium transport in root and nodule cells. The regulatory control of *GmAMF3* and *GmbHLLHm1* remains poorly understood. It is expected that a range of activators (protein, hormone) may be involved in their regulation. To identify possible candidates that interact with *GmbHLLHm1* or *GmAMF3*, Yeast One-Hybrid assays were conducted using soybean nodule cDNA as possible targets to bind or interact with the promoters of both genes.

Five annotated proteins were found to interact with the promoter of *GmbHLLHm1*, and eleven for *GmAMF3* (Table 4.1 and 4.2). This study wasn't able to follow up on these candidates and confirm direct interactions with the promoters using EMSA-based shift analysis or other similar approaches. Instead, a preliminary analysis of the cDNAs was conducted based on sequence analysis and interrogation of DNA databases to identify annotated homologs. Proteins related to nodulation and symbiotic nitrogen fixation processes were identified. These, include an MYB family transcription factor and an MT2 protein that interacted with *GmbHLLHm1*, and nodulin 22 which interacted with the promoter region of the *GmAMF3* (Mohammad et al., 2004; Hayashi et al., 2008; Panther, 2022). Some proteins share membrane localization patterns with *GmbHLLHm1* and *GmAMF3*, such as the sphingomyelin synthetase-like domain, some plasma membrane-bound lipoxygenases (Fornaroli et al., 1999) and the G-protein coupled receptors (GPCRs) (Millner and Causier, 1996; Junghans et al., 2004; Hayashi et al., 2008; Panther, 2022). The co-localization in the membranes could also preclude a possible interaction. Other proteins are related to important processes to plant development such as gene transcription and protein translation (TMA7, EIF5A), small subunit ribosomal protein, and large subunit ribosomal protein, hormone signalling, and stress (F-box and GRAS) (Fleischer et al., 2006; Dubos et al., 2010; Li et al., 2011; Takahara et al., 2013a; Tauc et al., 2021). The mechanisms of how they regulate the *GmAMF3* and *GmbHLLHm1* are unclear. Further studies are required to explain the mechanism of their regulation.

As a potential TF of *GmAMF3*, the Yeast One-Hybrid assay failed to identify *GmbHLHm1* as probably an interactor of *GmAMF3*. This does not mean that *GmbHLHm1* does not bind to the promoter region of *GmAMF3* in nodules, because the construction of the cDNA library has a certain randomness. To further investigate the regulation of *GmbHLHm1* on *GmAMF3*, another Yeast One-Hybrid experiment could be conducted using the *GmbHLHm1* as the prey and the *GmAMF3* promoter as the bait. Moreover, this Yeast One-Hybrid experiment helped to target several candidate proteins that potentially bind to the promoter of the *GmbHLHm1* and *GmAMF3*. Future research could emphasis on proteins that are related to nodulation regulation, for example, how nodulin 22 interacts with *GmAMF3* promoter, and whether and how MYB family protein regulates *GmbHLHm1*.

4.4. Material and method

4.4.1 Promoter-GUS fusion construct and GA responsive element editing *GmbHLHm1* Promoter-GUS fusion construct and hairy root transformation.

Soybean (*Glycine max L. cv Snowy*) genomic DNA was isolated from nodules using the PureLink™ Genomic Plant DNA Purification Kit. An 1863 bp section upstream of the *GmbHLHm1* start codon was cloned using primers (FWD: agcatggccgtgatttaacctaaagaaaaccaattc; REV: gacgtaacattataactcaaactacaacatcc). The promoter was cloned into the pCR™8 vector and then recombination cloned into the pKGWFS7 vector with the Gateway™ cloning system. The promoters with edited GA responsive elements were constructed by PCR mutagenesis using the primers listed in Table 4.3. The intact *GmbHLHm1* promoter in pKGWFS7 was used as the template. Phusion High-Fidelity DNA Polymerase was used to amplify the edited promoter-pKGWFS7 construct. The PCR products were circularized using NEBuilder® HiFi DNA Assembly. Constructs were transformed into the *Agrobacterium rhizogenes* K599 strain.

The Promoter-GUS fusion construct was used for hairy root transformation with the method illustrated in Chapter 2.4.1 (Mohammadi-Dehcheshmeh et al., 2014). The presence of the

promoter–GUS construct in the hairy roots was confirmed by PCR analysis on isolated root genomic DNA with primers (FWD: ctccgaattcgccttgatttaacc; REV: ccagtgcacctgcaggcat). Only nodules on confirmed hairy roots (PCR positive) were further studied in the promoter analyses in later experiments.

Soybeans with transgenic hairy roots were inoculated with NoduleNTM Legume Inoculant Peat and cultivated in controlled temperature chambers as described in Chapter 2.4.1. Plants with 23-day-old nodules were treated with/without 4ppmM GA₃ or 1ppm IAA in the -N nutrient solution for five days. 28-day-old transgenic nodules and hairy roots attached were harvested, and GUS staining was performed on both tissues. The GUS staining was performed according to the Mohammadi Dehcheshmeh (2014). The harvested transgenic hairy roots with nodules were soaked in 90% ice-cold acetone in a 50ml centrifuge tube as samples. Each sample was rinsed twice in sodium phosphate buffer for 5 min, before being transferred into GUS staining buffer. GUS staining buffer-covered samples were transferred in a vacuum for infiltration for 30 min before being incubated at 37°C for another 5 hrs.

Nodules containing the Promoter-GUS cassettes were fixed and embedded and then analysed under light microscopy (Márquez et al., 2005; Weigel and Glazebrook, 2008), with modifications illustrated below. After GUS staining, nodules were cut in half and placed in a 1.5 ml centrifuge tube and fixed in fresh 4% (w/v) paraformaldehyde solution for 2 hrs under vacuum. Each tissue sample was then dehydrated by sequentially immersing it in 30%, 50%, 80%, and 100% ethanol (20 min for each concentration and one hr for 100% ethanol). The infiltration was performed with the Technovit[®] 7100. The embedding and mounting steps were performed according to Márquez et al. (2005).

Tissues in the resin blocks were sectioned with the Leica RM2255 Fully Automated Rotary Microtome in slow mode and thickness of 10-20um. The sectioned tissue-resin slices were placed on a glass slide and a drop of water was added followed by a cover slip and sealed in resin glue to obtain a glass specimen for optical microscope observation. The Leica DM2500 M Materials Analysis Microscope was used for microscopy screening.

4.4.2 Yeast One-Hybrid

The Matchmaker® Gold Yeast One-Hybrid Library Screening System was used for the Yeast One-Hybrid experiment. The *GmbHLHm1* promoter and *GmAMF3* promoter were amplified as target genes for the transcription factors-promoter (protein-DNA) Interaction study. The library constructing and screening protocols were from the Matchmaker® Gold Yeast One-Hybrid Library Screening System User Manual, with some modifications illustrated in detail below.

For *GmAMF3* (Glyma08g06880), 1451bp's upstream of the start codon was amplified from soybean genomic DNA using primers (FWD: AAGCTTGAATTCGAGCTC gaaggggtgaattgcccgtt; REV: ACATGCCTCGAGGTCGACTccaggtggtgtttgctgtt). The primers allowed overlap bases (Capital) from the pAbAi vector. Likewise, the *GmbHLHm1* promoter was amplified from the promoter-GUS fusion construct (see Figure 4.1) with pAbAi overlap (Capital) with primers (FWD: GAATTGAAAAGCTTGAATTCGAGCTCT gatttaacctaagaaaaccaattccttattttgtattagg; REV: TACAGAGCACATGCCTCG aggtcgactatactcaactacaacatccatgtacatgc). The linearised pAbAi vector with the blunt end was amplified with primers (FWD: gtcgacctcgaggcatgtgctc; REV: gagctcgaattcaagcttttcaattcatc). The circular pAbAi vector was used as a template, using VELOCITY® DNA Polymerase Bioline™. The Gibson Assembly® HiFi Kit was used to assemble PCR products of each promoter fragment with the PCR amplified linear pAbAi product, building *GmAMF3/GmbHLHm1* promoter- pAbAi constructs as the bait plasmid for yeast transformation.

GmAMF3 or *GmbHLHm1* promoter - pAbAi constructs were transformed into the Y1HGOLD yeast strain to prepare two individual bait yeast strains, respectively. The bait strains were then grown on SD/-Ura medium plates with 100/200/300 ng/ml Aureobasidin A (AbA), respectively, to determine the minimal inhibitory concentration of AbA for each bait strain. Both strains were completely inhibited at the AbA concentration of 200 ng/ml. Therefore, 250 ng/ml concentration was used as a reference for the library screening to further eliminate the false positive.

The cDNA library constructions were generated according to the Matchmaker® Gold Yeast One-Hybrid Library Screening System User Manual. Total RNA was extracted from the 28-day-old soybean nodules with Monarch® Total RNA Miniprep Kit. First-strand cDNA was synthesized with oligo-dT primers and the RNA samples as a template. Double-stranded cDNA (ds cDNA)

was amplified by long-distance PCR (LD-PCR) with an optimized PCR cycle of 20, according to the concentration of the total RNA sample extracted from nodules (detailed calculation illustrated in the kit manual).

The ds cDNA was co-transformed into the constructed bait yeast strains with pGADT7-Rec AD Cloning Vector (Sma I-linearized), using the YeastmakerTM Yeast Transformation System 2, to create One-Hybrid cDNA libraries of *GmAMF3* or *GmbHLHm1* promoters, respectively. For each transformation reaction, the yeast culture was serially diluted into 1/10, 1/100, 1/1000, and 100 μ l of each dilution was spread on SD/-Leu and SD/-Leu/AbA²⁵⁰ agar plates (TakaraTM Yeast Media Set 1 Plus, Cat. No. 630493). 5-10 plates were made for each dilution, respectively. After five days of incubation, the colonies were screened, and colonies grown on SD/-Leu/AbA²⁵⁰ agar plates were picked for positive interaction confirmation. The Matchmaker[®] Insert Check PCR Mix 2 was used to confirm the positive interaction and eliminate insertions shorter than 400 bp and the positive colony with more than one prey plasmid (more than one band on the gel electrophoresis) inserted.

Each selected colony was grown for 2-3 days in 3 ml SD/-Leu liquid culture. 1.5 ml of each liquid culture was transferred into a 2 ml centrifuge tube with 100 μ l of 100 μ m diameter glass beads (Burke et al., 2000). The yeast cell wall was disrupted in the centrifuge tube by shaking in the Geno/Grinder[®] at high speed for 5 min. After the cell wall disruption, the yeast plasmid extraction was performed using the QIAprep[®] Spin Miniprep Kit. Plasmids extracted from yeast had low concentrations and poor purity. To obtain high-quality plasmid samples, each plasmid extracted from the yeast strains was transformed into *E. coli* (XL1-Blue) and grown for plasmid extraction.

To further eliminate the false positive interaction, each plasmid extracted from the *E. coli* was transformed into the compatible bait yeast strain (yeast strain with *GmAMF3* or *GmbHLHm1* promoter- pAbAi construct only) again and grown on the SD/-Leu/AbA²⁵⁰ agar plates. The plasmid interacts with the promoter in the bait yeast strain and showed colonies on plates after five days of incubation (positive). The plasmid generated positive results were sent for sequencing and analysis. The sequencing results were analysed and processed with the Geneious software. The processed sequences were blasted in the Phytozome (<https://phytozome-next.jgi.doe.gov/blast-search>) against the soybean genome (version: Glycine max Wm82.a2.v1).

Chapter 5 Functional analysis of the nodule transcription factor *LjbHLHm1.1* in *Lotus japonicus*

5.1 Introduction

Lotus japonicus (*Lotus*) is a well-characterized model legume. *Lotus* has a small diploid genome (472Mb, six chromosomes), self-pollinated, extensive seed population, short growing cycle and readily permits *Agrobacterium tumefaciens*-mediated transformation (Handberg and Stougaard, 1992; Sato and Tabata, 2006; Sato et al., 2008). *Lotus* is widely used in the study of rhizobia legume interactions. After the genome structure of *L. japonicus* was reported, it provided the first chance to study the genetic system of legumes (Sato et al., 2008). *Lotus* nodules do not have a continuous growing meristem, resulting in a determinate nodule (Lotocka et al., 2012). *Lotus* nodules are a good reference for determinate nodule research observed in other legume crops, such as common bean and soybean.

LORE1 (*Lotus retrotransposon 1*) is a long terminal repeat (LTR) retrotransposon, that belongs to a low-copy-number, TY3-gypsy retrotransposon family (Madsen et al., 2005). The insertion of *LORE1* into functional genes creates potential gene-disruption mutations (Madsen et al., 2005). This character provides a tool for studying the function of genes through loss-of-function in the *L. japonicus* genome. A *LORE1* gene tagging insertion population was established containing 120,000 *L. japonicus* mutant lines, accessible for research use (Madsen et al., 2005; Fukai et al., 2012; Mun et al., 2016). This population are widely used for the legume plant study, especially plant-microbe interactions (Mun et al., 2016). The *LORE1* insertion also found in *LjbHLHm1.1*

and *1.2*, homolog of *GmbHLHm1*. Lines with these insertions are ideal plant materials to investigate the function of bHLHm1 in nodulation in *L. japonicus*.

The nodulation of *L. japonicus* is affected by gibberellins. The inhibiting effect of GA was counteracted by the application of uniconazole P, a GA biosynthesis inhibitor (Maekawa et al., 2009). The SLEEPY1 (SLY1) protein contains an F box motif and functions as a positive regulator in GA signalling by facilitating the degradation of the GA signalling negative regulators, such as GRAS proteins (containing DELLA domain), leading to the up-regulated production of endogenous GA (Dill et al., 2004). In *L. japonicus*, the overexpressed SLEEPY inhibited root nodule formation despite normal root development (Maekawa et al., 2009). *L. japonicus* inoculated with a GA-synthesis-deficient *M. loti* strain developed more nodules than those inoculated with the wild-type. The result indicates that GA from rhizobia can inhibit lateral nodule formation (Tatsukami and Ueda, 2016). Moreover, the genes for GA synthesis are only found in rhizobia that inhabit determinate nodules (Tatsukami and Ueda, 2016). The results suggest that GA-associated negative regulation of nodule number, by incorporating rhizobia helps to prevent a delayed infection of other rhizobia (Tatsukami and Ueda, 2016).

Akamatsu et al. (2021) reported that the GA signalling acts as a key regulator in the AON. GA biosynthesis is activated around the nodule vascular bundles, and synthesized GA accumulates in the nodule. Accumulated GA induces the expression of the *NIN* via a *cis*-acting region of the *NIN* promoter, while deletions of the *cis*-acting region increase *L. japonicus* susceptibility to rhizobia (Akamatsu et al., 2021) These results suggest that endogenous GA signalling negatively regulates nodulation through AON (Akamatsu et al., 2021)

According to previous studies, does *LjbHLHm1*, homolog of *GmbHLHm1*, play the same role in Lotus requires further study. Moreover, given the nodulation of Lotus is regulated by GA, the GA regulation of *LjbHLHm1* deserves further investigation. In this chapter, *LjbHLHm1.1*-expression-interrupted *LORE1* lines were used to investigate the function of the *LjbHLHm1.1* in *L. japonicus* nodulation and plant development. Exogenous GA was applied to the mature nodules (both wildtype and mutant) to study the effect of GA on *L. japonicus* nodule regulation, nitrogen fixation, and plant development.

5.2 Results

5.2.1 *L. japonicus* line selection and seedling genotyping

Lotus retrotransposon 1 (LORE1) is an active low-copy-number TY3-gypsy retrotransposon expressed in the model legume *L. japonicus* (Madsen et al., 2005). Five *L. japonicus* lines with LORE1 insertions in *LjbHLHm1.1* and three lines with insertions in *LjbHLHm1.2* were selected from the Lotus Base seed repository (<https://lotus.au.dk>) (Table 5.1). Seeds were initially cultivated (1st generation) in the glasshouse for preliminary genotyping. Four-week-old seedlings were genotyped using PCR. Primers and cycle times for genotyping were performed according to the protocols and primer sequences outlined in Table 5.1 and 5.2A. The LORE1 insertion is 5406 bp in size (GenBank: AJ966990.1), which should effectively disrupt subsequent transcriptional activity of the allele and block flanking primers to amplify a full-length genomic fragment with 1min extension time in PCR cycle. Using LJPrimer F and LORE1-LC2-rev (Figure 5.1A), PCR analysis revealed that line 30056892 showed a clear DNA band for the LORE1 insertion and the absence of a band using flanking primers on either side of the predicted LORE1 insertion, LJPrimer F and LJPrimer R (Figure 5.1 B). Comparable controls were identified as heterozygous and wild type (loss of LORE1 insertion) in the seed population. According to the genotype interpretation listed in Table 5.3, wild-type, heterozygous and homozygous LORE1 lines were identified in the population of seeds obtained from Lotus Base. Of the lines received, only one was identified (line 30056892) that contained a single insertion in the second exon of *LjbHLHm1* (Table 5.1), this line was used in subsequent experiments to test the functionality of *LjbHLHm1.1*.

The expressions of *LjbHLHm1.1* in wild-type, heterozygous, and homozygous (*bhlhm1.1 mutant*) nodules were tested by RT-PCR. cDNA converted from total RNA (RNA of each sample was adjusted to the same concentration in cDNA synthesis reaction) was used as a PCR template with forward (tcatggcagcgtgatgctcttgc) and reverse (aaaccaattccacgcatagcttctctg) primers. A DNA band of the correct size was amplified from both wild-type and heterozygous (30056892) seedlings. The wild-type plant had a brighter band than the heterozygous plants, while no band was observed in the homozygous *bhlhm1.1 mutant* (Figure 5.2A). This result indicated that *LjbHLHm1.1*

expression levels in the heterozygous plant were lower than in the wild-type plant, and the *LjbHLHm1.1* expression was too low to be observed using RT-PCR in the homozygous *bhlhm1.1* mutant. To quantify the expression level of the *LjbHLHm1.1*, a qPCR assay was performed. The qPCR result (Figure 5.2B) indicated that *LjbHLHm1.1* expression is significantly reduced in nodule tissues of the *bhlhm1.1* mutant (30056892), though not absent.

Seedlings from the 1st generation of 30056892 seeds were genotyped as homozygous, heterozygous or wild type (absent) for the LORE1 insert in a 1:2:1 ratio. Seedlings were transferred into larger pots with a turface and sand mixture (ratio 1:1) and inoculated with rhizobia. Each plant was fertigated daily with B&D nutrient solution (no nitrogen applied to induce nodulation), using a semi-hydroponic reticulated system. Plants were grown in a temperature-controlled chamber (26°C/24°C Day/night regime). Only wild-type and heterozygous seedlings survived and were found to be nodulated. After 4 months of further growth, both the heterozygous and wild-type lines developed flowers and set seeds. Unfortunately, none of the homozygous plants survived past 3 months of growth and failed to set seed without an exogenous nitrate supply. Actually, homozygous mutant growth for more than three months had to be supplemented with the supply of exogenous nitrate (5 mM KNO₃) to keep the plants alive (Table 5.6). About 1000 seeds from the wild-type and heterozygous plants were harvested and used as plant material for the following experiments (2nd generation).

After 5 weeks of growth, the F2-generation (Line 30056892) was genotyped using leaf DNA samples. Among 192 seedlings tested, 37 failed to deliver a PCR signal. For those that did, there was a population of 41 seedlings identified as wild-type, 79 showing heterozygosity for the LORE1 insertion, and 35 lines with a homozygous (*bhlhm1.1 mutant*) genotype – again a 1:2:1 ratio. All seedlings from the three genotypes were cultivated in soil inside plastic containers (with lids) inside a glasshouse with a day/night temperature regime of 26°C/24°C. Only wild-type and heterozygous seedlings showed repeat flowering and seed generations up to 18 months (these plants were kept for harvesting seeds). All *bhlhm1.1 mutants* were petite, had no flowers, stopped growing, and died between 6 to 12 months after planting with the supply of exogenous nitrate (5 mM KNO₃) (Table 5.6). The survival rate of the seedlings with different genotypes (Table 5.6) showed that with a significantly reduced *LjbHLHm1.1* expression level (Figure 5.2), the *bhlhm1.1*

mutants were sterile and insensitive to the luxury growing conditions including N from nodulation or the supply of exogenous N fertilisers. As a result, all subsequent experiments utilised the heterozygote line to generate F1 seeds which were planted and genotyped to identify the three segregating genotypes. Confirmed genotypes were then used in experiments to test the functionality of *LjbHLHm1.1*.

5.2.2 Promoter analysis and GA responsive element identification.

The sequence of the 2000bp 5'-upstream region of the *LjbHLHm1.1* start codon (promoter) was analysed. Sequence analysis identified two putative GA responsive elements (GARE) as described by Skriver et al. (1991), indicating that the *LjbHLHm1.1* could also be regulated by GA signalling like its homolog in soybean (Figure 5.3).

5.2.3 The effect of GA on the *L. japonicus* nodulation phenotype and *LjbHLHm1.1* expression

The NZP2235 *Mesorhizobium loti* inoculated plants were grown for 90 days in the glasshouse in river sand until each plant to establish sufficient biomass for root and nodule sampling (Lotus are small plants, nodules of younger seedlings (the diameter of each root nodule is less than 0.5mm) are not enough to be sampled for RNA extraction). The expression level of *LjbHLHm1.1* in wild-type nodules was significantly higher than in roots, in control groups, indicating that *LjbHLHm1.1* is highly expressed in nodules than roots (Figure 5.4A), like its homolog *GmbHLHm1* (Figure 2.2 A). After 3 weeks of GA treatment (by irrigating the root system with 0.4 PPM GA₃ every second day), *LjbHLHm1.1* expression was significantly reduced in the wild-type nodules and induced in the wild-type roots, indicating that GA has opposite effects on *LjbHLHm1.1* expression in roots and nodules. Short-term (0-48hr) GA treatments with 0.4 ppm GA₃ on nodule *LjbHLHm1.1* expression were investigated to study how fast the *LjbHLHm1.1* could respond to GA treatment. There were no significant differences in *LjbHLHm1.1* expression from 0 to 3 h compared with the wild-type control. However, *LjbHLHm1.1* expression level was significantly induced between 6 to 24 h of the GA₃ treatment. After 48 h, the difference became insignificant (Figure 5.4 B).

To investigate the effect of *LjbHLHm1.1* expression and long-term GA treatment on *L. japonicus* growth, three weeks of GA treatments were applied to the wild-type, heterozygous and

homozygous *bhlhm1.1 mutant* lines. Extended exposure to GA₃, promoted shoot height in plants of all genotypes (Figure 5.5 A). Shoot dry weights (Figure 5.5 B) and the nodule dry weight (Figure 5.5 C) of all genotypes were not affected by the GA treatment relative to the control. The nodule number was increased with GA treatment in the wild type (Figure 5.5 D). No significant difference in nodule number was observed \pm GA treatment in heterozygous and *bhlhm1* groups (Figure 5.5 D). These results indicated that exogenous GA promotes *L. japonicus* shoot height regardless of the *LjbHLHm1.1* expression level in the plant. When *LjbHLHm1.1* expresses normally, GA increased nodule number in *L. japonicus*, while not affecting shoot dry weight or nodule dry weight. When *LjbHLHm1.1* expression is significantly reduced, plants are short, and weak, with suppressed nodulation. In this condition, the effect of GA on nodulation disappeared.

Plants of different genotypes are shown in Figure 5.6. In the normal growth condition (Figure 5.6, control groups, no GA treatment), the *bhlhm1.1 mutants* were much shorter, with yellowing leaves, fewer root nodules, and in general a stunted growth, compared to that of wild-type plants. Despite the height of the plants (heterozygous plants were shorter than wild-types), the phenotypes of heterozygous plants were similar to the wild-type group, plants remained healthy and robust, with normal nodulation patterns. This result is consistent with Figure 5.5, revealing that a significant reduction of *LjbHLHm1.1* expression results in stunted growth, and suppressed nodulation.

Plants with/without GA treatment are compared in Figure 5.6. After 3 weeks of GA treatment (Figure 5.6A), seedlings of all genotypes were taller, while wild-type and heterozygous lines were slender, with fewer and longer branches compared. In the wild-type and heterozygous groups, plants with 5 weeks of GA₃ treatment (Figure 5.6A) showed a more pronounced increase in shoot height than plants with 3 weeks of GA treatment (Figure 5.6B). In the *bhlhm1.1* mutant, a longer GA₃ treatment did not further increase shoot height (relative to 3-week-old plants). These results indicated that GA₃ treatment promotes the shoot height of *L. japonicus*. When the *LjbHLHm1.1* expression is reduced in plants, a longer GA₃ treatment increases shoot height independent of *LjbHLHm1.1*.

5.2.5 The effects of *LjbHLLHm1.1* expression and long-term GA application on *L. japonicus* nodule phenotype and function

Nodule phenotypes of different genotypes and GA treatment were observed and photographed (Figure 5.7 and Figure 5.8). The *bhlhm1.1* nodules (Figure 5.7 C) were smaller than wild-type and heterozygous nodules (Figure 5.7 A and B). The effective fixation area of wild-type nodules (Figure 5.8 A and E) was bigger than heterozygous nodules (Figure 5.8 B, C, F, and G). The *bhlhm1.1 mutant* nodules (Figure 5.8 D and H) had few effective fixation areas. These results indicate that the nodule size and the effective nitrogen fixation area are positively correlated with the expression of the *LjbHLLHm1.1*.

Wild-type and heterozygous groups have smaller nodules and effective nitrogen fixation areas after GA treatment (Figure 5.7 D and E; Figure 5.8 E and F, G) compared to the control groups (Figure 5.7 A and B; Figure 5.8 A and B, C). For heterozygous plants, big differences in nodule sizes from the same seedling were observed in the control condition (Figure 5.7 B), while the differences were reduced after GA treatment (Figure 5.7 E). GA treatment did not affect the nodule size and effective nitrogen fixation areas of the *bhlhm1.1 mutant* (Figure 5.7 C and F). Nodule size was reduced after GA treatment when the *LjbHLLHm1.1* expressed normally (Figure 5.7 A, B, D, E, Figure 5.8 A, B, C, E, F, G). GA treatment does not affect the size and the effective fixation area in the *LjbHLLHm1.1*-suppressed nodules (Figure 5.7 C, F, Figure 5.8 D, H).

To investigate the effects of long-term GA₃ application on *L. japonicus* nodule function, NH₄⁺ levels in nodules were measured. The NH₄⁺ level reduced significantly after a 3-week GA₃ treatment (Figure 5.9A). At shorter GA₃ treatment periods, NH₄⁺ levels increased at 1 h but then recovered (24 h) and then fell again at 48 and 72 h (Figure 5.9B).

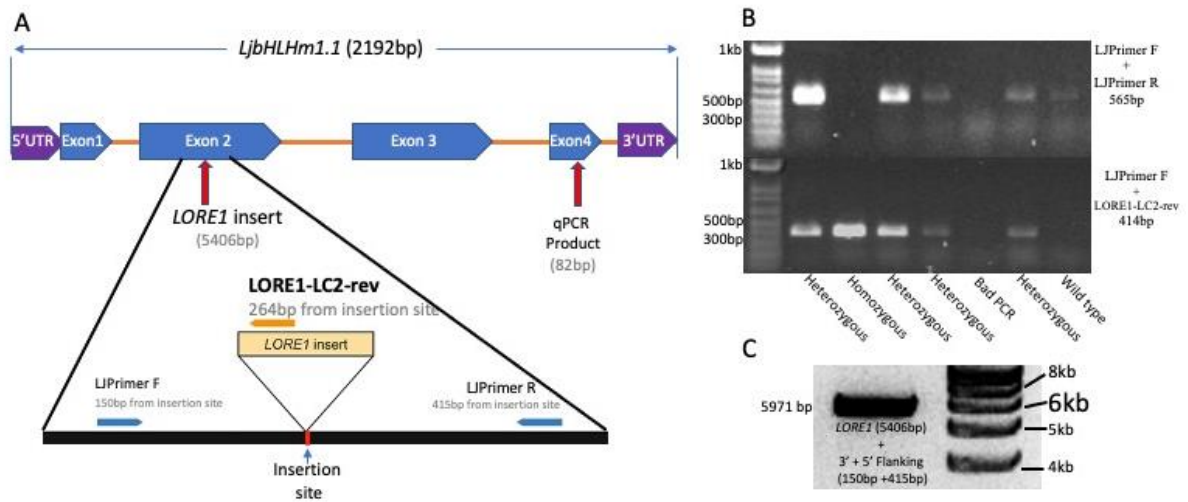


Figure 5. 1 Structure of *LjbHLHm1.1*, the LORE1 insertion site and genotyping result of line 30056892. (A) The LORE1 insert was in the second exon of the *LjbHLHm1* gene (Plant ID: 30056892). (B) Genotype analysis of 1st generation seedlings from Lotus Base seed. Primer combinations (LJPrimer F and LJPrimer R) were used to identify plant lines with or without the LORE1 insertion (565 bp products would identify genomic sequences without a LORE1 insertion). Primer combinations (LJPrimer F and LORE1-LC2-rev) were used to amplify the 5'-flanking DNA region at the insertion site. A positive PCR for LORE1 will amplify a 414 bp product. (C) PCR confirmation of homozygous plants with primers (LJPrimer F and LJPrimer R). Putative homozygous lines were examined using PCR with 5 min extension cycles. A positive PCR result is a band that is 5406 bp in size.

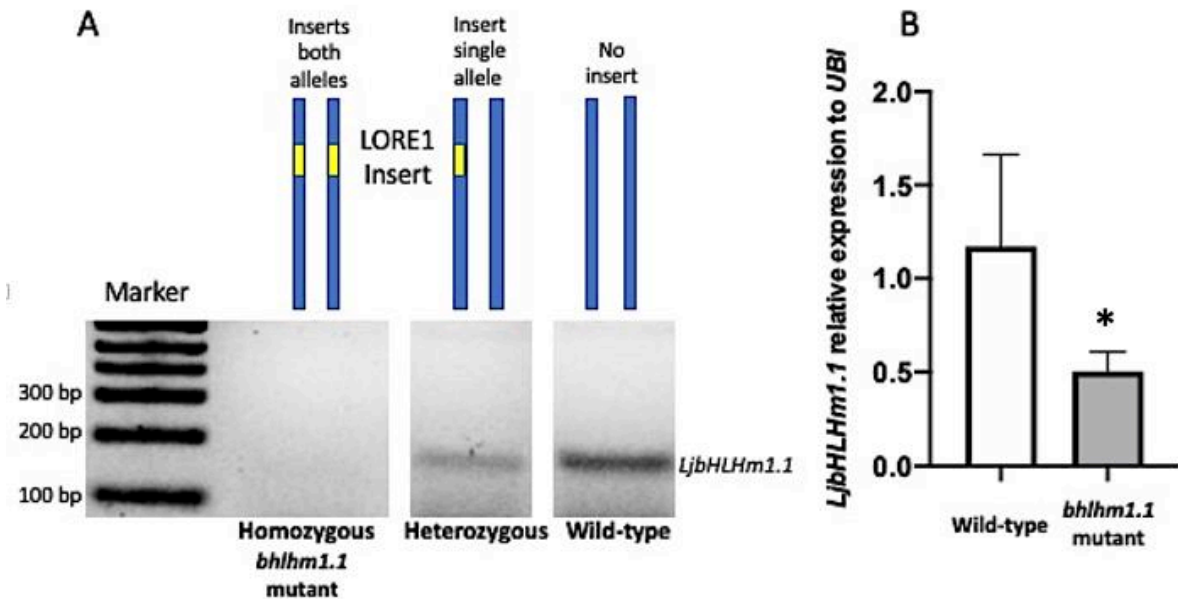


Figure 5. 2 The *LORE1* insertion in *LjbHLHm1.1* disrupts gene expression (line 30056892). (A) *LORE1* insertion could be on one allele (heterozygous) or both alleles (homozygous, the *bhlhm1.1* mutant). (A) The *LORE1* insertion can be observed to disrupt *LjbHLHm1* mRNA expression in both heterozygous and homozygous lines relative to the wild-type control. (B) The relative expression of *LjbHLHm1* in nodules of wild-type and homozygous *bhlhm1.1* lines. The expression of *LjbHLHm1* levels was normalized with *UBI* as a reference gene and was calculated using the $2^{-\Delta\Delta C_t}$ method (Libault et al., 2008). Values were means \pm SE (n=4) biological replicates. The * indicates the significant differences compared to wild-type based on the T-test ($P < 0.05$).

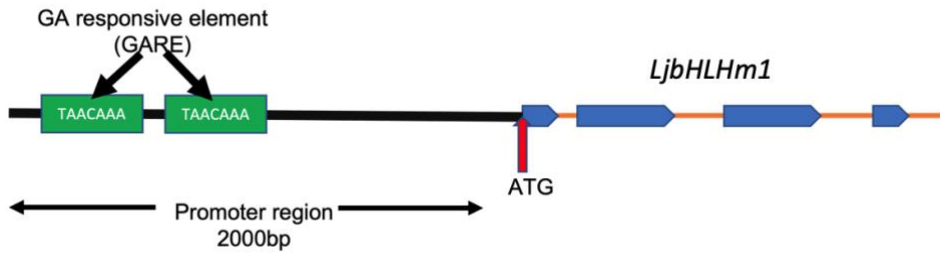


Figure 5.3 GA responsive elements in the promoter region of *LjbHLHm1.1*.

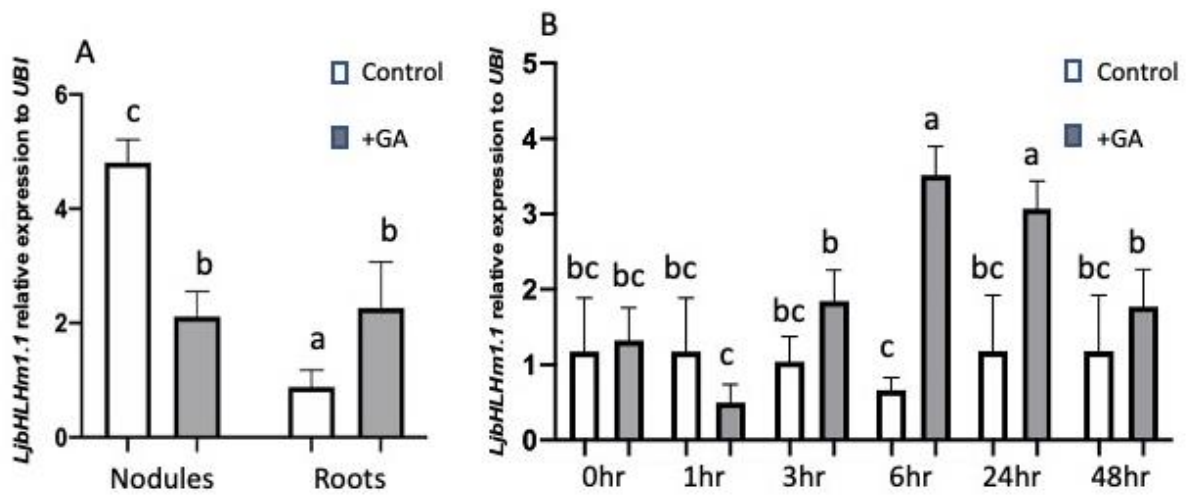


Figure 5.4 Contrasting expression of *LjbHLHm1.1* in nodules and roots of wild-type plants. *LjbHLHm1.1* mRNA expression is measured in (A) separated nodules and roots or (B) Four-month-old wild-type plants were treated with/without 4ppm GA₃ (10⁻⁶ M) at 10 am followed by nodule harvests at 1, 3, 6, 24 and 48 h after treatment. The expression of *LjbHLHm1.1* was normalized with *ubiquitin* as a reference gene and was calculated using the 2^{-ΔΔCt} method. Values were means ± SE (n=4) of four biological replicates.

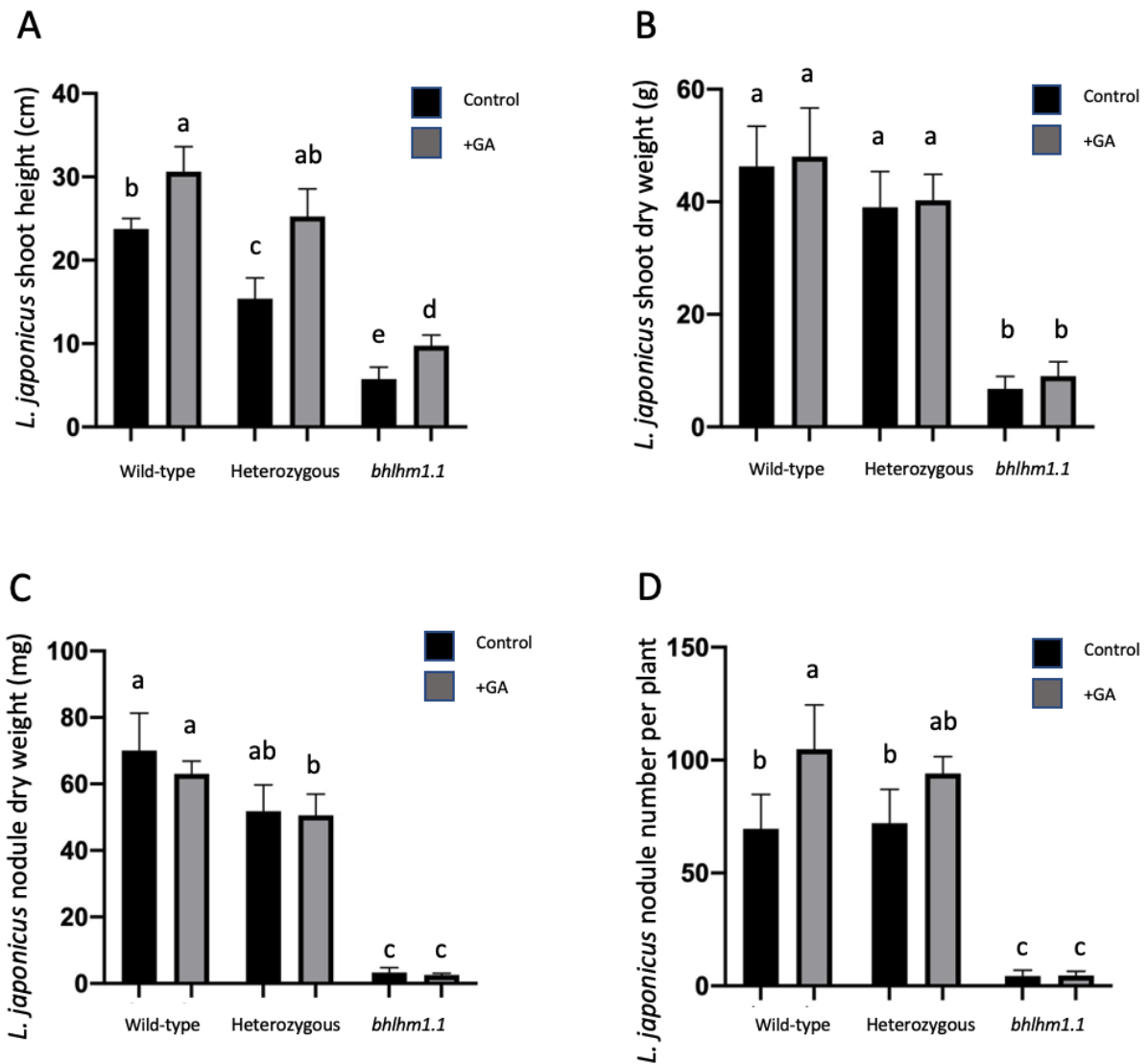


Figure 5. 5 The effects of long-term GA application on *Lotus japonicus* nodule and shoot growth. (A) Shoot height, (B) shoot dry weight, (C) nodule dry weight, and (D) nodule number per plant after 3 weeks of growth in the presence/absence of 10^{-6} M GA₃. At three months, plants were treated with/without GA₃ for three weeks. Values are means \pm SE (n=4). Values with different letters indicate significant differences between the treatments based on the two-way ANOVA ($P < 0.05$).

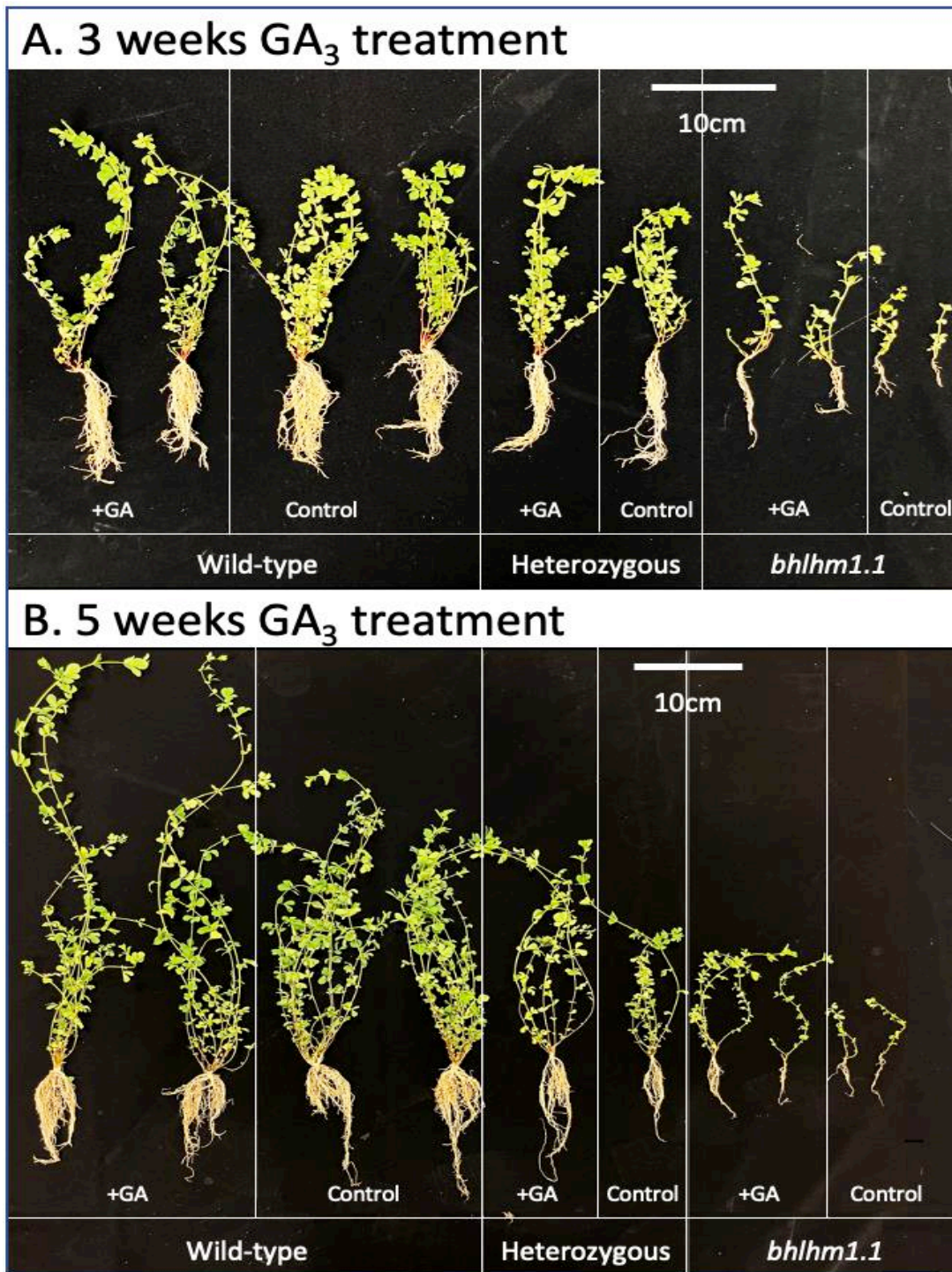


Figure 5. 6 *Lotus japonicas* phenotypes influenced by extended GA₃ treatment. Phenotypes of wild-type, heterozygous and homozygous *bhlhm1.1* mutant plants after 3 w (A) and 5 w GA₃ treatment. Seedlings were grown for 90 d in river sand and watered every day or supplied with B&D nutrient solution (Broughton and Dilworth 1971) containing 5 mM KNO₃ three times a week. The 10⁻⁶ M GA₃ solution was directly applied into pots every 48 h.

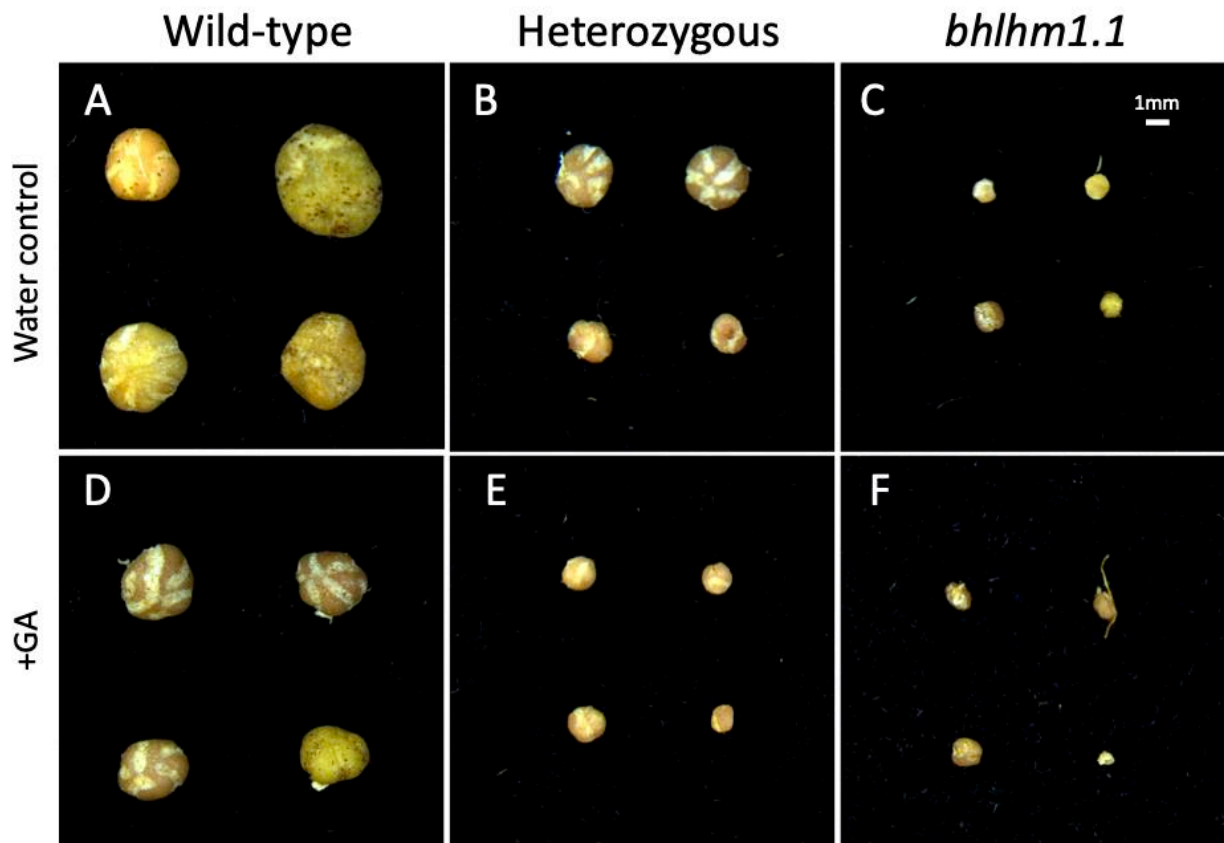


Figure 5. 7 *Lotus japonicas* nodule size of wild-type, heterozygous and homozygous *bhlhm1.1* mutant plants with/without GA₃ treatment. 4ppm GA₃ was applied to 90 d old plants for 3 weeks. A random selection of nodules is presented from each treatment.

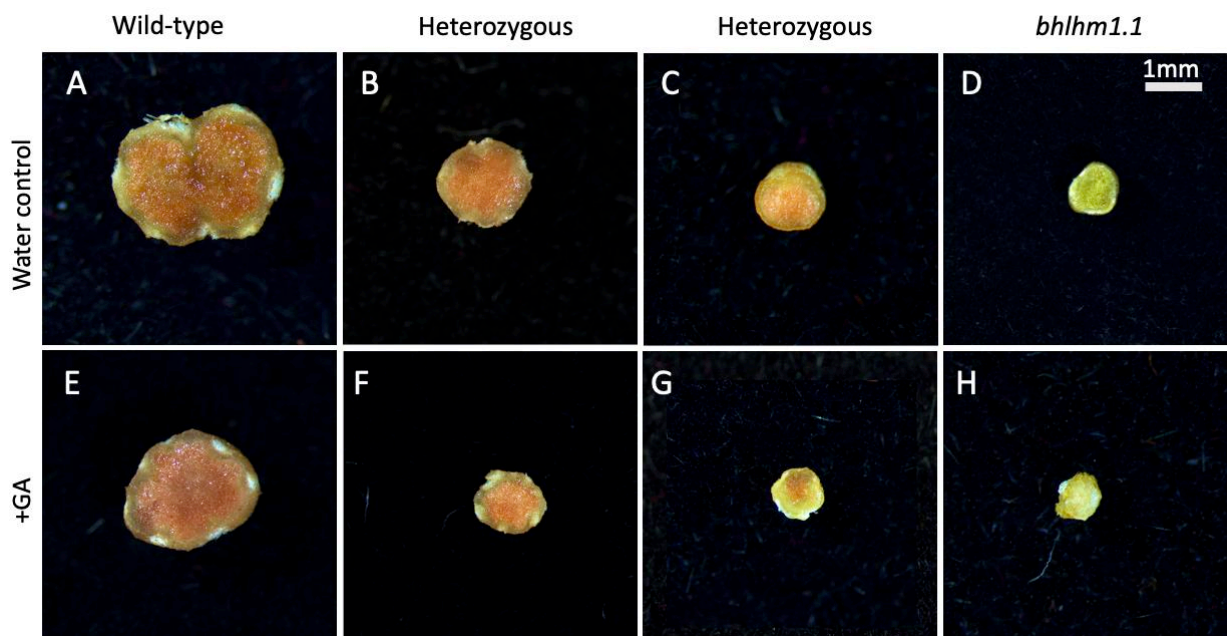


Figure 5. 8 Nodule cross-sections of wild-type, heterozygous and homozygous *bhlhm1.1* mutant plants with/without GA₃ treatment. The pink-to-orange area inside the nodule is the effective nitrogen fixation area. 90 d plants were treated with/without 4ppm GA₃ for 3 weeks and nodules were harvested and sectioned.

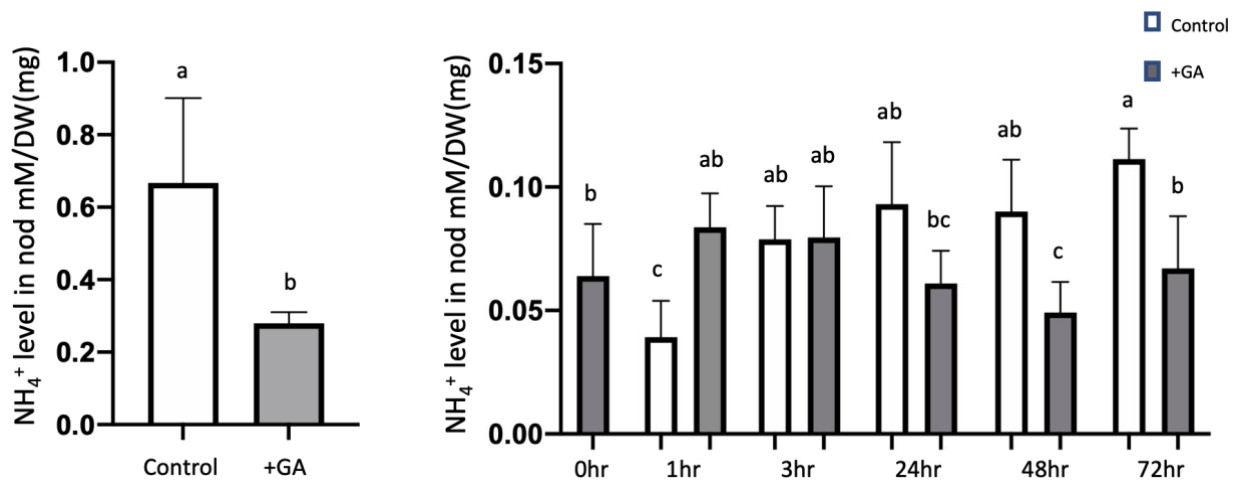


Figure 5. 9 NH_4^+ concentration in *L. japonicus* GA_3 treated nodules. Nodulated 90 d plants were treated with/without 4ppm GA_3 for up to 3 weeks. Concentrations of NH_4^+ were measured in nodules by ammonium assay. (A) Reduced NH_4^+ in GA_3 treated nodules after 3 w. (B) Four-month-old nodules were treated with/without 4ppm GA_3 at 10 am, and four biological repeats for each treatment were harvested after 1, 3, 6, 24 and 48 h. Values are means \pm SE (n=4).

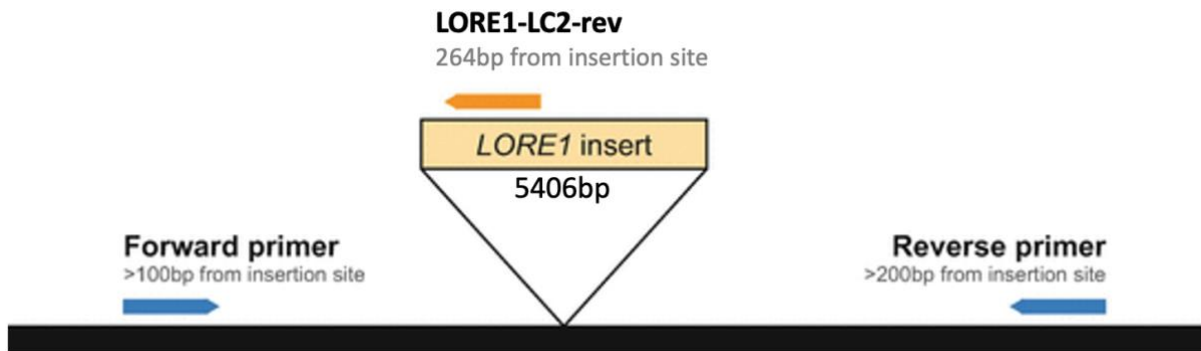


Figure 5. 10 The design of LORE1 genotyping primers. Forward and reverse primers are designed using Primer 3 and are located at least 100 and 200 bp away from the LORE1 insertion site, respectively. The LORE-LC2-rev primer binds to a region 264 bp downstream of the LORE1 5' LTR. Figure edited from Mun et al. (2017).

Homologous of <i>GmbHLHm1</i>	Gene ID number	Plant ID	Insertion in <i>LjbHLHm1</i>	Insertion in other genes	LJPrimer F	LJPrimer R
<i>LjbHLHm1.1</i>	Lj0g3v029 2969.1	300561 24	1 exonic	2 exonic 2 intronic 1 intergenic	GCCAATGGC TGCTGCTTTT GGAGA	TTCTTGTGAAA CCCGGGCGAC AAC
		300568 92	1 exonic		GCCAATGGC TGCTGCTTTT GGAGA	TTCTTGTGAAA CCCGGGCGAC AAC
		300206 13	1 intronic	1 intronic	GAAAGCGGC GAGAGAAGC TCAGCC	CAAGGGCACA GCTCCCAAAT GTCA
		301466 91	1 intronic	1 intronic	GAAAGCGGC GAGAGAAGC TCAGCC	CAAGGGCACA GCTCCCAAAT GTCA
		300725 08	1 intronic	2 exonic 5 intronic 1 intergenic	TGCAAAATC CCACATCCA TCTGCAA	TGAGGGCTCTT GAGGAGGAGC AGA
<i>LjbHLHm1.2</i>	Lj6g3v217 1830.1	300069 27	2 exonic	1 exonic	TGATCAATG TTCATTTTGC GGGAGGG	ATCTGTGACG GAATTTGCGA CGGA
		300836 93	1 exonic	1 intergenic	TCACGGGTT GTTGATGTG AACTGGC	TGTGGGGACC CTCCTTCAAAA CCA
		301439 48	1 intronic	2 intronic	TGAAGCAGC TAGGGAATC AGCAGCA	CATGTGTCATC AACTATCTAG CCTGCAGAA

Table 5. 1 Information of *LORE1* lines and Primers for genotyping

A

Step	Temperature	Time	Cycles
Initial denaturation	95 °C	1 min	1
Denaturation	95 °C	15 s	30
Annealing*	55 °C	15 s	
Extension*	72 °C	60 s	
	72 °C	10min	1

B

Step	Temperature	Time	Cycles
Initial denaturation	95 °C	1 min	1
Denaturation	95 °C	15 s	30
Annealing*	55 °C	15 s	
Extension*	72 °C	6 min	
	72 °C	10min	1

Table 5. 2 PCR cycles for genotyping (A) and conformation (B)

Summary of PCR verification of the LORE1 insertion in 30056892					
	Genotyping PCR		Genotype	Full-length confirmation PCR	Comment
	LJPrimer F + LJPrimer R	LJPrimer F + LORE1-LC2-rev		LJPrimer F + LJPrimer R	
Correct sized DNA band in gel	+	+	Heterozygous		LORE1 insertion in one allele. The <i>LjbHLHm1</i> in the other allele is functional.
	+	-	Wild type		No insertion
	-	+	Homozygous	Only One band (5971bp)	LORE1 Insertion in both alleles. The <i>LjbHLHm1</i> expression is disrupted.

Table 5.3 Genotype interpretation from gel electrophoresis results.

Plant ID	Gene	Primer Name	Primer sequence
Reference gene	Ubiquitin gene	Ubi-qF	TTCACCTTGTGCTCCGTCTTC
		Ubi-qR	AACAACAGCACACACAGACAATC
30056892	LjbHLHm1.1	892 QPCR F	ACATTTGGGAGCTGTGCCCT
		892 QPCR R	GAACTTCCAGCTTTGGGCCA
30020613		613 QPCR F	GACATTTGGGAGCTGTGCC
		613 QPCR R	TGAACTTCCAGCTTTGGGCCA
30083693	LjbHLHm1.2	693 QPCR F	TGGTTTTGAAGGAGGGTCCCC
		693 QPCR R	GCCAATTCCCAAAGAGCAAGTG
30143948		948 QPCR F	CAGTGGCGCTTTGGCTCTATTG
		948 QPCR R	GTTTTGTGGTTGAAGTTTGGGC

Table 5. 4 Primers used for Real-time quantitative PCR

Stock concentration	Volume for single reaction
1M Tricine, pH 8.0	10 μ L
10 mM CaCl ₂	10 μ L
5 mM NADH	10 μ L
150 mM α -ketoglutarate	10 μ L
L-Glutamic Dehydrogenase Type II, 50% glycerol solution, ≥ 35 units/mg protein (Sigma TM G2626)	0.1 μ L
Water	9.9 μ L
Total	50 μ L

Table 5. 5 The reaction solution for ammonium assay.

Line 30056892	1st generation (grown without N)			2nd generation (seeds from 1st generation heterozygous plants, grown with low N)		
Genotypes	Homozygous	Heterozygous	Wild-type	Homozygous mutant	Heterozygous	Wild-type
Genotype identification seedlings (4 weeks)	5	10	6	35	79	41
3-month survival seedlings	0	8	5	24	75	39
Death rate after 3 months	Without N supply			With 5 mM KNO ₃		
	100%	20%	16.7%	31.4%	5.1%	5.9%
Seedlings have flowers and seeds	0	8	5	0 out of 3 seedlings kept	10 out of 10 seedlings kept	5 out of 5 seedlings kept
18-month survival seedlings	N/A	N/A	N/A	0 out of 3	10 out of 10	5 out of 5

Table 5. 6 The survival seedling number and death rate of different genotypes (Line 30056892) with/without N supply

5.3 Discussion

Nitrogen is an essential macro-element for plants. It is a constituent of nucleic acids, proteins and other indispensable organic compounds such as chlorophyll and vitamins (Ohyama, 2010). Nitrogen deficiency leads to stunted growth, pale leaves, and reduced flower, while severe deficiency can result in plant death (Uchida, 2000). *bHLHm1* is a transcription factor related to legume nodule nitrogen fixation and ammonium transport processes in legume nodules and roots (Chiasson et al., 2014). The homologs of *GmbHLHm1*, *LjbHLHm1.1* and *LjbHLHm1.2*, were identified in the *L. japonicus* genome by sequence comparisons. This chapter investigated the relationship between the expression of *LjbHLHm1.1* and GA on *L. japonicus* growth and nodulation.

Suppressed expression of *LjbHLHm1.1* resulted in stunted, fragile, sterile plants that rarely nodulated. This is a consistent trait linked to the reduction in *bHLHm1* expression in soybean (Chiasson et al., 2014). Gibberellins (GAs) are plant hormones that regulate cell and tissue growth and influence various developmental processes such as seed germination, root and shoot elongation, flowering, and fruit patterning (Binenbaum et al., 2018). GA also affects nodulation by regulating nodulation-related genes, but effects vary between different leguminous plants, exogenous/endogenous GA₃, GA concentrations, and nodulation stage. To investigate the GA regulation of *LjbHLHm1.1*, the promoter of *LjbHLHm1.1* was analysed, and two GA responsive elements (GARE) were identified within 2000bp upstream of the start codon, indicating the potential role of GA regulation of the *LjbHLHm1* expression. Long-term GA treatment inhibited the *LjbHLHm1.1* expression and nitrogen fixation rate in nodules. like its homolog *GmbHLHm1* (Figure3.4). However, the GA inhibition of *LjbHLHm1.1* expression in roots versus nodules is less clear as changes to expression levels diverge in opposite directions. The reason of how these two tissues differ in the *LjbHLHm1.1* expression profiles after GA treatment requires further investigation. Short-term GA treatment induced the *LjbHLHm1.1* expression after 6 h and then returned to normal level at 48 h. This result shows that the *LjbHLHm1.1* expression responds to

GA treatment in a relatively short time period (6 hours), however, plants are able to regulate the gene expression back to normal level after the short induction to maintain growth.

During early nodulation stages, GA is known to inhibit nodulation in *L. japonicas* by compromising infection thread formation, leading to a reduced nodulation phenotype (Maekawa et al., 2009). GA then promotes cell division of the nodule primordium, and the required organogenesis to form nitrogen-fixing organs (Ferguson et al., 2011). Three weeks of GA treatment on wild-type plants increased shoot height and nodule numbers but inhibited nodule size and had no effect on shoot dry weight or nodule dry weight. According to the growth profile of the plants, GA treatment induced shoot height making them tall and slim, compared to water control. As the biomass of the shoot was not changed by the GA treatment, the nutrients and N required for plant growth would remain similar. The total amount of biologically fixed nitrogen is related to nodule number, the total mass of nodules and the nitrogen fixation rate of each nodule. GA inhibited nodule size and nodule fixation rates of mature wild-type nodules. This would suggest that alternative sources of N acquisition (roots) may have helped to compensate for a reduced N₂-fixation capacity. With a significantly reduced *LjbHLLHm1.1* expression in the *bhlhm1.1* mutant, GA still managed to induce a response to shoot height, while the effect of GA on nodule number and nodule size is less clear due to the poor level of nodulation in the *bhlhm1.1* line.

5.4 Materials and method

5.4.1 Lotus line identification

The *GmbHLLHm1* mRNA sequence was identified in the NCBI (Transcripts: Glyma.15G061400.1, Glycine max Wm82.a2.v1; Alias: Glyma15g06680 .v1.1). The protein sequence was translated with the Geneious Prime software. The protein sequence was used to blast against the Phytozome (*Lotus japonicus* Lj1.0v1). Two homologous *LjbHLLHm1.1* (Lj4g0022968.2) and *LjbHLLHm1.2* (Lj6g0028057.1) genes similar to *GmbHLLHm1* were identified. The sequences of these two homologs were blasted against the Lotus BLAST (<https://lotus.au.dk>) to identify the available lines

that have insertions in each gene. Seeds of 5 lines that have inserts in the *LjbHLHm1.1* (Lj0g3v0292969.1, *Lotus japonicus* MG20 v3.0 cDNA, Lotus Base) and 3 lines that have inserts in the *LjbHLHm1.2* (Lj6g3v2171830.1, *Lotus japonicus* MG20 v3.0 cDNA, Lotus Base) were identified and ordered from the seed bank.

5.4.2 Plant material preparation of *LOREI* line

5.4.2.1 Seeds germination and inoculation

Seeds were scarified by scratching gently with fine sandpaper to disrupt the seed coat. Seeds were then soaked in sodium hypochlorite [2% (v/v) containing 0.1% (v/v) Tween 20] for 20 min to surface sterilize the seeds and then rinsed 3 times (20 min each time) with sterile distilled water (Nishida et al., 2020). Swollen seeds were transferred onto several layers of clean wet filter paper in Petri dishes. Sealed Petri dishes were incubated in a 24°C dark incubator for a week or until the cotyledons are fully expanded with the seed teguments removed. The germinated seedlings were transferred to pots with sand and irrigated with B&D medium around the seedling roots (Broughton and Dilworth, 1971). Six pots were put in one tray for irrigation and covered with a transparent plastic lid to reduce evaporation until the roots were established.

5.4.2.2 Inoculation

The *L. japonicus* inoculant, NZP2235 *Mesorhizobium loti* (obtained from La Trobe University), was spiked into a 200 ml YEM culture and incubated at 28°C, with shaking at 120 rpm for 3 days. The culture was diluted to a final OD600 of 0.02 and carefully dispensed at 10ml per seedling around the roots of the seedlings. The inoculation was repeated on the second day and irrigated with B&D medium from a bottom tray to avoid dilution of the inoculant.

5.4.2.3 Genotyping

Seedlings were grown in the glasshouse and watered daily with added nitrogen-free B&D medium three times a week. Leaf tissue samples were collected for genotyping when the plants had grown about 4 cm tall or 3 fully expanded leaves were evident. Plant DNA was extracted with the PureLink™ Genomic Plant DNA Purification Kit (according to the manufacturer's instructions). Extracted DNA samples were used as template DNA with two primer combinations as listed in Table 5.1. Two PCRs were performed for each DNA sample using the flanking forward and reverse primers (LJPrimer F + LJPrimer R) and the forward primer of each line with the reverse primer in LORE1 (LJPrimer F + LORE1-LC2-rev). PCR cycles for both primer combinations are listed in Table 5.2A under the Genotyping PCR section. Homozygous plants identified from the previous PCR genotyping were confirmed with the LJPrimer F + LJPrimer R and PCR cycles listed in Table 5.2B (Confirmation PCR). The genotyping result of the different *LORE1* lines is listed in Table 5.3. All PCR-positive plants were selected and allowed to grow to seed (F1).

5.4.2.4 Plant cultivation and harvesting

Germinated seedlings were transferred into pots with river sand and watered daily in a greenhouse with a 14hr/10hr and 26°C/24°C day/night regime. B&D nutrient solution with 5mM KNO₃ was applied twice a week to support plant growth. GA treatments were performed with 4ppm GA₃ supplied daily on 3-month-old plants for three weeks until the shoot height was significantly increased (Maekawa et al., 2009). Phenotypic data (photos, fresh weights, and shoot heights) were immediately collected at harvest. A proportion of the tissues were then frozen with liquid N₂ and desiccated in a freeze dryer (LABCONCO™) for 48 h to obtain final dry weights. The other tissue proportions were kept at -80°C till used for RNA extraction.

5.4.3 RNA extraction and quantitative polymerase chain reaction (qPCR) analysis

Plant samples were harvested around 11 a.m. Nodules were detached from the roots and the remaining tissues were kept in separate centrifuge tubes and rapidly frozen in liquid nitrogen before being transferred into -80°C freezer. RNA extraction was performed using the Monarch® Total RNA Miniprep Kit. First-strand cDNA synthesis was performed using the SuperScript™ IV Reverse Transcriptase (Invitrogen™). Primers for *LjbHLHm1* expression (primers listed in Table

5.4) were designed using Geneious software. Primer efficiency was tested with SYBR Green Real-Time PCR Master Mix and 1, 1/5, 1/25, 1/125, 1/625 dilutions of synthesized cDNA. The primer efficiency was between 90%-110%. 2 µl of a 1/5 dilution of cDNA was used as the qPCR templates. The SYBR Green Real-Time PCR Master Mix was used for qPCR. Results were normalized against *UBI* as the reference gene and calculated using the $2^{-\Delta\Delta C_t}$ method (Libault et al., 2008). Values were means \pm SE (n=4) biological replicates. Significant differences between groups were based on a T-test ($P < 0.05$).

5.4.4 Ammonium assay

The NH_4^+ content of *L. japonicus* nodules was measured using an ammonium assay. Three-month-old (> 21 days for long-term GA treatment experiments) nodules were harvested around 11 a.m. Nodules were detached from the root and freeze-dried for 24 hours. 50 mg dry nodule tissue was put into a 1.5 ml Eppendorf tube. Each sample was soaked in 500 µL of 0.1M Tris buffer (pH 7.3) for one hour till the samples were soft. Excess liquid was pipetted from tubes and each sample was ground in the tube with disposable pellet pestles (Fisherbrand™). 1 ml of 1M Tris buffer (pH 7.3) was added to each tube and mixed to extract the soluble NH_4^+ released from nodules. Samples were centrifuged at 14,000 rpm for 5 min. The supernatant of each sample was transferred to one tube of an 8-tube strip. A standard curve was established with a serial dilution of NH_4Cl (0, 0.01, 0.02, 0.04, 0.08, 0.16, 0.64 and 1.28 mM). A reaction solution was made according to Table 5.4. 50 µL of each nodule-extracted liquid and 50 µL of reaction solution were mixed in a well of 96 well optical microplates. Absorbance at 340 nm was measured at 25°C with an interval of 6 seconds for each measure for 5 min with SpectraMax® Plus 384 Absorbance Plate Reader. The NH_4^+ level of each sample was calculated according to the standard curve and nodule dry weight. Four biological repeats were used for each treatment.

Chapter 6 Conclusion and Future Directions

Soybean is an important crop grown globally for its high protein and oil content. As a legume, soybeans can fix atmospheric N₂ to NH₃ through their symbiotic partnership with rhizobia bacteria. This symbiosis is an important addition to overall nitrogen use efficiencies in plant and animal-based agricultural systems. With the increasing demand for protein in the food industry, oil for food and fuel, and reduced nitrogen for other agricultural purposes (rotation crops and animal feeds), a solid understanding of the mechanisms that legumes (soybean) use to manage their nitrogen acquisition and utilisation requirements, will help target breeding programs to identify varieties with improved nitrogen use efficiencies. An important gene linked to nodule activity is *GmbHLHm1*. Previous research has characterized *GmbHLHm1* as a transcription factor that co-regulates nodulation, nodule development and activity through changes in the expression of nodule and root-expressed genes. This study investigated the functional activities of *GmbHLHm1* and its response to phytohormones. The study also investigated a homolog of *GmbHLHm1* in *L. japonicus* (*LjbHLHm1*) using an *LjbHLHm1*-disrupted LORE line. This research aimed to further investigate the role of *bHLHm1* and how GA and Auxin regulate the nodulation and expression of *bHLHm1* in nodules in different legumes.

6.1 Function analysis of *GmbHLHm1* in soybean roots and nodules

RNAi-Silenced *GmbHLHm1* transgenic hairy roots led to reduced nodule size, nodule number, nitrogen fixation rate, and impaired plant growth. This is constant with that previously reported by

Chiasson et al. (2014) and Mohammadi-Dehcheshmeh et al. (2014), indicating that *GmbHLHm1* plays an important role in nodulation and symbiotic nitrogen fixation. With disrupted *LjbHLHm1.1* expression in *Lotus japonicus*, the *bhlhm1.1* mutants were sterile, unable to generate functional nodules, require N supply to survive, and grew poorly with a short lifespan. These phenotypes are consistent with the *bhlhm1* of soybean, the significantly reduced *LjbHLHm1.1* expression inhibiting nodulation and nitrogen fixation, leading to a nitrogen deficiency outcome (Uchida, 2000).

Interestingly, soybeans grown on non-nodulated, RNAi-silenced *GmbHLHm1* transgenic hairy roots showed enhanced shoot growth with an exogenous N supply. Similar results were reported by Mohammadi Dehcheshmeh (2014), where N application increased shoot height of soybean seedlings when uninoculated. In this study, *GmbHLHm1*-silenced hairy roots showed significantly induced shoot height and dry weights in the same growth condition Mohammadi illustrated. This observation implies that in the absence of *GmbHLHm1* expression and a reduction in nodule activity, shoot growth responds strongly to exogenous N. As a transcription factor, the disruption of *GmbHLHm1* has been shown to down-regulate different genes, including *AMT2*, *NRT1.7*, *NRT2.4*, and *DUR3*, which are induced by N deficiency (Mohammadi Dehcheshmeh, 2014). On the other hand, the disruption of *GmbHLHm1* up-regulates genes induced by exogenous NO₃, such as *NIA1*, *WRKY27*, and *NRT1.1* (Mohammadi Dehcheshmeh, 2014).

Nodulation is metabolically expensive for soybeans, as extra C is required from the host plant to support the growth of nodules and bacteroids in exchange for reduced N (Ferguson et al., 2019). Therefore, non-nodulated soybean seedlings with sufficient KNO₃ supply do not spend extra C from photosynthesis on nodules, allowing for enhanced growth compared to those relying on symbiotic nitrogen fixation. Moreover, in this case, the disruption of *GmbHLHm1* and exogenous KNO₃ supply both induce the expression of the low-affinity nitrogen transporter *NRT1.1*, potentially improving nitrate acquisition of the seedlings (Mohammadi Dehcheshmeh, 2014; Maghiaoui et al., 2020). This could explain the enhanced growth of seedlings on non-nodulated, *GmbHLHm1*-silenced hairy roots with exogenous KNO₃ supply.

Overexpression of the *GmbHLHm1* significantly increased nodule size, nodule dry weight, nitrogen fixation rates, and enhanced plant growth. However, nodule number (nodulation) was not influenced. The nodule distribution of the *GmbHLHm1*-OEX group showed extra-large nodules at the crown and a few smaller nodules attached to the middle and tip area of the root, compared to the control groups, which showed a relatively even distribution (no extra-large nodules) of the nodule. This explained the enhanced nodule dry weight, promoted shoot growth, and unaffected nodule number of the *GmbHLHm1*-OEX group. The unique nodule distribution of the *GmbHLHm1*-OEX group could be explained by AON. Overexpression of *GmbHLHm1* induced the size of nodules established earlier, and these extra-large nodules have a larger effective nitrogen fixation area, which could synthesize more nitrogen to support plant growth. The nitrogen from those extra-large nodules was transported to the shoot influencing AON activities, which inhibited the growth of new lateral nodules in the middle and tip area of the root.

In summary, the expression of the *GmbHLHm1* is related to nodule development, especially nodule size and nitrogen fixation activities. Silencing the *GmbHLHm1* led to impaired nodule development while overexpressing the *GmbHLHm1* enhanced the primary nodule size and nitrogen fixation area. However, the impact of *GmbHLHm1* on nodulation was still under the autoregulation of nodulation. Moreover, the *GmbHLHm1* does not seem essential for nitrogen transport processes from root to shoot. Soybean seedlings grown on *GmbHLHm1*-silenced, non-nodulated hairy roots showed enhanced shoot growth with the supply of exogenous NO_3^- .

6.2 Interaction between *bHLHm1* expression with N, GA_3 , and IAA

The exogenous supply of NO_3^- promotes plant growth while simultaneously suppressing nodulation (Xia et al., 2017). Long-term N treatments inhibit *GmbHLHm1* expression. Previously, the GA-responsive genes *MTO3*, *GASA6*, and *GAMMA-TIP*, were shown to be deregulated with the loss of *GmbHLHm1* expression, based on microarray gene expression experiments (Mohammadi Dehcheshmeh, 2014). In this study, when *GmbHLHm1* expression was suppressed under a long-term supply of exogenous N, the expression of *MOT3* and *GAMMA-TIP* did not change, in contrast to the previous microarray results. However, consistent with previous

microarray results, *GASA6* was upregulated. Homolog of *GASA6* in *Arabidopsis* is reported as a GA, abscisic acid, and glucose inducible gene, promoting seed germination and cell elongation (Zhong et al., 2015). This could also be related to the promoted shoot growth of soybean grown on non-nodulated, RNAi-silenced *GmbHLHm1* transgenic hairy roots grown with exogenous N source (Figure 2.6). Future experiments could focus on the regulation of N, *GmbHLHm1* on *GASA6* and how *GASA6* expression regulates shoot growth, with *GmbHLHm1* silenced and overexpressed transgenic soybean plants.

Promotor analysis GA-responsive elements, P-BOX and TATC-BOX and the putative auxin-responsive TGA elements (AACGAC) have been identified in the promoter region of the *GmbHLHm1*, indicating that the gene could be regulated by GA and Auxin (Mohammadi Dehcheshmeh, 2014). Two GA responsive elements (GARE) are also identified in the promotor of *LjbHLHm1* as described by Skriver et al. (1991), indicating that *LjbHLHm1.1* could also be regulated by GA signalling.

The effect of a long-term GA treatment on *bHLHm1* expression in mature nodules was investigated. GA inhibited *GmbHLHm1* expression, nodule size, nitrogen fixation rate, and increased nodule number, nodule dry weight, and shoot height in the empty vector soybean groups. Shoot dry weight and %N in leaves remain unchanged. In the *GmbHLHm1*-silenced group, shoot height increased independent of *GmbHLHm1* expression, indicating that the shoot height was not controlled by *GmbHLHm1* expression in the root system. However, *GmbHLHm1*-silenced nodules did affect shoot growth under GA treatment, most likely due to unhealthy nodules and N deficiencies, compared to that of the empty vector control. On the other hand, overexpression of the *GmbHLHm1* promoted nodulation in soybean and enhanced the nitrogenase activity in nodules, further promoting shoot height and shoot dry weight with GA treatment.

Similar results are obtained from GA-treated Lotus. Three weeks of GA treatment resulted in increased shoot heights, and nodule numbers, but inhibited nodule size, and NH_4^+ concentration in nodules. With significantly reduced *LjbHLHm1.1* expression in the *bhlhm1.1* mutant, GA was still able to stimulate shoot growth (height). This indicates GA inhibits nodulation and nitrogen

fixation and regulates shoot height independent of the expression of *LjbHLLHm1.1* in roots and nodules.

According to the above experiment, we concluded that GA is a negative regulator of *GmbHLLHm1*. To find out how fast the *GmbHLLHm1* expression responds to GA treatment, short-term GA treatment was applied to the wild-type nodule. A loss of *GmbHLLHm1* expression was observed after 1h of GA treatment, recovering after 3 h, then significantly suppressed by 24 h (Figure 3.2 A). The ammonium level and ARA of nodules did not significantly change within 48 h of GA treatment. Results indicate that the fluctuation of *GmbHLLHm1* expression caused by the short-term GA is reversible and had no instant impact on nodule activities; only extended GA treatments cause structural change of nodules and lead to a stable inhibited *GmbHLLHm1* expression and nitrogenase activity.

In Lotus, short-term GA treatment significantly induced *LjbHLLHm1.1* expression at 3 h and then returned to normal levels at 48 h. Nitrogen fixation activity fluctuated after 1 hr of GA treatment and returned to normal level, then significantly reduced after 48 hours of GA treatment. Short-term GA treatments induced *LjbHLLHm1.1* expression initially before returning to normal levels. These results are consistent with the results from the soybean.

Nodulation is also regulated by the auxin (Kohlen et al., 2017). Opposite to GA, auxin positively regulates IF elongation by controlling cell cycle reactivation, vascular tissue differentiation, and rhizobial infection (Breakspear et al., 2014; Kohlen et al., 2017). An elevated level of endogenous IAA is detected in the nodule primordium during initiation, and an optimized level of exogenous IAA can promote nodulation on roots (Van Noorden et al., 2006a; Kuppusamy et al., 2009; Kohlen et al., 2017). In this study, a short-term (1ppm) IAA treatment had no impact on *GmbHLLHm1* expression in soybean nodules and roots, while a longer exposure to IAA-induced *GmbHLLHm1* expression, nodule size, nitrogen fixation area, and shoot dry weight. In the empty vector groups, an increased number of large nodules were observed in the root with IAA treatment (Figure 3.10). The nitrogen fixed from the large nodules on the root system was sufficient to support the increased shoot dry weight after the IAA treatment. When *GmbHLLHm1* was overexpressed, IAA did not

affect the size of the nitrogen fixation area, but it made the colour darker in the nitrogen fixation region. (Figure 3.12).

In contrast, IAA helped to maintain nodule size in the *GmbHLHm1*-silenced nodules, but the nitrogen fixation area (pink) was not improved (Figure 3.10 C). The result indicates that IAA improves the nodule size independent of the nitrogen fixation activity and *GmbHLHm1* expression. In line with this, the IAA treatment further enhanced the nodule size of the *GmbHLHm1*-overexpressed nodules. However, the nitrogen fixation rate and %N in leaves were not significantly different between the IAA and water controls. Although we found that GA and IAA have a regulatory effect on the expression of *bHLHm1*, and there are GA-responsive elements on the promoter of *bHLHm1*. Whether this regulation is via direct interaction with GA-responsive elements in promoter or indirectly through other regulatory pathways, requires further investigation.

6.3 Promoter analysis of *GmbHLHm1* and *GmAMF3*

Three GA-responsive elements and two Auxin-responsive elements were identified in the promoter region of *GmbHLHm1* (Mohammadi Dehcheshmeh, 2014). Transgenic hairy roots and nodules with inserted promoter-GUS constructs were treated with water, GA, or IAA, to investigate the effect of GA and IAA on *GmbHLHm1* promoter expression patterns.

qPCR and GUS staining results revealed that GA treatment inhibited *GmbHLHm1*-promoter-GUS expression in nodules and IAA enhanced GUS expression in the root. The cross-sections of GUS-stained nodules show that promoter-GUS was mainly expressed in infected cells in the infected zone and had a small amount expressed in the IC and OC (Figure 4.4 A and B). GA treatment suppressed GUS expression in nodules, especially in the peripheral cells of the infected area. Each of the GA-responsive elements in the promoter region of *GmbHLHm1* was edited to investigate their function, respectively. No GUS expression was observed in edited constructs, indicating that each of the GA-responsive elements is individually important in facilitating the expression of the *GmbHLHm1*. These results reveal that the GA and IAA regulate the promoter of *GmbHLHm1*.

GmAMF3 was suggested to be an NH_4^+ permeable transport protein, and *GmbHLHm1* is a TF of *ScAMF1* (homologs of *GmAMF3*) in yeast (Chiasson et al., 2014). *GmAMF3* localized to the plasma membrane when expressed in yeast cells (Chiasson et al., 2014). RNAi silencing of *GmAMF3* gene disrupts the nodulation process, indicating that the AMF3 is essential for nodule development (Evgenia Ovchinnikova, 2014). However, in the *GmbHLHm1*-silenced nodules, no significant change in *GmAMF3* expression was observed (Chiasson et al., 2014). To test if other TFs regulate the expression of the *GmAMF3* and *GmbHLHm1* in the nodule, Yeast One-Hybrid experiments were performed to identify potential TFs that regulate the expression of the *GmbHLHm1* and *GmAMF3*. Five annotated proteins were found to bind to the promoter of *GmbHLHm1*, and eleven were found to bind to the promoter of *GmAMF3*.

With *GmbHLHm1*, preliminary sequence analysis identified binding proteins related to nodulation and symbiotic nitrogen fixation. This included an MYB family transcription factor previously shown to possibly be related to the AON, for binding to the AON-related peptide NIN under Pi deficiency (Isidra-Arellano et al., 2020). Other proteins include sphingomyelin synthetase-like domain protein (SMS1 and SMS2) which localized to the Golgi and PM, sharing the localization with *GmbHLHm1* (Subathra et al., 2011). With *GmAMF3*, nodulin 22 was identified as a potential interacting protein. Nodulin 22 is located in the ER and is responsible for preventing the induction of cell death during plant-microbe interactions (Rodriguez-López et al., 2014). This is an interesting outcome as AMF's have been associated with early senescence in Arabidopsis when activities are disrupted (Wenjing Li, unpublished results). Lipoxygenases were also found bound to the AMF3 promoter. These are enhanced in the lumen of the infection threads, and increased lipoxygenase activities are observed in mature nodules (28 dpi) (Gardner et al., 1996; Junghans et al., 2004). LOX9 and LOX10 may be involved in lipid metabolism and membrane modification in parenchyma cells of nodules (Hayashi et al., 2008).

Some of the identified proteins share a similar localization with *GmAMF3* in nodules. MTs (types 1-4) are a group of metal-binding proteins involved in metal tolerance and reactive oxygen species response expressed in the cytoplasm and nucleus (Coyle et al., 2002; Hassinen et al., 2011). MT2 is expressed in soybean roots, leaves, and seeds (Pagani et al., 2012; Leszczyszyn et al., 2013). G-protein coupled receptors (GPCRs) are a family of membrane proteins existing in animals and

plants that are responsible for the gene signalling (Taddese et al., 2013). Both proteins bind to the promoter region of *GmAMF3*. The co-localization in the nucleus and membranes, respectively, could also preclude a possible interaction. There were proteins related to basic processes of cell development, such as gene transcription and protein translation (TMA7, EIF5A, Small subunit ribosomal protein, and Large subunit ribosomal protein), hormone signalling (GRAS), and stress (F-box and MTs) (Fleischer et al., 2006; Dubos et al., 2010; Li et al., 2011; Takahara et al., 2013a; Tauc et al., 2021). The mechanisms of how they regulate the *GmAMF3* and *GmbHLHm1* via interacting with their promoters are still to be determined. Further studies are required to explain the mechanism of their interaction.

GmbHLHm1 was not identified as a possible DNA-binding protein in this Yeast One-Hybrid experiment. This does not mean that *GmbHLHm1* does not bind to the promoter region of *GmAMF3*. Subsequent experiments are required to test whether *GmbHLHm1* was presented in the cDNA library and whether the interactions can occur in situ using the Yeast One-Hybrid system. To further investigate the regulation of *GmbHLHm1* on *GmAMF3*, another Yeast One-Hybrid experiment should be conducted using the *GmbHLHm1* as the prey and the *GmAMF3* promoter as the bait.

In summary, *bHLHm1* is involved in the regulation of nodulation, symbiotic nitrogen fixation and transportation in legumes. GA negatively regulates the expression of the *GmbHLHm1* through regulating its promoter. IAA is a positive regulator of the *GmbHLHm1*. Similar regulatory effects of GA and IAA were observed in soybean and Lotus.

Reference

- Ahmad, M.Z., Sana, A., Jamil, A., Nasir, J.A., Ahmed, S., Hameed, M.U., and Abdullah.** (2019). A genome-wide approach to the comprehensive analysis of GASA gene family in Glycine max. *Plant molecular biology* **100**, 607-620.
- Akamatsu, A., Nagae, M., Nishimura, Y., Romero Montero, D., Ninomiya, S., Kojima, M., Takebayashi, Y., Sakakibara, H., Kawaguchi, M., and Takeda, N.** (2021). Endogenous gibberellins affect root nodule symbiosis via transcriptional regulation of NODULE INCEPTION in *Lotus japonicus*. *Plant J* **105**, 1507-1520.
- Alves, B.J.R., Boddey, R.M., and Urquiaga, S.** (2003). The success of BNF in soybean in Brazil. *Plant and Soil* **252**, 1-9.
- Batenburg, F.H.D., Jonker, R., and Kijne, J.W.** (1986). Rhizobium induces marked root hair curling by redirection of tip growth: a computer simulation. *Physiologia Plantarum* **66**, 476-480.
- Batzenschlager, M., Masoud, K., Janski, N., Houlné, G., Herzog, E., Evrard, J.-L., Baumberger, N., Ehrardt, M., Nominé, Y., and Kieffer, B.** (2013). The GIP gamma-tubulin complex-associated proteins are involved in nuclear architecture in *Arabidopsis thaliana*. *Frontiers in plant science*, 480.
- Belliény-Rabelo, D., Oliveira, A.E.A., and Venancio, T.M.** (2013). Impact of whole-genome and tandem duplications in the expansion and functional diversification of the F-box family in legumes (Fabaceae). *PloS one* **8**, e55127.
- Berry, E.A., Huang, L.S., and DeRose, V.J.** (1991). Ubiquinol-cytochrome c oxidoreductase of higher plants. Isolation and characterization of the bc1 complex from potato tuber mitochondria. *Journal of Biological Chemistry* **266**, 9064-9077.
- Binenbaum, J., Weinstain, R., and Shani, E.** (2018). Gibberellin localization and transport in plants. *Trends in plant science* **23**, 410-421.
- Breakspear, A., Liu, C., Roy, S., Stacey, N., Rogers, C., Trick, M., Morieri, G., Mysore, K.S., Wen, J., Oldroyd, G.E.D., Downie, J.A., and Murray, J.D.** (2014). The Root Hair “Infectome” of *Medicago truncatula* Uncovers Changes in Cell Cycle Genes and Reveals a Requirement for Auxin Signaling in Rhizobial Infection *The Plant Cell* **26**, 4680-4701.

- Breullin-Sessoms, F., Floss, D.S., Gomez, S.K., Pumpllin, N., Ding, Y., Levesque-Tremblay, V., Noar, R.D., Daniels, D.A., Bravo, A., Eaglesham, J.B., Benedito, V.A., Udvardi, M.K., and Harrison, M.J.** (2015). Suppression of Arbuscule Degeneration in *Medicago truncatula* phosphate transporter4 Mutants Is Dependent on the Ammonium Transporter 2 Family Protein AMT2;3. *The Plant Cell* **27**, 1352-1366.
- Broughton, W.J., and Dilworth, M.J.** (1971). Control of leghaemoglobin synthesis in snake beans. *Biochem J* **125**, 1075-1080.
- Burke, D., Dawson, D., and Stearns, T.** (2000). *Methods in yeast genetics: a Cold Spring Harbor Laboratory course manual* (2000 edition). Plainview, NY: Cold Spring Harbor Laboratory Press.[Google Scholar].
- Caetano-Anollés, G., and Gresshoff, P.M.** (1991). Plant genetic control of nodulation. *Annual Review of Microbiology* **45**, 345-382.
- Caetano-Anollés, G., Paparozziz, E.T., and Gresshoff, P.M.** (1991). Mature Nodules and Root Tips Control Nodulation in Soybean. *Journal of Plant Physiology* **137**, 389-396.
- Cai, K., Yin, J., Chao, H., Ren, Y., Jin, L., Cao, Y., Duanmu, D., and Zhang, Z.** (2018). A C3HC4-type RING finger protein regulates rhizobial infection and nodule organogenesis in *Lotus japonicus*. *Journal of integrative plant biology* **60**, 878-896.
- Cesco, S., Neumann, G., Tomasi, N., Pinton, R., and Weiskopf, L.** (2010). Release of plant-borne flavonoids into the rhizosphere and their role in plant nutrition. *Plant and Soil* **329**, 1-25.
- Chaudhary, M.I., Adu-Gyamfi, J.J., Saneoka, H., Nguyen, N.T., Suwa, R., Kanai, S., El-Shemy, H.A., Lightfoot, D.A., and Fujita, K.** (2008). The effect of phosphorus deficiency on nutrient uptake, nitrogen fixation and photosynthetic rate in mashbean, mungbean and soybean. *Acta Physiologiae Plantarum* **30**, 537-544.
- Chiasson, D.M., Loughlin, P.C., Mazurkiewicz, D., Mohammadidehcheshmeh, M., Fedorova, E.E., Okamoto, M., McLean, E., Glass, A.D., Smith, S.E., Bisseling, T., Tyerman, S.D., Day, D.A., and Kaiser, B.N.** (2014). Soybean SAT1 (Symbiotic Ammonium Transporter 1) encodes a bHLH transcription factor involved in nodule growth and NH₄⁺ transport. *Proc Natl Acad Sci U S A* **111**, 4814-4819.
- Chu, X., Su, H., Hayashi, S., Gresshoff, P.M., and Ferguson, B.J.** (2022). Spatiotemporal changes in gibberellin content are required for soybean nodulation. *New Phytologist* **234**, 479-493.
- Clontech Laboratories, I.** (2012). Matchmaker® Gold Yeast One-Hybrid Library Screening System User Manual.
- Couzigou, J.-M., Zhukov, V., Mondy, S., Abu el Heba, G., Cosson, V., Ellis, T.H.N., Ambrose, M., Wen, J., Tadege, M., Tikhonovich, I., Mysore, K.S., Putterill, J., Hofer, J., Borisov, A.Y., and Ratet, P.** (2012). NODULE ROOT and COCHLEATA Maintain Nodule Development and Are Legume Orthologs of *Arabidopsis* BLADE-ON-PETIOLE Genes *The Plant Cell* **24**, 4498-4510.

- Coyle, P., Philcox, J., Carey, L., and Rofo, A.** (2002). Metallothionein: the multipurpose protein. *Cellular and Molecular Life Sciences CMLS* **59**, 627-647.
- Di Giacomo, E., Laffont, C., Sciarra, F., Iannelli, M.A., Frugier, F., and Frugis, G.** (2017). KNAT3/4/5-like class 2 KNOX transcription factors are involved in *Medicago truncatula* symbiotic nodule organ development. *New Phytol* **213**, 822-837.
- Dill, A., Thomas, S.G., Hu, J., Steber, C.M., and Sun, T.-p.** (2004). The *Arabidopsis* F-box protein SLEEPY1 targets gibberellin signalling repressors for gibberellin-induced degradation. *The Plant Cell* **16**, 1392-1405.
- Dobert, R.C., Rood, S.B., and Blevins, D.G.** (1992a). Gibberellins and the Legume-*Rhizobium* Symbiosis I. Endogenous Gibberellins of Lima Bean (*Phaseolus lunatus* L.) Stems and Nodules. *Plant Physiology* **98**, 221-224.
- Dobert, R.C., Rood, S.B., Zanewich, K., and Blevins, D.G.** (1992b). Gibberellins and the Legume-*Rhizobium* Symbiosis III. Quantification of Gibberellins from Stems and Nodules of Lima Bean and Cowpea. *Plant Physiology* **100**, 1994-2001.
- Doerks, T., Strauss, M., Brendel, M., and Bork, P.** (2000). GRAM, a novel domain in glucosyltransferases, myotubularins and other putative membrane-associated proteins. *Trends in biochemical sciences* **25**, 483-485.
- Dubos, C., Stracke, R., Grotewold, E., Weisshaar, B., Martin, C., and Lepiniec, L.** (2010). MYB transcription factors in *Arabidopsis*. *Trends in Plant Science* **15**, 573-581.
- Duca, D., Lorv, J., Patten, C.L., Rose, D., and Glick, B.R.** (2014). Indole-3-acetic acid in plant-microbe interactions. *Antonie van Leeuwenhoek* **106**, 85-125.
- Endre, G., Kereszt, A., Kevei, Z., Mihacea, S., Kaló, P., and Kiss, G.B.** (2002). A receptor kinase gene regulating symbiotic nodule development. *Nature* **417**, 962.
- Evgenia Ovchinnikova, D.C., Jana Kolesik, and Brent N. Kaiser.** (2014). The role of ammonium facilitator 3 (AMF3) for the nodule formation and functioning in soybean and *Medicago truncatula*. In 17th Australian Nitrogen Fixation Proceedings, B.N. Kaiser, ed (The University of Adelaide).
- Feller, A., Machemer, K., Braun, E.L., and Grotewold, E.** (2011). Evolutionary and comparative analysis of MYB and bHLH plant transcription factors. *The Plant Journal* **66**, 94-116.
- Ferguson, B.J., Ross, J.J., and Reid, J.B.** (2005). Nodulation Phenotypes of Gibberellin and Brassinosteroid Mutants of Pea. *Plant Physiology* **138**, 2396-2405.
- Ferguson, B.J., Foo, E., Ross, J.J., and Reid, J.B.** (2011). Relationship between gibberellin, ethylene and nodulation in *Pisum sativum*. *New Phytologist* **189**, 829-842.
- Ferguson, B.J., Indrasumunar, A., Hayashi, S., Lin, M.-H., Lin, Y.-H., Reid, D.E., and Gresshoff, P.M.** (2010). Molecular Analysis of Legume Nodule Development and Autoregulation. *Journal of Integrative Plant Biology* **52**, 61-76.

- Ferguson, Brett J., Mens, C., Hastwell, April H., Zhang, M., Su, H., Jones, Candice H., Chu, X., and Gresshoff, Peter M.** (2019). Legume nodulation: The host controls the party. *Plant, Cell & Environment* **42**, 41-51.
- Fleischer, T.C., Weaver, C.M., McAfee, K.J., Jennings, J.L., and Link, A.J.** (2006). Systematic identification and functional screens of uncharacterized proteins associated with eukaryotic ribosomal complexes. *Genes Dev* **20**, 1294-1307.
- Fonouni-Farde, C., Miassod, A., Laffont, C., Morin, H., Bendahmane, A., Diet, A., and Frugier, F.** (2019). Gibberellins negatively regulate the development of *Medicago truncatula* root system. *Scientific Reports* **9**, 2335.
- Fonouni-Farde, C., Tan, S., Baudin, M., Brault, M., Wen, J., Mysore, K.S., Niebel, A., Frugier, F., and Diet, A.** (2016). DELLA-mediated gibberellin signalling regulates Nod factor signalling and rhizobial infection. *Nature Communications* **7**, 12636.
- Fornaroli, S., Petrusa, E., Braidot, E., Vianello, A., and Macrì, F.** (1999). Purification of a plasma membrane-bound lipoxygenase from soybean cotyledons. *Plant Sci.* **145**, 1-10.
- Fujita, K., Ofosu-Budu, K.G., and Ogata, S.** (1992). Biological nitrogen fixation in mixed legume-cereal cropping systems. *Plant and Soil* **141**, 155-175.
- Fukai, E., Soyano, T., Umehara, Y., Nakayama, S., Hirakawa, H., Tabata, S., Sato, S., and Hayashi, M.** (2012). Establishment of a *Lotus japonicus* gene tagging population using the exon-targeting endogenous retrotransposon LORE1. *The Plant Journal* **69**, 720-730.
- Gage, D.J.** (2004). Infection and Invasion of Roots by Symbiotic, Nitrogen-Fixing Rhizobia during Nodulation of Temperate Legumes. *Microbiology and Molecular Biology Reviews* **68**, 280-300.
- Gardner, C., Sherrier, D., Kardailsky, I., and Brewin, N.** (1996). Localization of lipoxygenase proteins and mRNA in pea nodules: identification of lipoxygenase in the lumen of infection threads.
- Gautrat, P., Laffont, C., and Frugier, F.** (2020). Compact root architecture 2 promotes root competence for nodulation through the miR2111 systemic effector. *Current Biology* **30**, 1339-1345. e1333.
- Geurts, R., and Bisseling, T.** (2002). Rhizobium Nod Factor Perception and Signalling. *The Plant Cell* **14**, s239-s249.
- Giles, J.** (2005). Nitrogen study fertilizes fears of pollution (Nature Publishing Group).
- Goto, T., Soyano, T., Liu, M., Mori, T., and Kawaguchi, M.** (2022). Auxin methylation by *IAMT1*, duplicated in the legume lineage, promotes root nodule development in *Lotus japonicus*. *Proceedings of the National Academy of Sciences* **119**, e2116549119.
- Göttfert, M.** (1993). Regulation and function of rhizobial nodulation genes. *FEMS Microbiology Reviews* **10**, 39-63.
- Grieneisen, V.A., Xu, J., Marée, A.F.M., Hogeweg, P., and Scheres, B.** (2007). Auxin transport is sufficient to generate a maximum and gradient guiding root growth. *Nature* **449**, 1008-1013.

- Guether, M., Neuhäuser, B., Balestrini, R., Dynowski, M., Ludewig, U., and Bonfante, P.** (2009). A mycorrhizal-specific ammonium transporter from *Lotus japonicus* acquires nitrogen released by arbuscular mycorrhizal fungi. *Plant Physiol* **150**, 73-83.
- Gupta, R., and Chakrabarty, S.** (2013). Gibberellic acid in plant: still a mystery unresolved. *Plant signaling & behavior* **8**, e25504.
- Hadri, A.-E., Spaink, H.P., Bisseling, T., and Brewin, N.J.** (1998). Diversity of root nodulation and rhizobial infection processes. In *The Rhizobiaceae* (Springer), pp. 347-360.
- Handberg, K., and Stougaard, J.** (1992). *Lotus japonicus*, an autogamous, diploid legume species for classical and molecular genetics. *The Plant Journal* **2**, 487-496.
- Haney, C.H., and Long, S.R.** (2010). Plant flotillins are required for infection by nitrogen-fixing bacteria. *Proceedings of the National Academy of Sciences* **107**, 478-483.
- Hao, D.-L., Zhou, J.-Y., Yang, S.-Y., Qi, W., Yang, K.-J., and Su, Y.-H.** (2020). Function and regulation of ammonium transporters in plants. *International Journal of Molecular Sciences* **21**, 3557.
- Hassinen, V.H., Tervahauta, A.I., Schat, H., and Kärenlampi, S.O.** (2011). Plant metallothioneins – metal chelators with ROS scavenging activity? *Plant Biology* **13**, 225-232.
- Hayashi, S., Gresshoff, P.M., and Kinkema, M.** (2008). Molecular analysis of lipooxygenases associated with nodule development in soybean. *Mol Plant Microbe In* **21**, 843-853.
- Hayashi, S., Reid, D.E., Lorenc, M.T., Stiller, J., Edwards, D., Gresshoff, P.M., and Ferguson, B.J.** (2012). Transient Nod factor-dependent gene expression in the nodulation-competent zone of soybean (*Glycine max* [L.] Merr.) roots. *Plant Biotechnology Journal* **10**, 995-1010.
- Herridge, D.F.** (1982). Use of the Ureide Technique to Describe the Nitrogen Economy of Field-Grown Soybeans. *Plant Physiology* **70**, 7-11.
- Hiltenbrand, R., Thomas, J., McCarthy, H., Dykema, K.J., Spurr, A., Newhart, H., Winn, M.E., and Mukherjee, A.** (2016). A Developmental and Molecular View of Formation of Auxin-Induced Nodule-Like Structures in Land Plants. *Frontiers in Plant Science* **7**.
- Hirsch, A.M.** (1992). Developmental biology of legume nodulation. *New Phytologist* **122**, 211-237.
- Hirsch, S., and Oldroyd, G.E.** (2009). GRAS-domain transcription factors that regulate plant development. *Plant Signal Behav* **4**, 698-700.
- Hoppe, T., Rape, M., and Jentsch, S.** (2001). Membrane-bound transcription factors: regulated release by RIP or RUP. *Current opinion in cell biology* **13**, 344-348.
- Ibiang, Y.B., and Sakamoto, K.** (2018). Synergic effect of arbuscular mycorrhizal fungi and bradyrhizobia on biomass response, element partitioning and metallothionein gene expression of soybean-host under excess soil zinc. *Rhizosphere* **6**, 56-66.
- Isidra-Arellano, M.C., Pozas-Rodríguez, E.A., del Rocío Reyero-Saavedra, M., Arroyo-Canales, J., Ferrer-Orgaz, S., del Socorro Sánchez-Correa, M., Cardenas, L., Covarrubias, A.A., and**

- Valdés-López, O.** (2020). Inhibition of legume nodulation by Pi deficiency is dependent on the autoregulation of nodulation (AON) pathway. *The Plant Journal* **103**, 1125-1139.
- Jia, Q., Xiao, Z.-X., Wong, F.-L., Sun, S., Liang, K.-J., and Lam, H.-M.** (2017). Genome-wide analyses of the soybean F-box gene family in response to salt stress. *International journal of molecular sciences* **18**, 818.
- Jin, J., Watt, M., and Mathesius, U.** (2012). The autoregulation gene SUNN mediates changes in root organ formation in response to nitrogen through alteration of shoot-to-root auxin transport. *Plant Physiology* **159**, 489-500.
- Jin, Y., Liu, H., Luo, D., Yu, N., Dong, W., Wang, C., Zhang, X., Dai, H., Yang, J., and Wang, E.** (2016). DELLA proteins are common components of symbiotic rhizobial and mycorrhizal signalling pathways. *Nature Communications* **7**, 12433.
- Junghans, T.G., Oliveira, M.G.d.A., and Moreira, M.A.** (2004). Lipoxygenase activities during development of root and nodule of soybean. *Pesquisa Agropecuária Brasileira* **39**, 625-630.
- Kaiser, B.N., Finnegan, P.M., Tyerman, S.D., Whitehead, L.F., Bergersen, F.J., Day, D.A., and Udvardi, M.K.** (1998). Characterization of an ammonium transport protein from the peribacteroid membrane of soybean nodules. *Science* **281**, 1202-1206.
- Karimi, M., Inzé, D., and Depicker, A.** (2002). GATEWAY™ vectors for Agrobacterium-mediated plant transformation. *Trends in Plant Science* **7**, 193-195.
- Khush, G.S.** (1999). Green revolution: preparing for the 21st century. *Genome* **42**, 646-655.
- Kinkema, M., Scott, P.T., and Gresshoff, P.M.** (2006). Legume nodulation: successful symbiosis through short- and long-distance signalling. *Functional Plant Biology* **33**, 707-721.
- Kohlen, W., Ng, J.L.P., Deinum, E.E., and Mathesius, U.** (2017). Auxin transport, metabolism, and signalling during nodule initiation: indeterminate and determinate nodules. *Journal of Experimental Botany* **69**, 229-244.
- Krusell, L., Madsen, L.H., Sato, S., Aubert, G., Genua, A., Szczyglowski, K., Duc, G., Kaneko, T., Tabata, S., and De Bruijn, F.** (2002). Shoot control of root development and nodulation is mediated by a receptor-like kinase. *Nature* **420**, 422-426.
- Krusell, L., Sato, N., Fukuhara, I., Koch, B.E., Grossmann, C., Okamoto, S., Oka-Kira, E., Otsubo, Y., Aubert, G., and Nakagawa, T.** (2011). The *Clavata2* genes of pea and *Lotus japonicus* affect autoregulation of nodulation. *The Plant Journal* **65**, 861-871.
- Kuppusamy, K.T., Ivashuta, S., Bucciarelli, B., Vance, C.P., Gantt, J.S., and VandenBosch, K.A.** (2009). Knockdown of CELL DIVISION CYCLE16 Reveals an Inverse Relationship between Lateral Root and Nodule Numbers and a Link to Auxin in *Medicago truncatula*. *Plant Physiology* **151**, 1155-1166.
- Lee, Y., and Kende, H.** (2002). Expression of α -expansin and expansin-like genes in deepwater rice. *Plant Physiology* **130**, 1396-1405.

- Lescot, M., Déhais, P., Thijs, G., Marchal, K., Moreau, Y., Van de Peer, Y., Rouzé, P., and Rombauts, S.** (2002). PlantCARE, a database of plant cis-acting regulatory elements and a portal to tools for in silico analysis of promoter sequences. *Nucleic Acids Res* **30**, 325-327.
- Leszczyszyn, O.I., Imam, H.T., and Blindauer, C.A.** (2013). Diversity and distribution of plant metallothioneins: a review of structure, properties and functions†. *Metallomics* **5**, 1146-1169.
- Lévy, J., Bres, C., Geurts, R., Chalhoub, B., Kulikova, O., Duc, G., Journet, E.-P., Ané, J.-M., Lauber, E., Bisseling, T., Dénarié, J., Rosenberg, C., and Debelle, F.** (2004). A Putative Ca²⁺ and Calmodulin-Dependent Protein Kinase Required for Bacterial and Fungal Symbioses. *Science* **303**, 1361-1364.
- Li, H., Wang, Y., Li, X., Gao, Y., Wang, Z., Zhao, Y., and Wang, M.** (2011). A GA-insensitive dwarf mutant of *Brassica napus* L. correlated with mutation in pyrimidine box in the promoter of *GID1*. *Molecular Biology Reports* **38**, 191-197.
- Li, Y., Pei, Y., Shen, Y., Zhang, R., Kang, M., Ma, Y., Li, D., and Chen, Y.** (2022). Progress in the self-regulation system in legume nodule development-AON (autoregulation of nodulation). *International Journal of Molecular Sciences* **23**, 6676.
- Libault, M., Thibivilliers, S., Bilgin, D.D., Radwan, O., Benitez, M., Clough, S.J., and Stacey, G.** (2008). Identification of Four Soybean Reference Genes for Gene Expression Normalization. *The Plant Genome* **1**.
- Lievens, S., Goormachtig, S., Den Herder, J., Capoen, W., Mathis, R., Hedden, P., and Holsters, M.** (2005). Gibberellins are involved in nodulation of *Sesbania rostrata*. *Plant Physiology* **139**, 1366-1379.
- Lim, C.W., Lee, Y.W., and Hwang, C.H.** (2011). Soybean nodule-enhanced CLE peptides in roots act as signals in GmNARK-mediated nodulation suppression. *Plant and Cell Physiology* **52**, 1613-1627.
- Lim, C.W., Lee, Y.W., Lee, S.C., and Hwang, C.H.** (2014). Nitrate inhibits soybean nodulation by regulating expression of CLE genes. *Plant Science* **229**, 1-9.
- Limpens, E., Franken, C., Smit, P., Willemsse, J., Bisseling, T., and Geurts, R.** (2003). LysM Domain Receptor Kinases Regulating Rhizobial Nod Factor-Induced Infection. *Science* **302**, 630-633.
- Lin, P.C., Pomeranz, M.C., Jikumar, Y., Kang, S.G., Hah, C., Fujioka, S., Kamiya, Y., and Jang, J.C.** (2011). The *Arabidopsis* tandem zinc finger protein AtTZF1 affects ABA-and GA-mediated growth, stress and gene expression responses. *The Plant Journal* **65**, 253-268.
- Liu, Y., Li, P., Fan, L., and Wu, M.** (2018). The nuclear transportation routes of membrane-bound transcription factors. *Cell Communication and Signaling* **16**, 1-9.
- Lotocka, B., Kopcińska, J., and Skalniak, M.** (2012). Review article: The meristem in indeterminate root nodules of Faboideae. *Symbiosis* **58**, 63-72.
- Madsen, L.H., Fukai, E., Radutoiu, S., Yost, C.K., Sandal, N., Schausser, L., and Stougaard, J.** (2005). LORE1, an active low-copy-number TY3-gypsy retrotransposon family in the model legume *Lotus japonicus*. *The Plant Journal* **44**, 372-381.

- Maekawa, T., Maekawa-Yoshikawa, M., Takeda, N., Imaizumi-Anraku, H., Murooka, Y., and Hayashi, M.** (2009). Gibberellin controls the nodulation signaling pathway in *Lotus japonicus*. *The Plant Journal* **58**, 183-194.
- Maghiaoui, A., Gojon, A., and Bach, L.** (2020). NRT1.1-centered nitrate signaling in plants. *Journal of Experimental Botany* **71**, 6226-6237.
- Márquez, A.J., Stougaard, J., Udvardi, M., Parniske, M., Spaink, H., Saalbach, G., Webb, J., and Chiurazzi, M.** (2005). *Lotus japonicus* handbook. (Springer).
- Mathur, M., Sharma, N., and Sachar, R.** (1993). Differential regulation of S-adenosylmethionine synthetase isozymes by gibberellic acid in dwarf pea epicotyls. *Biochimica et Biophysica Acta (BBA)-Protein Structure and Molecular Enzymology* **1162**, 283-290.
- McAdam, E.L., Reid, J.B., and Foo, E.** (2018). Gibberellins promote nodule organogenesis but inhibit the infection stages of nodulation. *Journal of Experimental Botany* **69**, 2117-2130.
- Mena, M.a., Cejudo, F.J., Isabel-Lamoneda, I., and Carbonero, P.** (2002). A Role for the DOF Transcription Factor BPBF in the Regulation of Gibberellin-Responsive Genes in Barley Aleurone. *Plant Physiol.* **130**, 111-119.
- Mens, C., Hastwell, A.H., Su, H., Gresshoff, P.M., Mathesius, U., and Ferguson, B.J.** (2021). Characterisation of *Medicago truncatula* CLE34 and CLE35 in nitrate and rhizobia regulation of nodulation. *New Phytologist* **229**, 2525-2534.
- Millner, P.A., and Causier, B.E.** (1996). G-protein coupled receptors in plant cells. *Journal of Experimental Botany* **47**, 983-992.
- Mitra, R.M., Gleason, C.A., Edwards, A., Hadfield, J., Downie, J.A., Oldroyd, G.E.D., and Long, S.R.** (2004). A Ca²⁺/calmodulin-dependent protein kinase required for symbiotic nodule development: Gene identification by transcript-based cloning. *Proceedings of the National Academy of Sciences of the United States of America* **101**, 4701-4705.
- Mohammad, A., Miranda-Ríos, J., Estrada Navarrete, G., Quinto, C., Olivares, J.E., García-Ponce, B., and Sánchez, F.** (2004). Nodulin 22 from *Phaseolus vulgaris* protects *Escherichia coli* cells from oxidative stress. *Planta* **219**, 993-1002.
- Mohammadi Dehcheshmeh, M.** (2014). Regulatory control of the symbiotic enhanced soybean bHLH transcription factor, GmSAT1. In School of Agriculture, Food and Wine (The University of Adelaide).
- Mohammadi-Dehcheshmeh, M., Ebrahimie, E., Tyerman, S.D., and Kaiser, B.N.** (2014). A novel method based on combination of semi-in vitro and in vivo conditions in *Agrobacterium rhizogenes*-mediated hairy root transformation of *Glycine* species. *In Vitro Cellular & Developmental Biology - Plant* **50**, 282-291.
- Mohd-Radzman, N.A., Laffont, C., Ivanovici, A., Patel, N., Reid, D., Stougaard, J., Frugier, F., Imin, N., and Djordjevic, M.A.** (2016). Different pathways act downstream of the CEP peptide receptor CRA2 to regulate lateral root and nodule development. *Plant Physiology* **171**, 2536-2548.

- Mun, T., Bachmann, A., Gupta, V., Stougaard, J., and Andersen, S.U.** (2016). Lotus Base: An integrated information portal for the model legume *Lotus japonicus*. *Sci Rep* **6**, 39447.
- Mun, T., Malolepszy, A., Sandal, N., Stougaard, J., and Andersen, S.U.** (2017). User Guide for the LORE1 Insertion Mutant Resource. In *Plant Genomics: Methods and Protocols*, W. Busch, ed (New York, NY: Springer New York), pp. 13-23.
- Mylona, P., Pawlowski, K., and Bisseling, T.** (1995). Symbiotic nitrogen fixation. *The Plant Cell* **7**, 869.
- Nagao, R.T., Goekjian, V.H., Hong, J.C., and Key, J.L.** (1993). Identification of protein-binding DNA sequences in an auxin-regulated gene of soybean. *Plant molecular biology* **21**, 1147-1162.
- Nett, R.S., Bender, K.S., and Peters, R.J.** (2022). Production of the plant hormone gibberellin by rhizobia increases host legume nodule size. *The ISME Journal* **16**, 1809-1817.
- Ng, J.L.P., and Mathesius, U.** (2018). Acropetal Auxin Transport Inhibition Is Involved in Indeterminate But Not Determinate Nodule Formation. *Front Plant Sci* **9**, 169.
- Ng, J.L.P., Welvaert, A., Wen, J., Chen, R., and Mathesius, U.** (2019). The *Medicago truncatula* PIN2 auxin transporter mediates basipetal auxin transport but is not necessary for nodulation. *Journal of Experimental Botany* **71**, 1562-1573.
- Ng, J.L.P., Hassan, S., Truong, T.T., Hocart, C.H., Laffont, C., Frugier, F., and Mathesius, U.** (2015). Flavonoids and auxin transport inhibitors rescue symbiotic nodulation in the *Medicago truncatula* cytokinin perception mutant cre1. *The Plant Cell* **27**, 2210-2226.
- Niemietz, C.M., and Tyerman, S.D.** (2000). Channel-mediated permeation of ammonia gas through the peribacteroid membrane of soybean nodules. *FEBS Lett.* **465**, 110-114.
- Nishida, H., Tanaka, S., Handa, Y., Ito, M., Sakamoto, Y., Matsunaga, S., Betsuyaku, S., Miura, K., Soyano, T., and Kawaguchi, M.** (2018). A NIN-LIKE PROTEIN mediates nitrate-induced control of root nodule symbiosis in *Lotus japonicus*. *Nature communications* **9**, 499.
- Nishida, Y., Hiraoka, R., Kawano, S., Suganuma, N., Sato, S., Watanabe, S., Anai, T., Arima, S., Tominaga, A., and Suzuki, A.** (2020). SEN1 gene from *Lotus japonicus* MG20 improves nitrogen fixation and plant growth. *Soil Science and Plant Nutrition* **66**, 864-869.
- Nishimura, R., Hayashi, M., Wu, G.J., Kouchi, H., and Imaizumi-Anraku, H.** (2002). HAR1 mediates systemic regulation of symbiotic organ development. *Nature* **420**, 426.
- Nutman, P.S.** (1952). Studies on the Physiology of Nodule Formation III. Experiments on the Excision of Root-tips and Nodules. *Annals of Botany* **16**, 79-103.
- Ohyama, T.** (2010). Nitrogen as a major essential element of plants. *Nitrogen assimilation in plants* **37**, 2-17.
- Okamoto, S., Ohnishi, E., Sato, S., Takahashi, H., Nakazono, M., Tabata, S., and Kawaguchi, M.** (2009). Nod factor/nitrate-induced CLE genes that drive HAR1-mediated systemic regulation of nodulation. *Plant Cell Physiol* **50**, 67-77.

- Okuma, N., and Kawaguchi, M.** (2021). Systemic optimization of legume nodulation: A shoot-derived regulator, miR2111. *Frontiers in Plant Science* **12**, 682486.
- Oldroyd, G.E., Murray, J.D., Poole, P.S., and Downie, J.A.** (2011). The rules of engagement in the legume-rhizobial symbiosis. *Annual review of genetics* **45**, 119-144.
- Oldroyd, G.E.D., and Downie, J.A.** (2004). Calcium, kinases and nodulation signalling in legumes. *Nature Reviews Molecular Cell Biology* **5**, 566.
- Olsson, J.E., Nakao, P., Bohlool, B.B., and Gresshoff, P.M.** (1989). Lack of systemic suppression of nodulation in split root systems of supernodulating soybean (*Glycine max [L.] Merr.*) mutants. *Plant Physiology* **90**, 1347-1352.
- Pagani, M.A., Tomas, M., Carrillo, J., Bofill, R., Capdevila, M., Atrian, S., and Andreo, C.S.** (2012). The response of the different soybean metallothionein isoforms to cadmium intoxication. *Journal of Inorganic Biochemistry* **117**, 306-315.
- Panther.** (2022). PANTHER family model Sphingomyelin synthetase.
- Pastuglia, M., Roby, D., Dumas, C., and Cock, J.M.** (1997). Rapid induction by wounding and bacterial infection of an S gene family receptor-like kinase gene in Brassica oleracea. *The Plant Cell* **9**, 49-60.
- Patterson, T.G., and LaRue, T.A.** (1983). Nitrogen Fixation by Soybeans: Seasonal and Cultivar Effects, and Comparison of Estimates I. *Crop Science* **23**, 488-492.
- Peng, J., Richards, D.E., Hartley, N.M., Murphy, G.P., Devos, K.M., Flintham, J.E., Beales, J., Fish, L.J., Worland, A.J., Pelica, F., Sudhakar, D., Christou, P., Snape, J.W., Gale, M.D., and Harberd, N.P.** (1999). 'Green revolution' genes encode mutant gibberellin response modulators. *Nature* **400**, 256.
- Peng, X.-Q., Ke, S.-W., Liu, J.-Q., Chen, S., Zhong, T.-X., and Xie, X.-M.** (2016). Deletion and hormone induction analyses of the 4-coumarate: CoA ligase gene promoter from Pennisetum purpureum in transgenic tobacco plants. *Plant Cell, Tissue and Organ Culture (PCTOC)* **126**, 439-448.
- Peoples, M., Herridge, D., and Ladha, J.** (1995). Biological nitrogen fixation: an efficient source of nitrogen for sustainable agricultural production? *Plant and soil* **174**, 3-28.
- Perret, X., Staehelin, C., and Broughton, W.J.** (2000). Molecular Basis of Symbiotic Promiscuity. *Microbiology and Molecular Biology Reviews* **64**, 180-201.
- Phillips, A.L., and Huttly, A.K.** (1994). Cloning of two gibberellin-regulated cDNAs from *Arabidopsis thaliana* by subtractive hybridization: expression of the tonoplast water channel, γ -TIP, is increased by GA 3. *Plant molecular biology* **24**, 603-615.
- Plet, J., Wasson, A., Ariel, F., Le Signor, C., Baker, D., Mathesius, U., Crespi, M., and Frugier, F.** (2011). MtCRE1-dependent cytokinin signaling integrates bacterial and plant cues to coordinate symbiotic nodule organogenesis in *Medicago truncatula*. *The Plant Journal* **65**, 622-633.

- Potten, B.** (2015). Molecular genetic and biochemical analysis of gibberellic acid involvement in the stages of soybean (*Glycine max* L.) nodule development. In School of Agriculture and Food Sciences (The University of Queensland).
- Prochaska, L.J., Geyer, R.R., Fisher, K.N., Pokalsky, C.N., Hosler, J., Omolwelu, R., and Ogunjimi, K.** (2017). Analysis of the Structural and Functional Role of the Dicyclohexylcarbodiimide (DCCD) Binding Site (E90-H212-Y246) in Subunit III of Bovine Heart and *Rhodobacter Sphaeroides* Cytochrome c Oxidase using Mutagenesis and Chemical Modification. *Biophysical Journal* **112**, 277a-278a.
- Qiao, Z., Brechenmacher, L., Smith, B., Strout, G.W., Mangin, W., Taylor, C., Russell, S.D., Stacey, G., and Libault, M.** (2017). The GmFWL1 (FW2-2-like) nodulation gene encodes a plasma membrane microdomain-associated protein. *Plant, Cell & Environment* **40**, 1442-1455.
- Radutoiu, S., Madsen, L.H., Madsen, E.B., Felle, H.H., Umehara, Y., Grønlund, M., Sato, S., Nakamura, Y., Tabata, S., Sandal, N., and Stougaard, J.** (2003). Plant recognition of symbiotic bacteria requires two LysM receptor-like kinases. *Nature* **425**, 585-592.
- Raun, W.R., and Johnson, G.V.** (1999). Improving nitrogen use efficiency for cereal production. *Agronomy journal* **91**, 357-363.
- Reid, D.E., Ferguson, B.J., and Gresshoff, P.M.** (2011a). Inoculation-and nitrate-induced CLE peptides of soybean control NARK-dependent nodule formation. *Mol Plant Microbe In* **24**, 606-618.
- Reid, D.E., Ferguson, B.J., Hayashi, S., Lin, Y.H., and Gresshoff, P.M.** (2011b). Molecular mechanisms controlling legume autoregulation of nodulation. *Ann Bot* **108**, 789-795.
- Rivers, R.L., Dean, R.M., Chandy, G., Hall, J.E., Roberts, D.M., and Zeidel, M.L.** (1997). Functional analysis of nodulin 26, an aquaporin in soybean root nodule symbiosomes. *Journal of Biological Chemistry* **272**, 16256-16261.
- Roberts, D.M., and Tyerman, S.D.** (2002). Voltage-dependent cation channels permeable to NH⁽⁺⁾(4), K⁽⁺⁾, and Ca⁽²⁺⁾ in the symbiosome membrane of the model legume *Lotus japonicus*. *Plant Physiol* **128**, 370-378.
- Rodriguez-López, J., Martínez-Centeno, C., Padmanaban, A., Guillén, G., Olivares, J.E., Stefano, G., Lledías, F., Ramos, F., Ghabrial, S.A., Brandizzi, F., Rocha-Sosa, M., Díaz-Camino, C., and Sanchez, F.** (2014). Nodulin 22, a novel small heat-shock protein of the endoplasmic reticulum, is linked to the unfolded protein response in common bean. *Molecular plant-microbe interactions : MPMI* **27**, 18-29.
- Rogato, A., D'Apuzzo, E., and Chiurazzi, M.** (2010). The multiple plant response to high ammonium conditions. *Plant Signaling & Behavior* **5**, 1594-1596.
- Rogato, A., D'Apuzzo, E., Barbulova, A., Omrane, S., Stedel, C., Simon-Rosin, U., Katinakis, P., Fletmetakis, M., Udvardi, M., and Chiurazzi, M.** (2008). Tissue-specific down-regulation of *LjAMT1*; 1 compromises nodule function and enhances nodulation in *Lotus japonicus*. *Plant molecular biology* **68**, 585-595.

- Roy Choudhury, S., Johns, S.M., and Pandey, S.** (2019). A convenient, soil-free method for the production of root nodules in soybean to study the effects of exogenous additives. *Plant Direct* **3**, e00135.
- Roy, S., Liu, W., Nandety, R.S., Crook, A., Mysore, K.S., Pislariu, C.I., Frugoli, J., Dickstein, R., and Udvardi, M.K.** (2019). Celebrating 20 Years of Genetic Discoveries in Legume Nodulation and Symbiotic Nitrogen Fixation[OPEN]. *The Plant Cell* **32**, 15-41.
- Roy, S., Robson, F., Lilley, J., Liu, C.-W., Cheng, X., Wen, J., Walker, S., Sun, J., Cousins, D., and Bone, C.** (2017). MtLAX2, a functional homologue of the *Arabidopsis* auxin influx transporter AUX1, is required for nodule organogenesis. *Plant Physiology* **174**, 326-338.
- Salvagiotti, F., Cassman, K.G., Specht, J.E., Walters, D.T., Weiss, A., and Dobermann, A.** (2008). Nitrogen uptake, fixation and response to fertilizer N in soybeans: A review. *Field Crops Research* **108**, 1-13.
- Sarkar, P.K., Haque, M.S., and Abdul Karim, M.** (2002). Effects of GA and IAA and their frequency of application on morphology, yield 3. *Pakistan journal of agronomy* **1**, 119-122.
- Sasaki, A., Ashikari, M., Ueguchi-Tanaka, M., and Itoh, H.** (2002). A mutant gibberellin-synthesis gene in rice. *Nature*, **416**, 701-702.
- Sasaki, A., Itoh, H., Gomi, K., Ueguchi-Tanaka, M., Ishiyama, K., Kobayashi, M., Jeong, D.-H., An, G., Kitano, H., and Ashikari, M.** (2003). Accumulation of phosphorylated repressor for gibberellin signaling in an F-box mutant. *Science* **299**, 1896-1898.
- Sato, S., and Tabata, S.** (2006). *Lotus japonicus* as a platform for legume research. *Curr Opin Plant Biol* **9**, 128-132.
- Sato, S., Nakamura, Y., Kaneko, T., Asamizu, E., Kato, T., Nakao, M., Sasamoto, S., Watanabe, A., Ono, A., and Kawashima, K.** (2008). Genome structure of the legume, *Lotus japonicus*. *DNA research* **15**, 227-239.
- Satomi, H., M., G.P., and J., F.B.** (2014). Mechanistic action of gibberellins in legume nodulation. *Journal of Integrative Plant Biology* **56**, 971-978.
- Saur, I.M., Oakes, M., Djordjevic, M.A., and Imin, N.** (2011). Crosstalk between the nodulation signaling pathway and the autoregulation of nodulation in *Medicago truncatula*. *New Phytologist* **190**, 865-874.
- Schauser, L., Roussis, A., Stiller, J., and Stougaard, J.** (1999). A plant regulator controlling development of symbiotic root nodules. *Nature* **402**, 191-195.
- Schlutzen, F., Tocilj, A., Zarivach, R., Harms, J., Gluehmann, M., Janell, D., Bashan, A., Bartels, H., Agmon, I., and Franceschi, F.** (2000). Structure of functionally activated small ribosomal subunit at 3.3 Å resolution. *cell* **102**, 615-623.
- Schnabel, E., Journet, E.-P., de Carvalho-Niebel, F., Duc, G., and Frugoli, J.** (2005). The *Medicago truncatula* SUNN gene encodes a CLV1-like leucine-rich repeat receptor kinase that regulates nodule number and root length. *Plant molecular biology* **58**, 809-822.

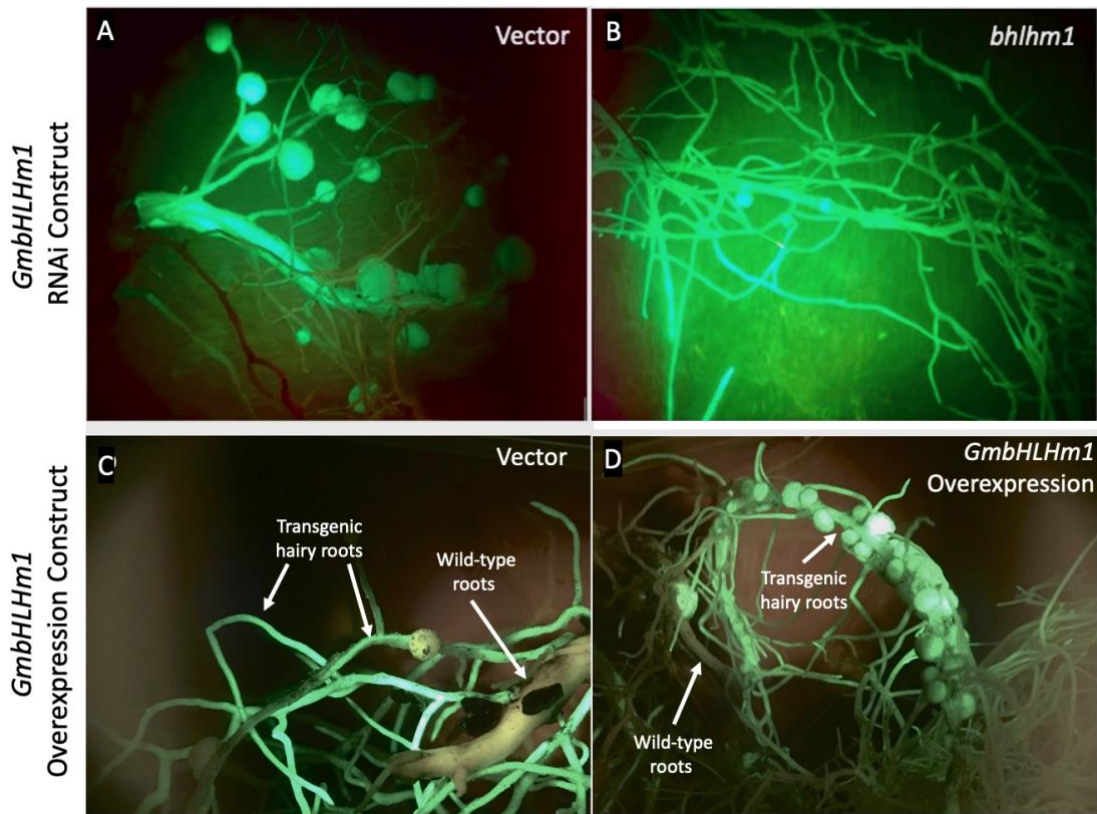
- Schwechheimer, C., Zourelidou, M., and Bevan, M.** (1998). Plant transcription factor studies. Annual review of plant biology **49**, 127-150.
- Searle, I.R., Men, A.E., Laniya, T.S., Buzas, D.M., and Iturbe-Ormaetxe, I.** (2003). Long-distance signaling in nodulation directed by a CLAVATA1-like receptor kinase. Science **299**, 109.
- Senoo, H., Araki, T., Fukuzawa, M., and Williams, J.G.** (2013). A new kind of membrane-tethered eukaryotic transcription factor that shares an auto-proteolytic processing mechanism with bacteriophage tail-spike proteins. J Cell Sci **126**, 5247-5258.
- Seo, P.J.** (2014). Recent advances in plant membrane-bound transcription factor research: Emphasis on intracellular movement. Journal of integrative plant biology **56**, 334-342.
- Sergeevich, S.A., Alexandrovich, Z.V., Yurievna, S.O., Yurievich, B.A., and Anatolievich, T.I.** (2015). Nod-Factor Signaling in Legume-Rhizobial Symbiosis. In Plants for the Future (InTech).
- Shimada, T.L., Shimada, T., and Hara-Nishimura, I.** (2010). A rapid and non-destructive screenable marker, FAST, for identifying transformed seeds of *Arabidopsis thaliana*. The Plant Journal **61**, 519-528.
- Simon-Rosin, U., Wood, C., and Udvardi, M.K.** (2003). Molecular and cellular characterisation of *LjAMT2;1*, an ammonium transporter from the model legume *Lotus japonicus*. Plant Mol Biol **51**, 99-108.
- Skriver, K., Olsen, F.L., Rogers, J.C., and Mundy, J.** (1991). cis-acting DNA elements responsive to gibberellin and its antagonist abscisic acid. Proceedings of the National Academy of Sciences **88**, 7266-7270.
- Soyano, T., Hirakawa, H., Sato, S., Hayashi, M., and Kawaguchi, M.** (2014). NODULE INCEPTION creates a long-distance negative feedback loop involved in homeostatic regulation of nodule organ production. Proceedings of the National Academy of Sciences **111**, 14607-14612.
- Spray, C.R., Kobayashi, M., Suzuki, Y., Phinney, B.O., Gaskin, P., and MacMillan, J.** (1996). The dwarf-1 (dt) Mutant of Zea mays Blocks Three Steps in the Gibberellin-Biosynthetic Pathway. Proceedings of the National Academy of Sciences of the United States of America **93**, 10515-10518.
- Stulen, I., Perez-Soba, M., De Kok, L., and Van der Eerden, L.** (1998). Impact of gaseous nitrogen deposition on plant functioning. The New Phytologist **139**, 61-70.
- Subathra, M., Qureshi, A., and Luberto, C.** (2011). Sphingomyelin synthases regulate protein trafficking and secretion. PloS one **6**, e23644.
- Sudadi, S., and Suryono, S.** (2015). Exogenous application of tryptophan and indole acetic acid (IAA) to induce root nodule formation and increase soybean yield in acid, neutral and alkaline soil. AGRIVITA, Journal of Agricultural Science **37**, 37-44.
- Sun, X., Wang, Y., and Sui, N.** (2018). Transcriptional regulation of bHLH during plant response to stress. Biochem Bioph Res Co **503**, 397-401.

- Suzaki, T., Yano, K., Ito, M., Umehara, Y., Suganuma, N., and Kawaguchi, M.** (2012). Positive and negative regulation of cortical cell division during root nodule development in *Lotus japonicus* is accompanied by auxin response. *Development* **139**, 3997-4006.
- Taddese, B., Upton, G.J.G., Bailey, G.R., Jordan, S.R.D., Abdulla, N.Y., Reeves, P.J., and Reynolds, C.A.** (2013). Do Plants Contain G Protein-Coupled Receptors? *Plant Physiology* **164**, 287-307.
- Takahara, M., Magori, S., Soyano, T., Okamoto, S., Yoshida, C., Yano, K., Sato, S., Tabata, S., Yamaguchi, K., and Shigenobu, S.** (2013a). Too much love, a novel Kelch repeat-containing F-box protein, functions in the long-distance regulation of the legume–rhizobium symbiosis. *Plant and cell physiology* **54**, 433-447.
- Takahara, M., Magori, S., Soyano, T., Okamoto, S., Yoshida, C., Yano, K., Sato, S., Tabata, S., Yamaguchi, K., Shigenobu, S., Takeda, N., Suzaki, T., and Kawaguchi, M.** (2013b). Too much love, a novel Kelch repeat-containing F-box protein, functions in the long-distance regulation of the legume-Rhizobium symbiosis. *Plant Cell Physiol* **54**, 433-447.
- Tatsukami, Y., and Ueda, M.** (2016). Rhizobial gibberellin negatively regulates host nodule number. *Scientific Reports* **6**, 27998.
- Tauc, M., Cougnon, M., Carcy, R., Melis, N., Hauet, T., Pellerin, L., Blondeau, N., and Pisani, D.F.** (2021). The eukaryotic initiation factor 5A (eIF5A1), the molecule, mechanisms and recent insights into the pathophysiological roles. *Cell & Bioscience* **11**, 219.
- Thompson, J.F., and Hearst, J.E.** (1983). Structure-function relations in *E. coli* 16S RNA. *Cell* **33**, 19-24.
- Tiwari, M., Pandey, V., Singh, B., and Bhatia, S.** (2021). Dynamics of miRNA mediated regulation of legume symbiosis. *Plant, Cell & Environment* **44**, 1279-1291.
- Tsikou, D., Yan, Z., Holt, D.B., Abel, N.B., Reid, D.E., Madsen, L.H., Bhasin, H., Sexauer, M., Stougaard, J., and Markmann, K.** (2018). Systemic control of legume susceptibility to rhizobial infection by a mobile microRNA. *Science* **362**, 233-236.
- Tyerman, S.D., Whitehead, L.F., and Day, D.A.** (1995). A channel-like transporter for NH₄⁺ on the symbiotic interface of N₂-fixing plants. *Nature* **378**, 629-632.
- Uchida, R.** (2000). Essential nutrients for plant growth: nutrient functions and deficiency symptoms. *Plant nutrient management in Hawaii's soils* **4**, 31-55.
- Udvardi, M., and Poole, P.S.** (2013). Transport and metabolism in legume-rhizobia symbioses. *Annu Rev Plant Biol* **64**, 781-805.
- Ueguchi-Tanaka, M., Nakajima, M., Katoh, E., Ohmiya, H., Asano, K., Saji, S., Hongyu, X., Ashikari, M., Kitano, H., and Yamaguchi, I.** (2007). Molecular interactions of a soluble gibberellin receptor, *GID1*, with a rice *DELTA* protein, *SLR1*, and gibberellin. *The Plant Cell* **19**, 2140-2155.
- Unkovich M., H.D., Peoples M., Cadisch G., Boddey R., Giller K., Alves B. and Chalk P.** (2008). Measuring plant-associated nitrogen fixation in agricultural systems, *ACIAR*, ed, pp. 258

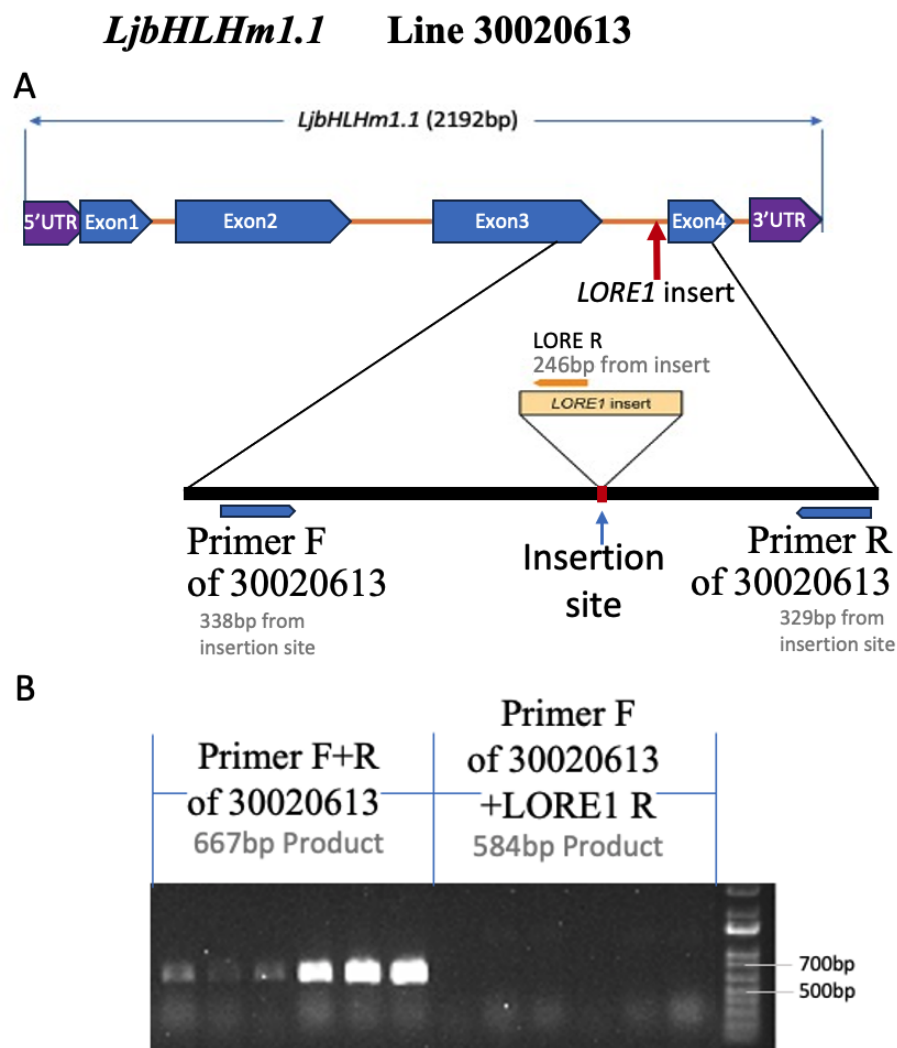
- Van Noorden, G.E., Ross, J.J., Reid, J.B., Rolfe, B.G., and Mathesius, U.** (2006a). Defective Long-Distance Auxin Transport Regulation in the *Medicago truncatula* super numeric nodules Mutant Plant Physiology **140**, 1494-1506.
- van Noorden, G.E., Ross, J.J., Reid, J.B., Rolfe, B.G., and Mathesius, U.** (2006b). Defective long-distance auxin transport regulation in the *Medicago truncatula* super numeric nodules mutant. Plant Physiol. **140**, 1494.
- Vinardell, J.M., Fedorova, E., Cebolla, A., Kevei, Z., Horvath, G., Kelemen, Z., Tarayre, S., Roudier, F.o., Mergaert, P., Kondorosi, A., and Kondorosi, E.** (2003). Endoreduplication Mediated by the Anaphase-Promoting Complex Activator CCS52A Is Required for Symbiotic Cell Differentiation in *Medicago truncatula* Nodules. The Plant Cell **15**, 2093-2105.
- Viswanath, K.K., Varakumar, P., Pamuru, R.R., Basha, S.J., Mehta, S., and Rao, A.D.** (2020). Plant Lipoxygenases and Their Role in Plant Physiology. Journal of Plant Biology **63**, 83-95.
- Walper, E., Weiste, C., Mueller, M.J., Hamberg, M., and Dröge-Laser, W.** (2016). Screen Identifying Arabidopsis Transcription Factors Involved in the Response to 9-Lipoxygenase-Derived Oxylipins. PLoS One **11**, e0153216.
- Wang, L., Sun, Z., Su, C., Wang, Y., Yan, Q., Chen, J., Ott, T., and Li, X.** (2019). A GmNINA-miR172c-NNC1 regulatory network coordinates the nodulation and autoregulation of nodulation pathways in soybean. Molecular Plant **12**, 1211-1226.
- Wang, Y., Wang, L., Zou, Y., Chen, L., Cai, Z., Zhang, S., Zhao, F., Tian, Y., Jiang, Q., and Ferguson, B.J.** (2014). Soybean miR172c targets the repressive AP2 transcription factor NNC1 to activate ENOD40 expression and regulate nodule initiation. The Plant Cell **26**, 4782-4801.
- Wang, Y., Li, K., Chen, L., Zou, Y., Liu, H., Tian, Y., Li, D., Wang, R., Zhao, F., Ferguson, B.J., Gresshoff, P.M., and Li, X.** (2015). MicroRNA167-Directed Regulation of the Auxin Response Factors GmARF8a and GmARF8b Is Required for Soybean Nodulation and Lateral Root Development Plant Physiology **168**, 984-999.
- Weigel, D., and Glazebrook, J.** (2008). Fixation, embedding, and sectioning of plant tissues. In CSH Protoc, pp. pdb.prot4941.
- Whitehead, L.F., Tyerman, S.D., Salom, C.L., and Day, D.A.** (1995). Transport of fixed nitrogen across symbiotic membranes of legume nodules. Symbiosis **19**, 141-154.
- William E. Balch, A.L.H., J. David Castle, Pat Shipman.** (2017). Chapter 12 - Protein Synthesis and Folding*. In Cell Biology (Third Edition), T.D. Pollard, W.C. Earnshaw, J. Lippincott-Schwartz, and G.T. Johnson, eds (Elsevier), pp. 209-222.
- Xia, X., Ma, C., Dong, S., Xu, Y., and Gong, Z.** (2017). Effects of nitrogen concentrations on nodulation and nitrogenase activity in dual root systems of soybean plants. Soil science and plant nutrition **63**, 470-482.
- Xiao, T.T., Schilderink, S., Moling, S., Deinum, E.E., Kondorosi, E., Franssen, H., Kulikova, O., Niebel, A., and Bisseling, T.** (2014). Fate map of *Medicago truncatula* root nodules. Development **141**, 3517-3528.

- Xie, F., Murray, J.D., Kim, J., Heckmann, A.B., Edwards, A., Oldroyd, G.E.D., and Downie, J.A.** (2012). Legume pectate lyase required for root infection by rhizobia. *Proceedings of the National Academy of Sciences* **109**, 633-638.
- Xue, H., Gao, X., He, P., and Xiao, G.** (2022). Origin, evolution, and molecular function of DELLA proteins in plants. *The Crop Journal* **10**, 287-299.
- Zažímalová, E., Petrášek, J., and Benková, E.** (2014). *Auxin and its role in plant development.* (Springer).
- Zhao, Y.** (2010). Auxin biosynthesis and its role in plant development. *Annu Rev Plant Biol* **61**, 49-64.
- Zhong, C., Xu, H., Ye, S., Wang, S., Li, L., Zhang, S., and Wang, X.** (2015). Gibberellic Acid-Stimulated Arabidopsis6 Serves as an Integrator of Gibberellin, Abscisic Acid, and Glucose Signaling during Seed Germination in Arabidopsis *Plant Physiology* **169**, 2288-2303.

Appendixes



Appendix 1. Comparison of Egfp signals in pK7GWIWG2D(II) (RNAi) and pFAST-G02 (Overexpression) vector identified in transformed hairy roots and nodules. (A) pK7GWIWG2D(II) empty vector transformed hairy roots and nodules, (B) pK7GWIWG2D(II)-*GmbHLHm1* transformed hairy roots and nodules. (C) pFAST-G02 empty vector transformed hairy roots and nodules, (D) pFAST-G02 *GmbHLHm1* transformed hairy roots and nodules. Transgenic hairy roots were made according to the protocol of (Mohammadi-Dehcheshmeh et al., 2014). Soybeans were grown in a mixed matrix of quartz sand and turface (1:1 ratio). B&D nutrient solution (Broughton and Dilworth, 1971) was applied twice a day using a semi-hydroponic growing system. 28 d nodules on wild-type roots and transgenic hairy roots were harvested for experiments and **Egfp** detection.



Appendix 2. Structure of *LjbHLHm1.1*, the LORE1 insertion site and genotyping result of line 30020613. (A) The LORE1 insert was in the second exon of the *LjbHLHm1* gene (Plant ID: 30020613). (B) Genotype analysis of 1st generation seedlings from Lotus Base seed. Primer combinations (Primer F and Primer R of 30020613) were used to identify plant lines with or without the LORE1 insertion (667 bp products would identify genomic sequences without a LORE1 insertion). Primer combinations (Primer F and LORE1 R) were used to amplify the 5'-flanking DNA region at the insertion site. A positive PCR for LORE1 will amplify a 584bp product. PCR cycles used for genotyping are described in Chapter 5. In this line, the LORE1 insertion is in the intron, no LORE1 insertion was detected by PCR.